Enhancing Materials through Controlled Architectures with Ring-Opening Metathesis Polymerization

Thesis by

Oren Alexander Scherman

In Partial Fulfillment of the Requirements

for the Degree of

Doctor of Philosophy

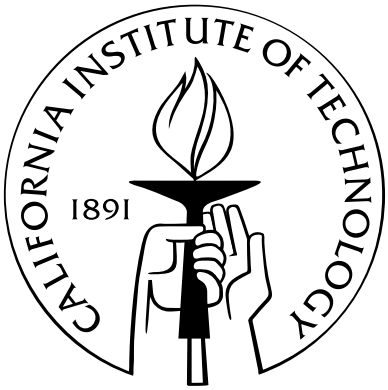

California Insititute of Technology

Pasadena, California

2004

(Defended February 19, 2004)

Acknowledgements

When I was ten years old, I recall sitting in my father's office at the University of Oklahoma; I heard a student address my father as "Dr. Scherman." This was indeed strange as my father has always insisted on being called "Avi." ***Doctor!?!*** *my dad's office didn't have a waiting room attached, full of sick people, but rather, only Psychology graduate students who loved to interrupt him in the middle of writing something on an old Macintosh computer.*

I guess there are two important things that came from that memory: first, it would be really neat to be called "Dr. Scherman" so that I could immediately insist on just being referred to as *Oren* again, and second, I was destined to be interrupted by graduate students while writing on a Macintosh computer!

In October 1999, I decided to *go west*, with the encouragement of Professors Dotsevi Sogah and Geoff Coates of Cornell University, and join the research group of Professor Robert H. Grubbs at Caltech to begin my quest for a PhD in Chemistry. After fifty-two rewarding months, I have accomplished this goal. It is difficult to express my immense gratitude to the many friends and family members and co-workers who not only helped and supported me throughout this challenging process, but made it extremely enjoyable as well. First and foremost, I am grateful to Professor Grubbs. The opportunity to work for Bob is what lured me to sunny California in the first place, and being part of his research group has been a wonderful experience. Bob has continually allowed me the space and freedom to pursue the chemistry that most interested me and has wisely advised me to "never talk myself out of doing a reaction!" His constant encouragement has helped me through the ups and downs of my research and he has taught me how to put things into perspective. The atmosphere

he creates for the group has helped me mature both as a chemist and as a person.

I would also like to thank the other members of my PhD committee for their support and encouragement: Professor Bill Goddard, Professor Brain Stoltz and Professor Dave Tirrell.

One of the earliest and strongest friendships I formed at Caltech were with my first-year roommate at 438 S. Catalina Avenue, # 103, Darren Beene, and with Chris Thomas. Darren and Chris have been great friends throughout my time at Caltech. Darren always offers a unique perspective, and I will miss our midnight conversations and more recent afternoon coffee breaks filled with friendly PAC-10 vs Big 12 banter and discussions over politics and current events, science, and life in general. Chris never ceases to impress me with his knowledge over a wide range of topics. He is an outstanding chemist and I wish him the best of luck with his new postdoc in San Diego.

The relationships I have formed with people in the Grubbs group have been instrumental to my success as a graduate student. When I first arrived, Chris Bielawski, John P. Morgan (JP), and Arnab Chatterjee helped me get off to a great start in the lab. I am grateful to Chris for teaching me how to use the glove box, the Schlenk lines and in general, how to be a successful chemist in the group. He is a creative polymer chemist and he encouraged me to be innovative and to show my creativity in my research. JP's approach to science is thorough and it was always refreshing to hear his well thought-out answers to my various questions. JP and I also both held strong opinions about politics and academia and I gained a lot of perspective from listening to his opinions. Arnab quickly became a wonderful friend and he always provided encouragement and advice during times of doubt in the course of my PhD. Arnab also introduced me to the wonders of Las Vegas and taught me how to play blackjack and craps, much to my wife's dismay. I have great memories of lazy days at sea and afternoons of Puerto Rican rum and fresh coconuts from a Caribbean cruise that Arnab, my wife, and I took together.

Several other graduate students were also instrumental in the successful completion of my PhD and I would like to thank all of the members of the Grubbs group

whose paths have crossed with mine during my time at Caltech. Diego Benitez, Tae Lim Choi (TLC), Dan Sanders, and I all started in the group at the same time. They have all been great friends and co-workers and I thank them for their input and suggestions during my PhD. Dan has also proven a great friend outside of the lab and I thank him for helping me climb 99% of the way up Half Dome in Yosemite National Park, pushing me to run a faster 5 K, and for midnight chats in the computer room. I have also had the honor and pleasure of carrying out several research projects with a wonderful co-worker and scientist, Isaac Rutenberg. Isaac has been a source of much needed skepticism when interpreting scientific data. He has always graciously provided excellent feedback on my countless drafts as I wrote papers or prepared presentations. And, he showed his acumen by quickly learning how to drive a manual car and simultaneously navigate through NYC traffic during one of my more robust drinking performances! Andy Hejl is responsible for my recent addiction to crossword puzzles and I wonder if I will ever again be able to enjoy morning coffee without them! I will always remember my road trip to Oklahoma with Andy and in particular the long ride back to LA on I-40 during which we passed the time performing out of tune duets to the songs on CD's 8–17.

A number of postdocs have also played an important role in my graduate career. Dr. Hyunjin Kim, my bench-mate for two years, shared his extensive knowledge of synthetic organic chemistry as I first started my chemistry research at Caltech. He taught me how to work efficiently and how to think about synthetic problems. From Dr. Andreas Kilbinger, a fantastic scientist and polymer chemist, I learned not only about chemistry but also about enjoying life and how to schedule a pub crawl. I enjoyed going with him to the Caltech pool for our daily swimming workouts so that I could make room for beers and yogurt on Wednesday evening....now I will need to go back to Barney's and get "Dr." added to my name plaque!

Dr. Jon Efskind is the first Norwegian I ever met and I immediately insulted him by calling him a Swede! I spent two years trying to convince him it was an honest mistake. He also kept me in shape with afternoon swimming workouts and occasional runs around the track. Jon and his wife, Dr. Camilla Haavik, are great friends and

during their tenure at Caltech we enjoyed many wonderful times together including trips to Las Vegas with front-row seats at a boxing match, drives down to San Diego, bar hopping, and great food in New Orleans. Jon was also crazy enough to take me up on my offer to drive to Oklahoma for Filet Mignon! I hope the steak was worth it after he risked deportation by the INS just outside of Whitesands, New Mexico!

Dr. Stuart Cantrill taught me, amongst other things, how to give a good presentation and write a respectable scientific paper. He is a very creative person and I always enjoyed talking with him about anything. I hope that one day we will find each other in a pub somewhere to watch the World Cup Finals! Dr. Christiane Marti has a wonderful sense of humor and an infectious smile, and she gave me many suggestions and encouragement over the last year of my research. I thank her for just being herself and introducing levity into my life every day. Dr. Sebastian Smidt helped me think about chemistry and offered many great suggestions during the writing of my proposals. I appreciate hearing his opinions about chemistry and life in general and I hope to share many more thoughts and ideas over an espresso in Europe. Dr. Brian Connell is an amazing synthetic organic chemist and he has helped me numerous times with his great suggestions. He is also a Mac-lover and I really appreciate the time and effort he has spent helping me keep the group computers and server up to par, and for constantly educating me about OS X! Thank you to Dr. Emmanuelle Despagnet-Ayoub for being a great bench-mate and desk-mate. We enjoyed discussing differences between the United States and Europe and I look forward to experiencing them first-hand. I had a great time interacting with Dr. Valeria Molinero on a computational project. I really enjoyed talking with her about life and why in general one should NOT trust a computer!

A special thanks to my other workout friends Sarah Monahan, Nelly Khidekel, and Anatoli Chlenov for helping me keep off the pounds after my Atkin's Diet with daily runs on the track or in San Marino or Friday afternoon laps in the pool. Also I want to thank Greg Drummond and Susan Schofer for making it possible to accomplish one of my goals while living in California and reach the summit of Mt. Whitney in October 2003.

I am very thankful for the last minute LaTeX help I received from Ross Moore and Wendy McKay....oh, if everyone just learned how to typeset things.....

I would like to thank my parents who have made tremendous sacrifices so that their children could find the best education. They have always supported my endeavors and have provided wise and much needed advice. It has been difficult being so far away from them while in school, but they have always known when I needed a little lift and have helped by visiting and sending great care packages. I want to thank my brother, Aric, and my sister, Dorit, for coming out to visit me while I have been in California. They both have a wonderful attitude towards life and their visits could not have come at better times to help me release some stress.

Also, thank you Pumpkin...a cat with personality is the biggest understatement!!! (his contribution →) lkjqwekljkgx93r

Lastly, I must thank Cora, my beautiful and loving wife, who is full of encouragement and always knows what to do and how to cheer me up! She is the bright beacon in my life and I cannot think where I would be right now without her. Thank you sweetie for being understanding of my late night or *early morning* returns from the lab, my really lousy ability to tell you when I'm ready to be picked up, and of my often-wandering mind during dinner.

Abstract

The focus of the research presented in this thesis is the synthesis of functional polymers and construction of controlled molecular architectures through a polymerization process referred to as ring-opening metathesis polymerization (ROMP). A brief overview of polymer chemistry as well as ring-olefin metathesis polymerization is discussed in introductory Chapter 1.

Chapters 2 and 3 discuss new synthetic routes to polyacetylene and polyacetylene block-copolymers from cyclooctatetraene and a new ruthenium olefin metathesis catalysts. Polyacetylene is an intractable material, as are most organic conducting polymers. Chapter 3, however, introduces a novel route to soluble telechelic polyenes and polyacetylene block-copolymers.

The construction of organic overlayers on semiconductor surfaces is important in the area of anti-fouling coatings as well as in organic electronic applications. Chapter 4 introduces a new route to polymer-covered silicon surfaces through a covalent Si-C linkage. ROMP of norbornene from a surface-attached ruthenium catalyst produces uniform polynorbornene overlayers with controlled thickness ranging from 10 Å to 5.5 μm. The work discussed in Chapter 5 elaborates on surface-initiated ROMP by constructing thin-film top-contact field effect transistors with a polynorbornene dielectric layer.

Chapter 6 explores the synthesis of polar-functionalized linear polymers from cyclopentene and cycloheptene derivatives. The challenge of polymerizing low-ring strain monomers *via* ROMP is also discussed. A method to *a priori* discern a monomer's ability to undergo ROMP is outlined in this chapter as well.

Chapters 7 and 8 describe the synthesis of both *regioregular* and *stereoregular*

polar-functionalized linear ethylene vinyl alcohol (EVOH) co-polymers by the ROMP of rationally designed, symmetric monomers. These polymers were made with the goal of producing materials with enhanced oxygen barrier properties. Controlling material architecture imparts a dramatic effect on both the solution and solid state morphologies of EVOH and the synthetic challenges and results are discussed.

Finally, Chapter 9 complements Chapters 7 and 8, and investigates the reason behind enhanced oxygen barrier properties of EVOH through molecular dynamics simulations. For EVOH polymers that differs only by the syn or anti orientation of neighboring diols, a clear difference is observed for the hydrogen bonding clusters. Moreover, the free volume accessible to any solute molecules is extremely low identified by a probe radius of less than 0.6 Å.

Contents

List of Figures

List of Schemes

List of Tables

Chapter 1

An Introduction to Functional Polymers and ROMP

1.1 Synthetic Polymer Basics

Put simply, polymers are large molecules that consist of a number of repeat units linked together in a repetitive fashion. The small molecules that make up polymers are called monomers. While each monomer has a singular molecular weight, synthetic materials do not. A polymeric material generally consists of many polymer chains of varying number of monomeric units and hence, different size and shape.

1.1.1 Synthesis

The synthesis of polymers can generally be described by two types of classifications: *condensation* and *addition* or *step growth* and *chain growth*.[1] The first, *condensation* and *addition*, describes the composition and/or structure of the polymer, while the second classification, *step growth* and *chain growth* relates to the polymerization mechanism.[1] The term "condensation" arises from the synthesis of polyesters and polyamides where small molecules such as water, alcohols, or acids are released upon forming covalent bonds between monomers. Removal of these condensation products serves to drive the reaction towards completion. These types of polymerizations occur in a *step*-wise fashion, first combining monomers and making *dimers*, and then *trimers* and *tetramers*, etc. The molecular weight of condensation polymers grows large only at the very end of the reaction ($> 99\%$ conversion). The number of repeat units in a condensation polymerization is defined as $X_{\mathrm{n}} = 1/(1\text{-}\rho)$, where ρ is the percent conversion.[1] Conversely, *addition* polymers are usually made by a *chain growth* mechanism. There are many ways to prepare *addition* polymers and these include anionic, cationic, free radical, and metal-catalyzed polymerizations of vinyl monomers to name a few.[1] These polymers can reach very high molecular weights at low conversions, and make up the bulk of industrial commodity polymers such as polyethylene (PE), polypropylene (PP), and polystyrene (PS).

Many commercially produced polymers are pure hydrocarbons like PE, PP, and PS. Much effort has been devoted to make versions of these polymers with slight differences in polymer architecture and stereochemistry. For example, PE that con-

tains a high amount of branching has very different properties than linear PE. The relative orientation (*tacticity*) of the pendent methyl groups in PP can determine whether the polymer is suitable to resist the high impact forces of a traffic accident or is better used as a plastic bag for groceries. There are also many polymers that contain polar functional groups. Functionalities that are pendent from the polymer main chain dramatically affect the properties of the resulting materials.[1] The regularity and relative spatial orientation (*tacticity*) of these functional groups can also produce large differences in polymer properties. Not all polymerization methods or catalysts, however, are amenable to polar monomers. Thus, the development of new methods to synthesize polar-functionalized polymers is an area of intense research.

1.1.2 Characterization

As mentioned earlier, since polymerizations produce materials with a broad distribution of molecular weights (MWs), it can be very misleading to report a single quantity for MW. Rather, it is much more useful to know something about the average and overall distribution of chain lengths in a polymer sample. Thus, MWs are reported as several values: the number average molecular weight, M_{n}, the weight average molecular weight M_{w}, as well as several others.[1, 2] The M_{n} value reported for a polymer states the average number of repeat units (monomers) times the monomer's MW for all of the polymer chains in the sample, while the M_{w} represents a weighted average whereby the longer chains bias the value. A measure of the distribution of a polymer's MW is termed *polydispersity index* (PDI) and is a ratio of two MW averages. The most common value of PDI is the ratio of $M_{\mathrm{w}}/M_{\mathrm{n}}$. As M_{w} is always $> M_{\mathrm{n}}$, the PDI of a polymer is always > 1. The PDIs of polymers made by step growth polymerizations are between 1 and 2 and are a function of conversion. On the other hand, the PDI of polymers made by chain growth polymerizations can vary greatly; controlled, "living" polymers can be made with PDIs of 1.01 while some metal-catalyzed or un-controlled free radical polymers have PDIs > 10.[2] Material properties can vary greatly depending on MW and PDI; therefore, the ability to

control these values through synthetic methodology is highly valued. Furthermore, much information about the polymerization mechanism can be obtained by evaluating trends observed in MW and PDI data.

There are many ways to measure M_n, M_w, and PDI values for synthetic polymers. These include size exclusion chromatography (SEC, also known as gel permeation chromatography, GPC), endgroup analysis (integration of ^{1}H NMR spectrum), light scattering, and matrix-assisted laser desorption ionization time-of-flight mass spectrometry (MALDI-TOF MS), are just a few of the common methods and are all used in the chapters that follow.[2] Unfortunately, the structure and functionality in many polymers can make their detailed characterization extremely difficult and in certain instances, impossible. For example, most conducting polymers are intractable materials and cannot be characterized in the solution state. Thus, developing methods of solubilizing such materials to enable detailed characterization is an active area of research.[3–6]

1.2 Olefin Metathesis

Synthetic chemists take pride in the ability to make almost any molecule that can be drawn on a piece of paper. The construction of these molecules occurs by making and breaking chemical bonds in discrete chemical reactions. In synthetic organic chemistry, the carbon-carbon double bond (C=C) is the basis for a large number of chemical transformations. The aptly named olefin metathesis reaction[7–9] allows for the formation of C=C bonds and is a simple "transposition of two elements"; it involves breaking a C=C bond followed by the formation of a new one. This process is mediated by a metal carbene catalyst as shown in Figure 1.1. Upon binding of an olefin to the metal carbene catalyst, formation of a metallocyclobutane occurs.[10–14] This species can either form a new olefin and metal carbene or revert to the original olefin in a non-productive metathesis event.

Many useful transformations can be carried out via olefin metathesis as depicted in Figure 1.2. A diene can undergo a ring-closing metathesis (RCM) event to form

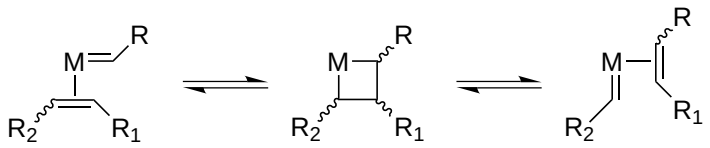

Figure 1.1: A simplified view of olefin metathesis.

a cyclic olefin, or, under conditions of very high concentration, may form a linear polymer through a process referred to as acyclic diene metathesis polymerization (ADMET).[14] The driving force behind both RCM and ADMET is the loss of a small molecule, ethlyene. In a process known as ring-opening metathesis polymerization (ROMP) cyclic olefins can be transformed into high molecular weight linear polymer. In contrast to RCM and ADMET, ROMP is driven by the release of ring strain inherent in cyclic olefin monomers. It is important to realize that all of these transformations are reversible and are controlled by a thermodynamic equilibrium.[9, 13]

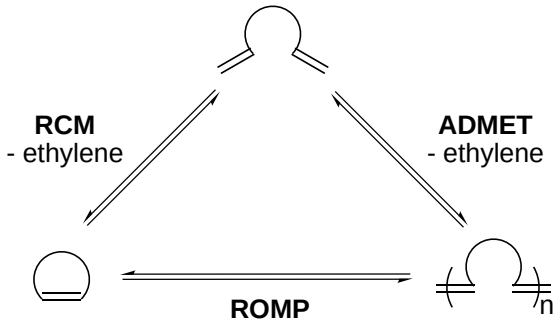

Figure 1.2: Chemical transformations by olefin metathesis.

1.2.1 Olefin Metathesis Catalysts

While a number of transition metals can catalyze olefin metathesis, early reports only focused on the ROMP of highly strained cyclic olefins with transition metal salts.[9, 14] Several decades of research produced well-defined early transition metal catalysts based on titanium, tungsten, and molybdenum as depicted in Figure 1.3.[9, 15] All of these catalysts, however, require very stringent handling conditions, are air sensitive, and do not tolerate many organic functional groups. While the reactivity of

these catalysts is high, their selectivity for reaction with olefins is poor. In the mid-1990s, Grubbs *et al.* reported a family of late transition metal, ruthenium-based olefin metathesis catalysts which were capable of operating in the presence of many polar functional groups (Figure 1.3) such as ketones, esters, aldehydes, and even alcohols. The activity of the ruthenium catalysts, however, was much lower than that of early metal catalysts.[13, 14, 16–19]

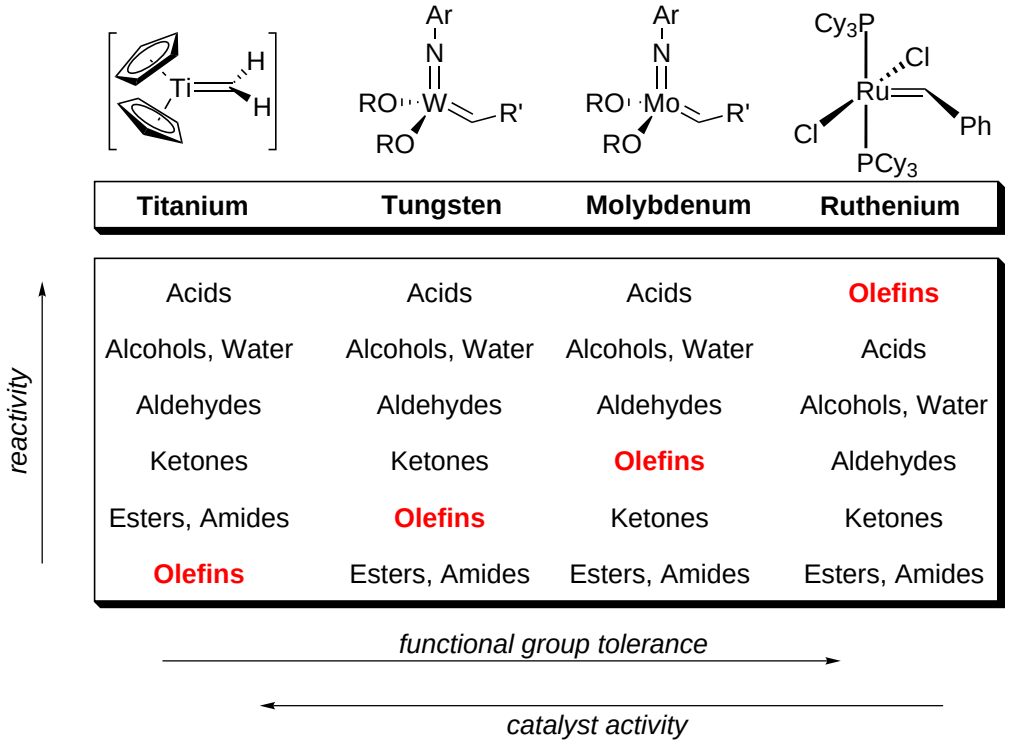

Figure 1.3: Reactivity of olefin metathesis catalysts.

Recently, further modifications of the ligand set addressed the lower activity of the ruthenium-based catalysts.[20] Figure 1.4 illustrates the replacement of a phosphine ligand with an N-heterocyclic carbene ligand. This ligand substitution greatly increased the catalyst activity while maintaining the functional group tolerance typical for the ruthenium systems.[12] In fact, the second-generation ruthenium catalyst is more active towards both RCM and ROMP than the first generation version by several orders of magnitude.[21] The development of well-defined, ruthenium-based catalysts has allowed for a wide variety of synthetically useful transformations and polymerizations

to occur in the presence of many functional groups.

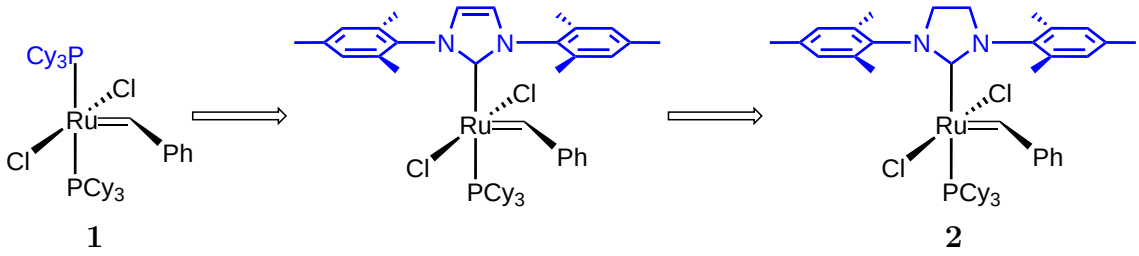

1 **2**

Figure 1.4: Recent advances in ruthenium olefin metathesis catalysts.

1.2.2 Ring-Opening Metathesis Polymerization

Both ADMET and ROMP are capable of producing linear polymers via olefin metathesis.[9] The driving forces for these reactions, however, are quite different, and the implications for the polymerizations are quite dramatic. For example, since the loss of ethylene drives ADMET polymerizations to high MW, the reaction follows a condensation, or step growth mechanism. Therefore high conversion is required for high MW polymer to form. Furthermore, high concentrations are necessary to ensure efficient coupling of terminal olefins and, unfortunately, slow diffusion due to high viscosity typically prevents the formation of high MW polymer.[9, 13]

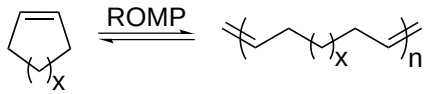

Figure 1.5: ROMP of a cyclic olefin.

Conversely, ROMP reactions use the release of ring strain inherent in the monomer to drive the reaction to completion (Scheme 1.5). Therefore, polymerizations can be carried out in dilute solutions which enable the formation of high MW material. Monomers which possess a high amount of ring strain such as cyclobutene and norbornene easily undergo ROMP at very low monomer concentrations.[9] However, monomers such as cyclopentene, cyclohexene, and cycloheptene are more difficult to polymerize as their strain energies are relatively low (Figure 1.6).[22] Since olefin

metathesis is a reversible reaction governed by thermodynamic equilibrium, the strain energy of the monomer plays a large role in determining the polymerization yield in ROMP reactions. As ROMP is reversible, depolymerization reactions can occur over the course of a metathesis polymerization, through processes known as chain transfer or "backbiting."[9, 23] This can have a great effect on the polymer MW and overall architecture.[24–26]

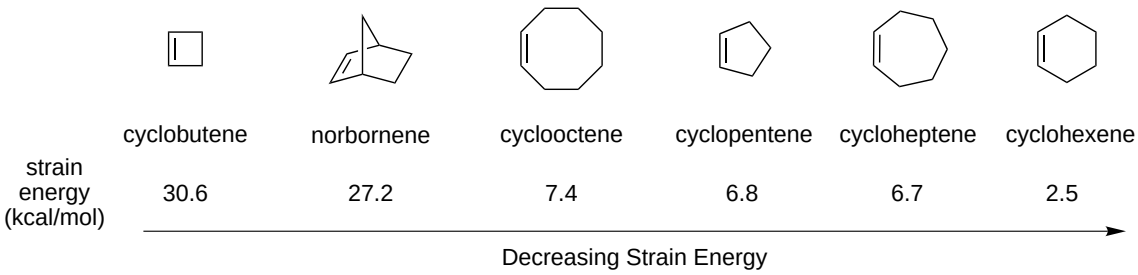

Figure 1.6: Representative cyclic olefin monomers and strain energies.[22]

As ROMP can be carried out in solution, facile control of polymer MW can be achieved in several different ways. For highly strained monomers such as cyclobutene, norbornene, and oxanorbornene, living polymerization can be attained with fast initiating olefin metathesis catalysts leading to precisely controlled polymer architectures and MW.[15, 27] ROMP has been used to prepare block-copolymers through the sequential addition of monomers. Another method to control the MW and architecture of ROMP polymers is through the use of chain transfer agents (CTAs).[23, 24] When ROMP of a cyclic olefin is carried out in the presence of a symmetric CTA, such as an acyclic olefin, a linear, telechelic polymer will be formed as illustrated in Scheme 1.1. Telechelic polymers are end-functionalized polymers that have found application in cross-linking and polymer network formation, chain-extention processes, and in the solubilization of materials.[28]

Scheme 1.1: ROMP in the presence of a CTA to produce a linear, telechelic polymer.

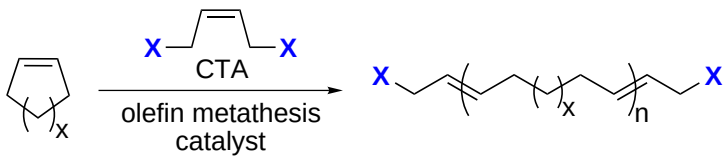

A general reaction mechanism for ROMP with a CTA is outlined in Scheme 1.2. The propagating polymer chain can react with either a cyclic olefin monomer or with an acyclic CTA molecule. If a metathesis event occurs with the CTA, the functionality (**X**) of the CTA gets transferred to one *end* of the polymer chain. Later in the reaction, the other chain *end* will be formed by reacting with another CTA molecule. Therefore, at the end of the reaction, all of the chains will have functionality (**X**) transferred to *both* chain ends.* Moreover, with the advances in catalyst design over

Scheme 1.2: Mechanism for the synthesis of telechelic polymers by ROMP.

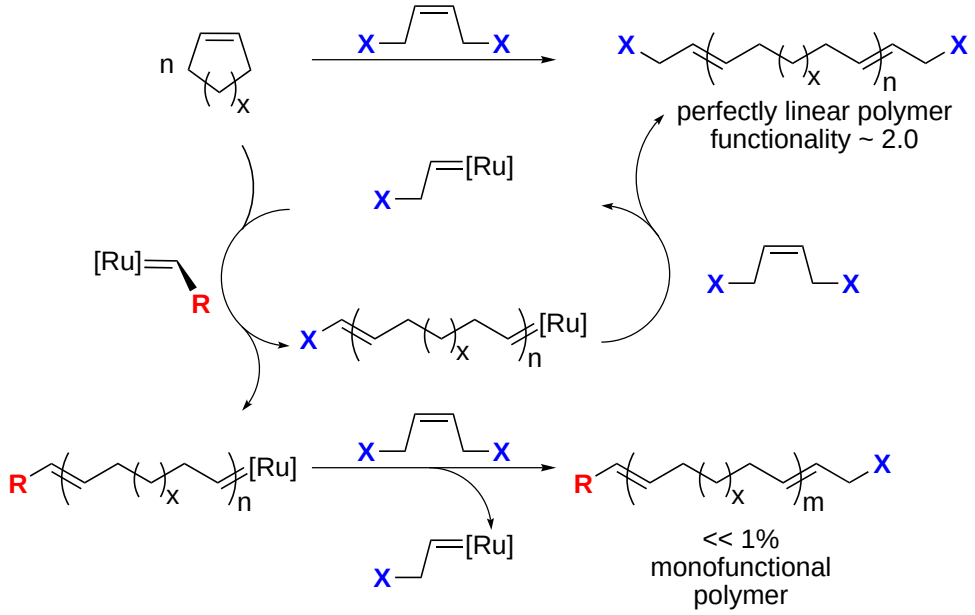

the last decade leading to late transition metal (ruthenium) catalysts, both cyclic and acyclic olefins bearing polar functional groups can now be employed in ROMP.[12] This has allowed for the synthesis of many new material architectures such as conducting polymers,[29–35] water-soluble polymers,[4] and surface-bound polymers,[36–38] all of which will be discussed in the following pages.

*This requires that a high excess of CTA relative to catalyst is used.[23, 24]

1.3 Objectives of this Work

The research presented in this thesis describes my contributions in the areas of conducting polymers, surface-inititated polymers, and well-defined polar functional polymers that are prepared by ROMP. Chapter 2 introduces the synthesis of conducting polymers via ROMP and illustrates that catalyst activity plays an important role in the preparation of polymers such as polyacetylene. The use of late transition metal olefin metathesis catalysts such as ruthenium to form polyacetylene (Chapter 2) was extended to form telechelic, solubilized polyenes and polyacetylene block-copolymers through the use of chain transfer agents; this work is discussed in Chapter 3. The use of ROMP in surface-initiated polymerization is discussed in Chapters 4 and 5. In a collaboration with Dr. Agnes Juang and Prof. Nathan Lewis (Caltech), organic overlayers consisting of polynorbornene were grown from a Si (111) surface (Chapter 4). The ROMP polymer was covalently attached to the silicon surface with a direct Si-C linkage instead of through the traditional Si/SiO_2 linkers previously employed. This concept was further explored in a collaboration with Mr. Isaac Rutenberg (also a member of the Grubbs group at Caltech) and Dr. Zhenan Bao (Lucent Technologies) in order to prepare top-contact field-effect thin film transistors with a ROMP polymer as the dielectric layer (Chapter 5). Chapter 6 evaluates the ROMP of low-strain monomers such as cyclopentene and cycloheptene and discusses the thermodynamic considerations involved in ROMP. A model for predicting the ability of a cyclic olefin to undergo ROMP ("ROMP*ability*") is presented. Novel materials possessing a range of both polar and apolar functionalities can now be prepared in large scale. These materials include both telechelic polymers, block-copolymers, and polymers with main-chain functionality. Chapters 7 and 8 describe a synthetic strategy for achieving both *regioregular* and *stereoregular* polymers bearing alcohol functionalities. A set of rationally designed ethylene vinyl alcohol (EVOH) copolymers allowed for the detailed study of property–function relationships for functional polymers. Complementary to the EVOH synthesis by ROMP, Chapter 9 describes some results from a collaborative effort with Dr. Valeria Molinero (a postdoc in the Goddard group at Caltech) for the

computational modeling of regioregular and stereoregular EVOH, and illustrates why the local polymer structure can effect material properties such as O_2 permeability.

References Cited

[1] Odian, G. *Principles of Polymerization;* Wiley & Sons: New York, 3rd ed.; 1991.
[2] Cowie, J. M. G. *Polymers: Chemistry and physics of modern materials;* Chapman and Hall: New York, 2nd ed.; 1991.
[3] Stelzer, F.; Grubbs, R. H.; Leising, G. *Polymer* **1991,** *32,* 1851–1856.
[4] Wagaman, M. W.; Grubbs, R. H. *Macromolecules* **1997,** *30,* 3978–3985.
[5] Knoll, K.; Schrock, R. R. *J. Am. Chem. Soc.* **1989,** *111,* 7989–8004.
[6] Krouse, S. A.; Schrock, R. R. *Macromolecules* **1988,** *21,* 1885–1888.
[7] Calderon, N.; Chen, H. Y.; Scott, K. W. *Tetrahedron Lett.* **1967,** *34,* 3327–3329.
[8] Calderon, N. *Acc. Chem. Res.* **1972,** *5,* 127–132.
[9] Ivin, K. J.; Mol, J. C. *Olefin Metathesis and Metathesis Polymerization;* Academic Press: London, 1997.
[10] Herisson, J. L.; Chauvin, Y. *Makromol. Chem.* **1971,** *141,* 161.
[11] Sanford, M. S.; Ulman, M.; Grubbs, R. H. *J. Am. Chem. Soc.* **2001,** *123,* 749–750.
[12] Sanford, M. S.; Love, J. A.; Grubbs, R. H. *J. Am. Chem. Soc.* **2001,** *123,* 6543–6554.
[13] Grubbs, R. H., Ed.; *Handbook of Metathesis;* Wiley-VCH: Weinheim, 2003.
[14] Trnka, T. M.; Grubbs, R. H. *Acc. Chem. Res.* **2001,** *34,* 18–29.
[15] Schrock, R. R.; Krouse, S. A.; Knoll, K.; Feldman, J.; Murdzek, J. S.; Yang, D. C. *J. Mol. Catal.* **1988,** *46,* 243–253.
[16] Nguyen, S. T.; Grubbs, R. H.; Ziller, J. W. *J. Am. Chem. Soc.* **1993,** *115,* 9858–9859.
[17] Schwab, P.; France, M. B.; Ziller, J. W.; Grubbs, R. H. *Angew. Chem., Int. Ed.* **1995,** *34,* 2039–2041.
[18] Schwab, P.; Grubbs, R. H.; Ziller, J. W. *J. Am. Chem. Soc.* **1996,** *118,* 100–110.
[19] Dias, E. L.; Nguyen, S. T.; Grubbs, R. H. *J. Am. Chem. Soc.* **1997,** *119,* 3887–3897.
[20] Scholl, M.; Ding, S.; Lee, C. W.; Grubbs, R. H. *Org. Lett.* **1999,** *1,* 953–956.
[21] Bielawski, C. W.; Grubbs, R. H. *Angew. Chem., Int. Ed.* **2000,** *39,* 2903–2906.
[22] Schleyer, P. v. R.; Williams, J. E.; Blanchard, K. R. *J. Am. Chem. Soc.* **1970,** *92,* 2377–2386.
[23] Hillmyer, M. A.; Grubbs, R. H. *Macromolecules* **1993,** *26,* 872–874.
[24] Hillmyer, M. A.; Grubbs, R. H. *Macromolecules* **1995,** *28,* 8662–8667.
[25] Hillmyer, M. A.; Nguyen, S. T.; Grubbs, R. H. *Macromolecules* **1997,** *30,* 718–721.

[26] Bielawski, C. W.; Scherman, O. A.; Grubbs, R. H. *Polymer* **2001,** *42,* 4939–4945.
[27] Choi, T. L.; Grubbs, R. H. *Angew. Chem., Int. Ed.* **2003,** *42,* 1743–1746.
[28] Jerome, R.; Henrioullegranville, M.; Boutevin, B.; Robin, J. J. *Prog. Polym. Sci.* **1991,** *16,* 837–906.
[29] Klavetter, F. L.; Grubbs, R. H. *J. Am. Chem. Soc.* **1988,** *110,* 7807–7813.
[30] Klavetter, F. L.; Grubbs, R. H. *Synth. Met.* **1989,** *28,* D99–D104.
[31] Klavetter, F. L.; Grubbs, R. H. *Synth. Met.* **1989,** *28,* D105–D108.
[32] Swager, T. M.; Grubbs, R. H. *J. Am. Chem. Soc.* **1989,** *111,* 4413–4422.
[33] Swager, T. M.; Dougherty, D. A.; Grubbs, R. H. *J. Am. Chem. Soc.* **1988,** *110,* 2973–2974.
[34] Edwards, J. H.; Feast, W. J. *Polymer* **1980,** *21,* 595–596.
[35] Scherman, O. A.; Grubbs, R. H. *Synth. Met.* **2001,** *124,* 431–434.
[36] Weck, M.; Jackiw, J.; Rossi, R.; Weiss, P.; Grubbs, R. H. *J. Am. Chem. Soc.* **1999,** *121,* 4088–4089.
[37] Kim, N.; Jeon, N.; Choi, I.; Takami, S.; Harada, Y.; Finnie, K.; Girolami, G.; Nuzzo, R.; Whitesides, G. M.; Laibinis, P. *Macromolecules* **2000,** *33,* 2793–2795.
[38] Juang, A.; Scherman, O. A.; Grubbs, R. H.; Lewis, N. S. *Langmuir* **2001,** *17,* 1321–1323.

Chapter 2

Polycyclooctatetraene (Polyacetylene) Produced with a Ruthenium Olefin Metathesis Catalyst

This has previously appeared as: Scherman, O. A. and Grubbs, R. H. *Synthetic Metals* **2001**, *124*, 431–434.

2.1 Abstract

Ring-opening metathesis polymerization (ROMP) of 1,3,5,7-cyclooctatetraene to form poly(COT), which is structurally polyacetylene (PA), has been accomplished using a well-defined ruthenium olefin metathesis catalyst. Physical and spectral properties of poly(COT) films are similar to PA obtained with previously published synthetic methodology.

2.2 Introduction

The area of highly conjugated organic polymers has commanded interest for quite some time. Polyacetylene (PA) is the (structurally) simplest conjugated organic polymer; however, its intractable nature has made its characterization quite difficult. The first successful PA film was produced in 1971 by Shirakawa and Ikeda from acetylene monomer and a highly concentrated Ziegler-Natta catalyst.[1] Over the last thirty years several methods have been introduced which allow for the synthesis of a precursor polymer that can subsequently be transformed into PA.[2, 3] Unfortunately, many of these techniques either involve the extrusion of large molecular fragments that can limit the processing of these polymers or produce very sensitive and even explosive materials.[4] Therefore, a forgiving and direct route to PA and substituted PA, such as ring opening metathesis polymerization (ROMP), which might lead to new substrates and amenable processing conditions is worth pursuing.

The metathesis polymerization of 1,3,5,7-cyclooctatetraene (COT) has been reported previously,[5–7] however the only successful routes to date have focused on early transition metal catalysts (tungsten) which are sensitive to air, moisture, and functional groups. It would be advantageous to use a late transition metal catalyst (ruthenium) which is more tolerant towards air, moisture and functional groups. Unfortunately, the $RuCl_2(=CHPh)(PCy_3)_2$, catalyst **1**, was not able to polymerize COT presumably due to its lower activity. Here we report the ROMP of COT by a highly active well defined ruthenium olefin metathesis catalyst, $RuCl_2(=CHPh)(PCy_3)(IMesH_2)$,

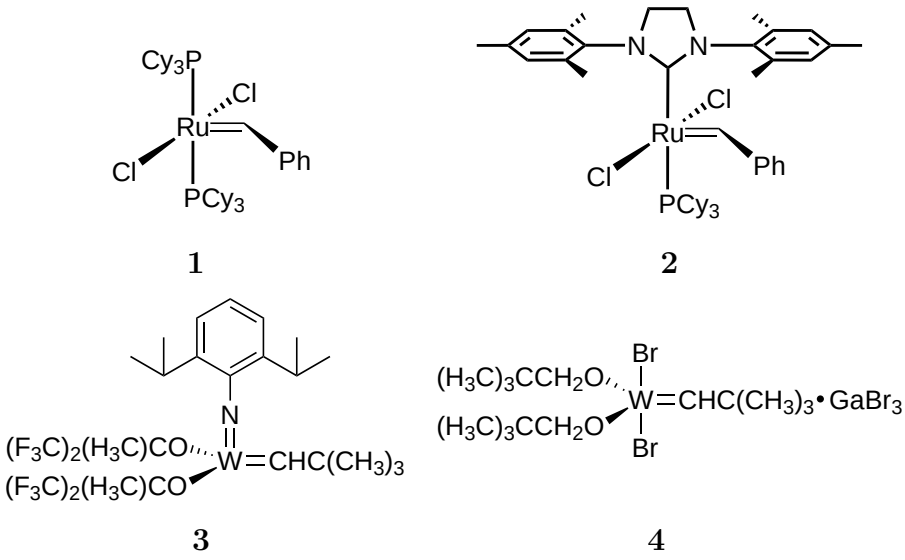

Figure 2.1: Several olefin metathesis active catalysts.

catalyst **2**, to produce films of polyacetylene (PA) with conductivities comparable to those first produced by Shirakawa.

2.3 Results and Discussion

Several years ago the ROMP of COT was reported using early metal tungsten catalysts, catalysts **3** and **4** (Figure 2.1).[6] Late metal metathesis catalysts have been developed in an effort to eliminate the rigorous conditions required by the early transition metal catalysts. Monomers such as norbornene and 1,5-cyclooctadiene which possess high to moderate ring strains of 27.2 kcal/mol[8] and 13.28 kcal/mol,[9] respectively, are well suited to ROMP with catalyst **1**, while COT has only 2.5 kcal/mol[8] ring strain and does not polymerize with **1**. Recently, it was reported that replacement of one of the phosphine ligands on catalyst **1** by a N-heterocyclic carbene ligand dramatically increases the activity of catalyst **2** towards ROMP.[10] Catalyst **2** is effective in the ROMP of COT to produce polyCOT (PA) (Figure 2.2).

Table 2.1 compares the properties of the polyCOT films produced by catalyst **2** to those produced with catalyst **3** and the standard Shirakawa method.[6] The most robust PA films were prepared by using 500 equivalents of COT to catalyst **2**, however up to

Table 2.1: Comparison of polyacetylenes properties produced by different routes and catalysts.

Property	Shirakawa PA	Poly(COT) from catalyst **3**	Poly(COT) from catalyst **2**
appearance	shiny, silver	shiny, silver	shiny, gold[a]
X-ray spacing *d*, Å	3.80-3.85 (*cis*)	3.90±0.05	3.79
σ (undoped)	10^{-5} (*trans*) 10^{-8} (*cis*)	$<10^{-8}$	$<10^{-8}$
σ (doped)	160 (*trans*) 550 (*cis*)	50-350	>25
SS CP-MAS ^{13}C NMR	126-9 ppm (*cis*)	126 (*cis*) 132 (*trans*)	127 (*cis*) 133 (*trans*)
IR major peaks	1015 (*trans*) 740 (*cis*)	930, 980, 765	1010, 992, 773, 745

[a]The shiny, gold appearance of poly(COT) produced from catalyst **2** is most likely due to the high *trans* content of the polymer.

2000 equivalents of COT also produced a film. The robust polyCOT films could be folded without cracking while films produced with higher monomer to catalyst ratios were quite fragile and often exhibited cracking. The undoped films are insulators,[6] however, exposure to iodine increased the conductivity in the range of 10^1 to 10^2 S/cm.

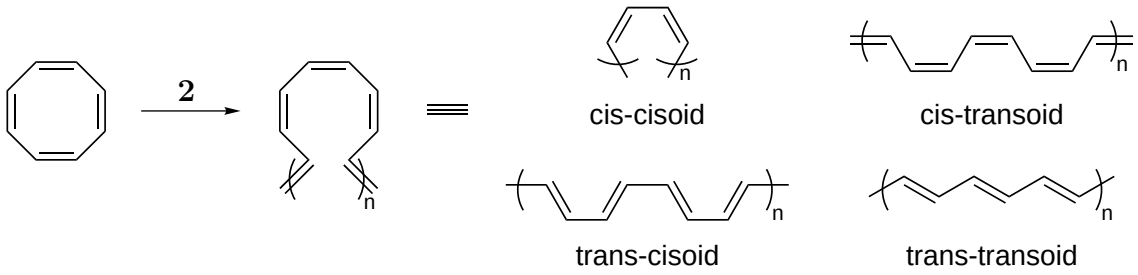

Figure 2.2: ROMP of COT and four isomeric microstructures of PA.

Four major isomeric structures exist for PA (Figure 2.2). The *cis* and *trans* isomers can be observed by solid-state ^{13}C NMR.[11, 12] Previous reports indicate that the thermodynamically favored all *trans* form of PA can be obtained upon heating of the polymer.[11] Catalyst **3** produced polyCOT with two sp^2 carbon types observed by solid-state CP-MAS ^{13}C NMR.[6] Upon heating of the sample, only one peak at 135.9

ppm was observed consistent with large trans-transoid segments in the sample.[6] The polyCOT produced by catalyst **2** also showed two sp^2 carbon types in the same region with shifts of 127 ppm (*cis*) and 133 ppm (*trans*), respectively. Bloch-decay MAS ^{13}C NMR indicates a *cis*:*trans* ratio of approximately 60:40. However, after one week the small amount of catalyst remaining in the solid sample appears active enough to isomerize the polyCOT to the thermodynamic all *trans* form, with a ^{13}C shift of 136 ppm, at room temperature (see Figure 2.3 a and b). This is consistent with previous reports for catalyst **2** to be long-lived and yielding the thermodynamic reaction product.[10*]

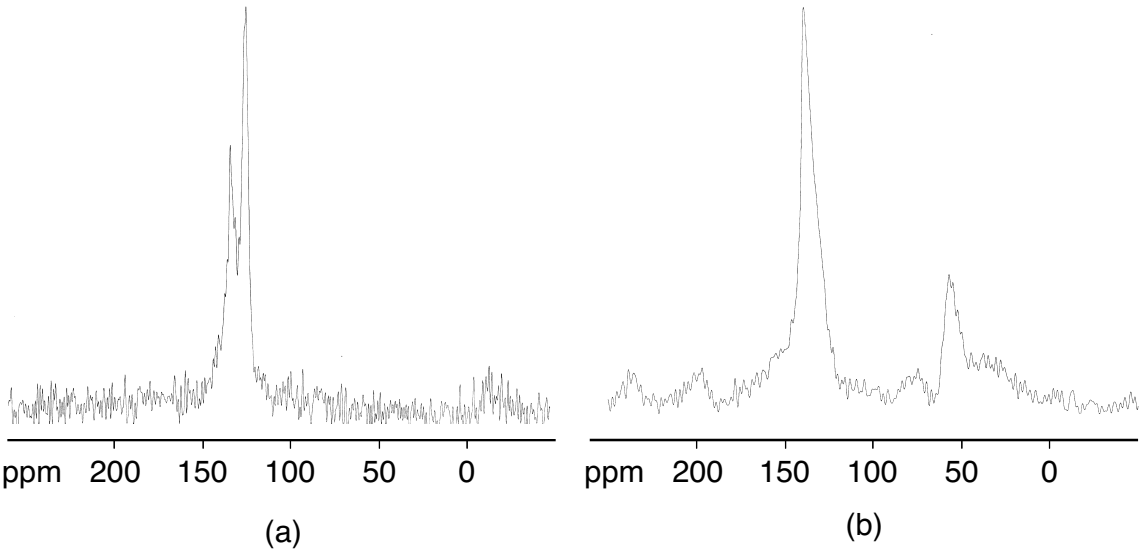

Figure 2.3: Solid-state ^{13}C NMR of poly(COT). (a) Bloch-decay MAS ^{13}C NMR of poly(COT), *cis*:*trans* ratio approximately 60:40. (b) Same sample after 1 week stored in the dark, under a nitrogen atmosphere. A small amount of oxidation is apparent, however, the large peak at ∼50 ppm falls at a spinning side band.

Vibrational spectroscopies also indicate a fair amount of *trans* double bond content in the polyCOT produced from catalyst **2**, as is evident by the large peak at 1010 cm^{-1} in the IR spectrum. As Table 2.1 suggests, the IR peaks observed for polyCOT correspond nicely with Shirakawa PA. Strangely FT-Raman results indicate only *trans* double bonds with a sharp C-C stretch between 1060–1090 cm^{-1} (maximum at 1070 cm^{-1}) and a sharp C=C stretch between 1450–1480 cm^{-1} (maximum at

*The original monomer to catalyst ratio for this sample was 500:1. The sample was kept out of the light and remained in a nitrogen atmosphere dry box for one week between NMR experiments.

1460 cm^{-1}). This lower Raman shift for the C=C stretch is indicative of longer average conjugation length as compared to polyCOT produced by **3** which Klavetter *et al.* observed between 1463–1531 cm^{-1}.[6, 13] FT-IR and solid-state ^{13}C NMR certainly indicate ample *cis* double bond content in the polyCOT while the FT-Raman spectrum is virtually void of *cis* character. While this may be due to selective resonance enhancements that can obscure the *cis* peak around 1250 cm^{-1}, we are unable to definitively say why the *cis* peak is omitted in the raman spectra.[14]

Unlike polyCOT produced with catalyst **3**,[6] scanning electron microscopy (SEM) images of polyCOT produced with catalyst **2** more closely resemble Shirakawa PA. Figure 2.4a illustrates the globular texture of polyCOT produced from **2**, which is similar to Shirakawa PA. It is interesting to note the cracking seen in Figure 2.4b. During the polymerization of COT a film forms on the polymerization substrate and after approximately 30 minutes, it begins to crack until fully dry. We believe that the highly active **2** backbites and extrudes small molecules, i.e., benzene, from the growing polymer chains in a similar fashion as is observed by ROMP of COT with **3**.[6] The cracking may be attributed to the shrinkage of the film during polymerization possibly due to the packing of trans segments in the polymer chains combined with the escaping of volatile small molecules such as benzene. The loss of benzene can also help explain the low yields of solid polyCOT obtained in the polymerization reactions (see general polymerization procedures in experimental section).

The ROMP of COT with catalyst **2** affords a direct synthetic route to PA with a late transition metal catalyst. The properties of polyCOT produced from **2** are nearly identical to PA produced from early transition metal catalysts. The high functional group tolerance exhibited by **2** combined with its high activity should allow for the synthesis of PA and other polyene substrates with controlled molecular weight and end-group functional handles. Furthermore, the processing of these materials will likely become easier as less rigorous techniques are required by the robust catalyst **2**. We are currently investigating the synthesis of telechelic polyenes by previously published methodology.[15]

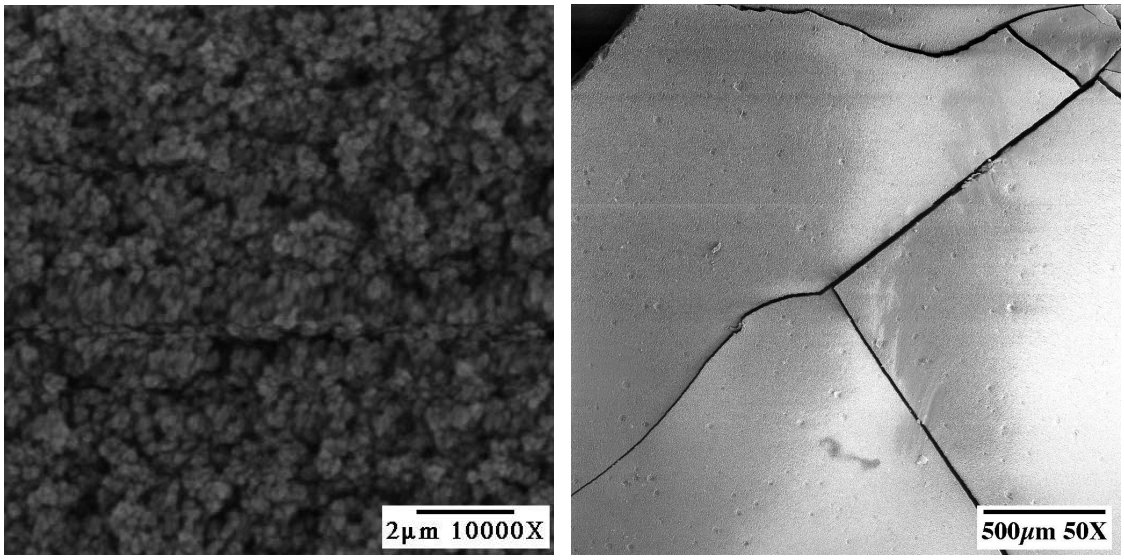

(a) (b)

Figure 2.4: SEM of poly(COT). (a) SEM of poly(COT) made from catalyst **2** magnified 10000x. (b) SEM of the same sample magnified 50x, depicting the cracking some poly(COT) films exhibit.

2.4 Experimental Section

General Procedures. Polymerization reactions were carried out in a nitrogen-filled dry box. COT was filtered through neutral alumina and distilled prior to use (45 °C, 25 mmHg). Purity was confirmed by GC analysis (> 99.9%). Purified COT was stored under argon in a -75 °C freezer. All solvents were passed through purification columns composed of activated alumina (A-2) and supported copper redox catalyst (Q-5 reactant).[16] Polymerization substrates (glass microscope slides and overhead transparencies) were cleaned thoroughly before use. Catalyst **2** was synthesized as previously described.[17] Solid-state CP-MAS ^{13}C NMR experiments were carried out on a Bruker 200 MHz spectrometer. Samples were subjected to magic angle spinning at 8.0 KHz in a high-pressure stream of nitrogen to protect the samples from atmospheric oxidation. FT-IR spectra (KBr pellet) obtained on a Perkin Elmer Paragon 1000. FT-Raman spectra were obtained on a Nicolet Raman 950 in a sample cell modified to hold a sealed NMR tube. Conductivity was measured by the four-point probe method with a Signatone apparatus. Film thickness was measured with

a Mitutoyo electronic micrometer. Doping of PA films by I_2 vapor were carried out in a glass schlenk tube which was evacuated and then closed, the films were allowed to sit under static vacuum for several hours.

Polymerization of COT. In a typical polymerization, approximately 5 mg of catalyst was placed in a 3 mL vial. 0.5 mL of COT (approximately 500 equivalents) was then added to the vial by syringe and the solution was swirled gently. Within 10–30 seconds the yellow solution suddenly turned dark red and subsequently purple. The purplish solution was then transferred to a pre-weighed polymerization substrate by pipet and allowed to polymerize under ambient temperature and pressure. The solution gelled and hardened within minutes yielding a shiny, black film, intractable in common solvents. The film was gently washed with a small amount of methanol to remove any unreacted monomer. The yields in these polymerization reactions ranged from 15-30% based on weight differential of the polymer substrate before and after deposition of the polyCOT.

References Cited

[1] Shirakawa, H.; Ikeda, S. *Polym. J. (Tokyo)* **1971,** *2,* 231.
[2] Edwards, J. H.; Feast, W. J. *Polymer* **1980,** *21,* 595–596.
[3] Swager, T. M.; Dougherty, D. A.; Grubbs, R. H. *J. Am. Chem. Soc.* **1988,** *110,* 2973–2974.
[4] Swager, T. M.; Grubbs, R. H. *J. Am. Chem. Soc.* **1989,** *111,* 4413–4422.
[5] Korshak, Y. V.; Korshak, V. V.; Kanischka, G.; Hocker, H. *Makromol. Chem., Rapid Commun.* **1985,** *6,* 685–692.
[6] Klavetter, F. L.; Grubbs, R. H. *J. Am. Chem. Soc.* **1988,** *110,* 7807–7813.
[7] Klavetter, F. L.; Grubbs, R. H. *Synth. Met.* **1989,** *28,* D99–D104.
[8] Schleyer, P. v. R.; Williams, J. E.; Blanchard, K. R. *J. Am. Chem. Soc.* **1970,** *92,* 2377–2386.
[9] Allinger, N. L.; Sprague, J. T. *J. Am. Chem. Soc.* **1972,** *94,* 5734–5747.
[10] Bielawski, C. W.; Grubbs, R. H. *Angew. Chem., Int. Ed.* **2000,** *39,* 2903–2906.
[11] Terao, T.; Maeda, S.; Yamabe, T.; Akagi, K.; Shirakawa, H. *Chem. Phys. Lett.* **1984,** *103,* 347–351.
[12] Maricq, M. M.; Waugh, J. S.; MacDiarmid, A. G.; Shirakawa, H.; Heeger, A. J. *J. Am. Chem. Soc.* **1978,** *100,* 7729–7730.
[13] Shibahara, S.; Yamane, M.; Ishikawa, K.; Takezoe, H. *Macromolecules* **1998,** *31,* 3756–3758.
[14] Kuzmany, H. *Phys. Stat. Sol.* **1980,** *97,* 521–531.
[15] Bielawski, C. W.; Scherman, O. A.; Grubbs, R. H. *Polymer* **2001,** *42,* 4939–4945.
[16] Pangborn, A. B.; Giardello, M. A.; Grubbs, R. H.; Rosen, R. K.; Timmers, F. J. *Organometallics* **1996,** *15,* 1518–1520.
[17] Scholl, M.; Ding, S.; Lee, C. W.; Grubbs, R. H. *Org. Lett.* **1999,** *1,* 953–956.

Chapter 3

Direct Synthesis of Soluble, End-Functionalized Polyenes and Polyacetylene Block-Copolymers

This has previously appeared as: Scherman, O. A.; Rutenberg, I. M.; Grubbs, R. H. *Journal of the American Chemical Society*, **2003**, *125*, 8515–8522.

3.1 Abstract

The ring-opening metathesis polymerization (ROMP) of 1,3,5,7-cyclooctatetraene (COT) in the presence of a chain transfer agent (CTA) with a highly active ruthenium olefin metathesis catalyst resulted in the formation of soluble polyenes. Small molecule CTAs containing an internal olefin and a variety of functional groups resulted in soluble telechelic polyenes with up to 20 double bonds. Use of polymeric CTAs with an olefin terminus resulted in polyacetylene block copolymers. These materials were subjected to a variety of solution and solid phase characterization techniques including ^{1}H NMR, UV/vis, and FT-IR spectroscopies, as well as MALDI-TOF MS and AFM.

3.2 Introduction

Intrinsically conducting polymers (ICP)s are of great interest due to their potential use in a wide variety of applications such as polymer light-emitting diodes (PLED)s, electrostatic dissipation (ESD) materials, and charge storage devices. As a consequence of their rigidity, most ICPs are insoluble materials, preventing thorough characterization and thereby slowing the development of this field. Moreover, the inherent instability of ICPs and associated processing difficulties create a large barrier for commercialization. In an effort to overcome these obstacles, the development of a practical synthesis of relatively stable and soluble conducting polymers with a controlled architecture is important.

The field of conducting polymers was founded upon the discovery of polyacetylene (PA), the simplest ICP, in the 1970s.[1–5] There have since been numerous accounts on the synthesis of PA including the Ziegler-Natta polymerization of acetylene,[6] the synthesis of precursor polymers followed by thermal evolution of a small molecule,[7, 8] and the ring-opening metathesis polymerization (ROMP) of 1,3,5,7-cyclooctatetraene (COT).[9–12] Despite these developments, applications of PA remain particularly elusive. Unlike PA, however, three decades of research involving other

ICPs such as polyaniline, poly(1,4-phenylenevinylene) (PPV), polypyrrole (PPy), and polythiopene (PTh) has resulted in their commercialization in applications such as anti-fouling coatings[13] and electrodes in batteries and capacitors.[14]

Since most ICPs are completely insoluble in organic solvents, several strategies have been employed to address this problem. One common approach is to add substitution along the polymer backbone thereby disturbing alignment between polymer chains and allowing for the penetration of solvating molecules. This approach has worked well for improving the solubilities of PPV and PTh in the forms of poly[2-(2-ethylhexyloxy)-5-methoxy-1,4-phenylenevinylene](MEH-PPV),[15] ester-substituted PPVs,[16] and poly(3-alkylthiophene).[17] While the materials' solubilities are greatly enhanced, they also maintain a suitable level of conductivity; unfortunately, this strategy is not amenable to PA. Both alkyl- and aryl-acetylene (R-acetylenes) derivatives have been polymerized to produce the corresponding soluble poly(R-acetylene)s. Although the disorder stemming from the substituents aids in solubilizing the R-PA, it simultaneously disrupts the π-conjugation along the polymer backbone. As a result, these materials exhibit substantially decreased conductivities in comparison to the parent PA.

Another synthetic method used to solubilize ICPs is to produce copolymers by introducing a second monomer with good solubility properties. Typically, in order to keep the conductive characteristics of the ICP, block copolymers are necessary. PA block copolymers have been previously synthesized via two approaches. In the first approach, using sequential addition of monomers, a soluble PA-precursor polymer such as poly(phenyl vinyl sulfoxide) is prepared as one of the blocks.[18] Upon heating, an elimination reaction converts the precursor polymer to PA. This method has been adapted both to anionic polymerization and, through the Durham route, to ROMP.[7] The second approach involves sequential addition copolymerization of COT and another ROMP-active monomer.[19] In both approaches, however, block copolymer composition is limited because both monomers must be polymerizable by the same method.

As many of the desirable characteristics of ICPs and PA are realized with a rela-

tively small number of repeat units, several groups have endeavored to produce soluble polyenes with up to 20 double bonds.[20, 21] Furthermore, the areas of natural product synthesis[22] and network polymer formation[23] would benefit if functional end groups were built into these soluble polyenes. It has been demonstrated that heating of a ROMP polymer, prepared from a Durham precursor monomer using highly active molybdenum and tungsten olefin metathesis catalysts, leads to polyenes with alkyl end groups.[19, 21, 24, 25] For polyenes with less than 16 double bonds, these alkyl groups enhance solubility and allow for more detailed characterization.[20] One drawback to producing polyenes via the Durham route is the need for a subsequent deprotection step.

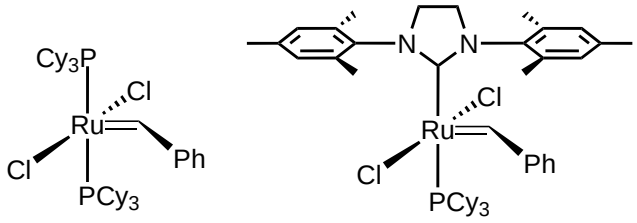

1 **2**

Figure 3.1: Ruthenium olefin metathesis catalysts.

Recently, we reported the direct synthesis of PA via the ROMP of COT with the highly active ruthenium catalyst **2**.[12] This reaction is not possible with the less active catalyst **1** as the ring strain of COT (2.5 kcal/mol) is extremely low.[26] Catalyst **2** has also been shown to form telechelic polymers with a variety of functional end groups when utilized in conjunction with a chain transfer agent (CTA).[27–29] Building upon this work, we report herein a method of forming telechelic polyenes by the ROMP of COT in the presence of a CTA. Furthermore, these polyenes are soluble in common organic solvents allowing for extensive solution-phase characterization. We also describe here the ROMP of COT in the presence of an olefin-terminated polymer, which allows PA block copolymers to be formed with a variety of commodity polymers such as polystyrene (PS), poly(methyl methacrylate) (PMMA), and poly(ethylene glycol) (PEG). Indeed, nearly any monomer that is polymerizable by living anionic or controlled radical techniques can be used as the solubilizing block. Furthermore, no elim-

ination step is necessary in forming the PA block, thus reducing synthetic complexity and material waste. Since the ROMP of COT forms PA directly without the need for deprotection steps,[11, 12] and olefin-terminated polymers are commercially available, this represents the first one-step synthesis of PA-containing block copolymers from commercially available materials.

3.3 Results and Discussion

3.3.1 Synthesis of Soluble Polyenes

We recently published a report detailing the ROMP of COT (**3**) to form PA with catalyst **2** (Equation 1).[12] The characteristics of the PA produced by **2** proved to

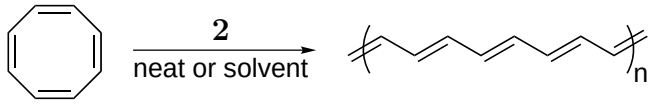

3 **4** **(1)**

be very similar to PA produced by previous synthetic routes.[12] Unfortunately, the characteristic insolubility of PA was also observed. The functional group tolerance of catalyst **2**, however, suggests the possibility of placing solubilizing functional groups at the chain ends by utilizing a chain transfer agent (CTA). It has been previously shown that the use of a CTA with **2** can produce telechelic oligomers and polymers from CTAs containing functional groups such as alcohols, halides, and esters.[27, 28] The same strategy can now be applied for the direct formation of telechelic PA. Furthermore, if the PA chain length can be controlled by this method, it would provide for the direct formation of soluble polyenes as outlined in Equation 2.

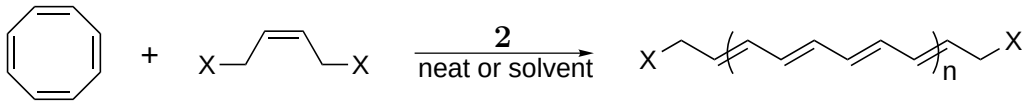

3 **5** **6** **(2)**

The synthesis of telechelic PA was successfully carried out both neat and in solution via the ROMP of COT with a CTA using catalyst **2** (see Table 3.1). Upon

Table 3.1: Effects of Monomer/CTA and Monomer/Catalyst Ratio on Yield of Polyenes

Entry	CTA	[COT]/ [CTA]	[COT]/[**2**]	% yield
1[a]	**5a**	1	500	76
2[a]	**5a**	2	500	83
3[b]	**5a**	1	540	78
4[b]	**5a**	2	480	69
5[b]	**5a**	3	520	49
6[b]	**5a**	1	980	40
7[b]	**5a**	3	1050	9
8[c]	**5b**	2	490	5
9[c]	**5b**	4	490	18
10[d]	**5c**	4	800	12
11[a]	**5d**	1	5000	0
12[e]	**5e**	1	500	0

[a]Reaction carried out in 1 mL of CH_2Cl_2. [b]Reaction carried out neat. [c]Reaction carried out in 1 mL of toluene. [d]Reaction carried out in 3 mL of toluene. [e]Reaction carried out in 1 mL of THF.

addition of **2**, the yellow COT solution turned light orange and then became progressively darker over the next 5 min depending on the ratio of COT to CTA. After 24 h, only a small amount of solid was observed to precipitate on the container walls. This result was visibly different from the large amount of solid (metallic in appearance) produced when a CTA was omitted from the reaction. After isolation, the resulting polymer was completely soluble in common organic solvents, enabling characterization by ^{1}H NMR, UV-vis, and FT-IR spectroscopies, as well as MALDI-TOF MS.

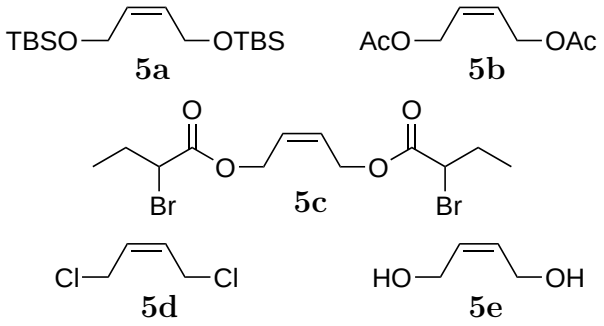

Figure 3.2: CTAs **5a**–**e**.

Attempts to use CTAs such as **5d** and **5e** were not successful (Figure 3.2). While no solids precipitated during the ROMP of COT with CTA **5d**, ^{1}H NMR spectroscopy of the crude reaction mixture showed very little polyene and no material could be isolated (entry 11). Immiscibility of COT and **5e** prevented neat polymerization and required solvents such as THF for ROMP in solution. Unfortunately, THF has been shown to dramatically decrease the rate of ROMP,[11] and no desired polyene product was observed in the ^{1}H NMR spectrum of the crude reaction mixture (entry 12).

As a consequence of the loss of material at each stage of preparation, obtaining the polyenes in high yield was somewhat difficult. Some polyene product was simply lost upon repetitive centrifuge/decant/wash cycles, while shorter polyene chains were most likely soluble in the MeOH washes. Entries 1 and 2 in Table 3.1 show that for ROMP carried out in solution, increasing the amount of COT relative to CTA **5a** has a very minimal effect on the yield of polyene **6a**. When the corresponding reactions are carried out neat (entries 3-5, Table 3.1), a decrease in yield of **6a** is observed with a decrease in the amount of CTA **5a**. This trend is likely due to insoluble PA chains precipitating out of solution when too few chain transfer groups are present to attenuate the molecular weight. When the amount of COT relative to catalyst **2** is increased to 1000:1 (entries 6 and 7, Table 3.1), the yields decrease substantially. This observation is likely due to the incomplete initiation of catalyst **2**[30] which would result in a "true" monomer to catalyst ratio far in excess of 1000. Finally, although it does not lead to chain termination, backbiting of catalyst **2** onto the growing polyene chain has previously been shown to eliminate benzene.[12] As benzene is not metathesis active, backbiting essentially removes monomer from the reaction.

3.3.1.1 Characterization of Soluble Polyenes

The loss of monomer over the course of the reaction because of backbiting also evidently hinders our attempt to control the molecular weight of the polyenes by adjusting the ratio of COT to CTA. Previous reports of ROMP reactions with catalyst **2** and a CTA have shown that molecular weight is dictated by the ratio of [monomer]:[CTA]if the reaction is allowed to reach thermodynamic equilibrium.[27, 28, 31] This result was

not found to be the case for COT. While accurate molecular weights and distributions could not be obtained for the polyenes, ^{1}H NMR spectroscopy as well as MALDI-TOF MS data indicated average chain lengths of around 10–13 double bonds for all reactions and did not vary with the ratio of COT:CTA. The average chain length of the isolated polyenes, however, may be misleading. When a higher COT to CTA ratio is employed, more polyene chains reach lengths that render them insoluble. For lower ratios, shorter, MeOH-soluble polyene chains are favored. As a result of likely fractionation of smaller and longer chains during workup, regardless of the starting COT to CTA ratio, the isolated polyene chains are heavily weighted to an average of 10–13 double bonds. Of course, the backbiting of **2** might be attenuated by decreasing the reaction temperature; however, if the polymerization of COT occurred without significant backbiting with a CTA molecule, an insoluble PA chain would result. Hence, in the direct synthesis of polyenes **6** with catalyst **2**, the ability to control molecular weight is limited.

The solution phase ^{1}H NMR spectrum of polyene **6a** (Figure 3.3) clearly shows signals corresponding to the backbone protons of the telechelic polyene between δ=6–7 ppm, which are characteristically shifted downfield due to the highly conjugated segment of olefins. The allylic CH_2 protons give rise to peaks around δ=4.2 ppm and the *tert*-butyl and methyl protons of the silane protecting group (from CTA **5a**) correspond to singlets at δ=0.9 and 0.05 ppm, respectively. The absense of a singlet at δ=5.79 ppm suggests that all of the unreacted COT was successfully removed from the polyene product. Integration of the methylene and polyene backbone peaks suggests an average of 10 double bonds for the sample, which is consistent with the MALDI-TOF MS data presented below.

Previous reports have provided very detailed UV-vis spectroscopy data on soluble polyenes containing up to 15 double bonds.[20, 21] As the number of conjugated double bonds increases, the absorption shifts to longer wavelengths and some detail of the higher energy transitions is lost. UV-Vis spectroscopy was carried out on polyene **6a** in both THF and CH_2Cl_2. Figure 3.4 shows the UV-vis spectrum in CH_2Cl_2 with 4 distinct transitions between 355 and 450 nm and a smooth absorption profile

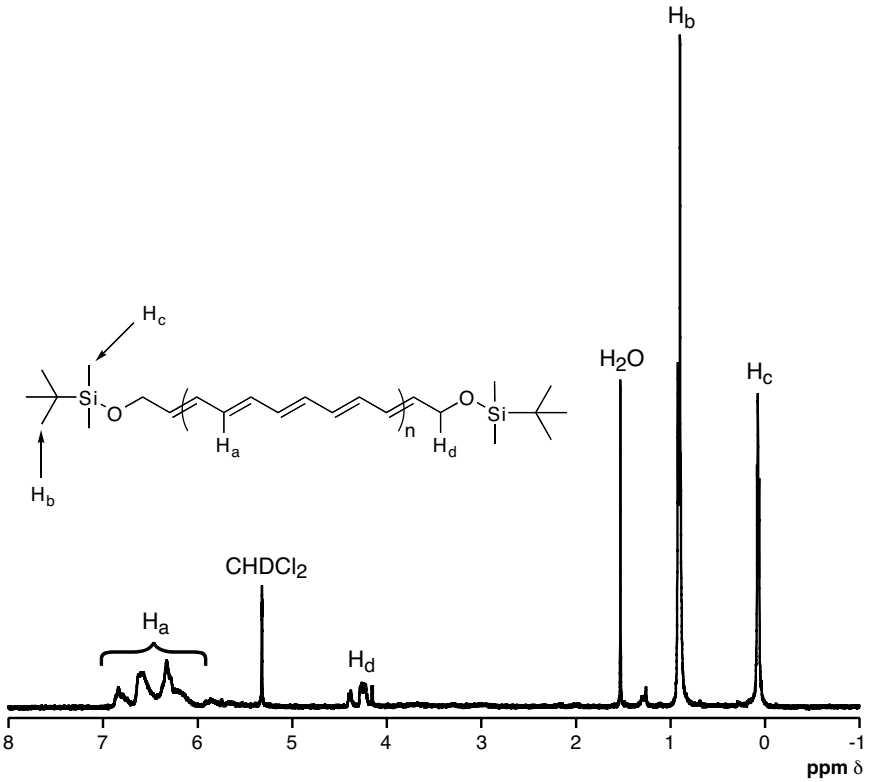

Figure 3.3: ^{1}H NMR spectrum of telechelic polyene **6a** in CD_2Cl_2.

extending past 500 nm. These transitions are consistent with a polyene composed of 10 to 20 double bonds.[20]

Infrared spectroscopy was also carried out on telechelic polyenes **6a** and **6b**. Figure 3.5 displays the FT-IR spectra for both telechelic polyenes. The bands at 745, 773, and 1011 cm^{-1} are visible in both polyene spectra and are conserved from the IR spectrum of poly(COT).[12] The peak at 743 cm^{-1} can be attributed to the *cis* C-H out-of-plane vibrational mode while the peak 1011 cm^{-1} is due to the *trans* C-H mode.[32] The presence of a much larger *trans* peak at 1011 cm^{-1} supports the mechanism of *trans*-selective catalyst **2** backbiting into the polymer chain to attach the endgroups and form telechelic polymers or to simply isomerize *cis* olefins to their *trans* counterparts.

Finally, mass spectrometry was carried out on the telechelic polyenes. Figure 3.6 shows the MALDI-TOF spectrum for **6a** acquired from a dithranol matrix. The first labeled peak with a mass of 628.9 Da corresponds exactly to telechelic polyene **6a**

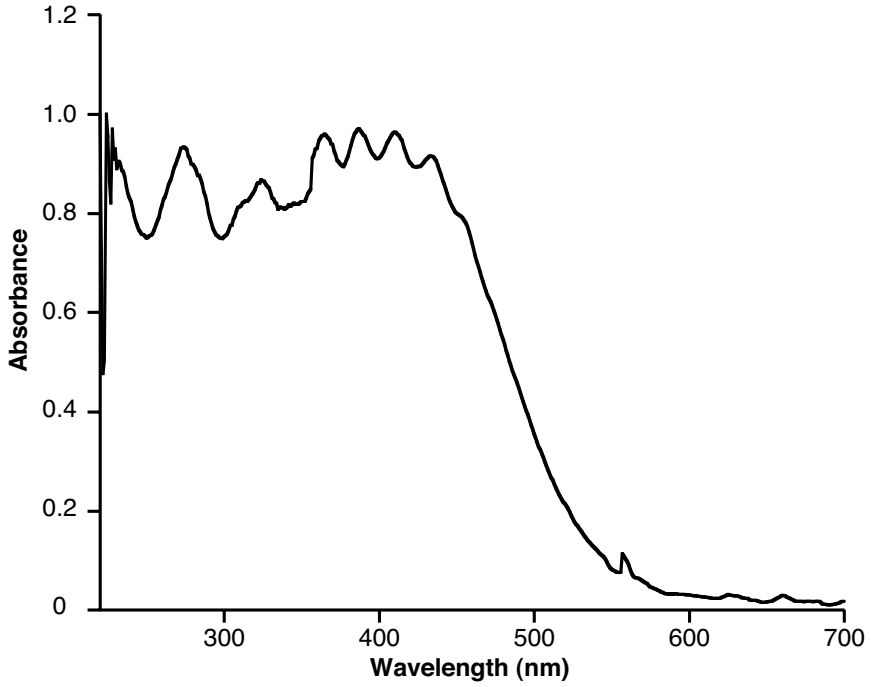

Figure 3.4: UV-Vis spectrum of telechelic polyene **6a** in CH_2Cl_2.

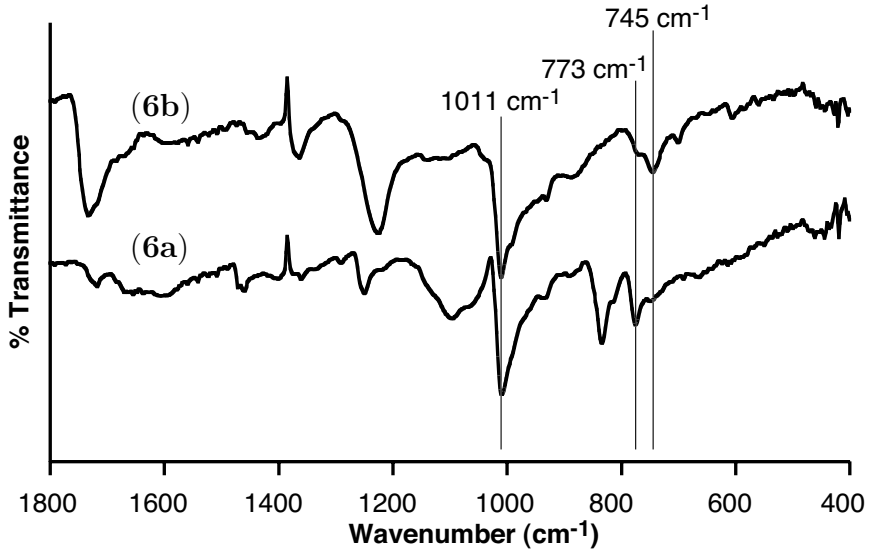

Figure 3.5: FT-IR % transmittance spectra of polyenes **6a** and **6b** in KBr pellets.

with 13 double bonds. There is a difference of 26.0 amu between each peak in the series corresponding to a C_2H_2 unit. The series is easily visible out to a mass peak of 811.0 amu, corresponding to a species with 20 double bonds. Furthermore, no other series with 26.0 amu mass differences are observed suggesting that all of the polyene

chains are capped at *both* ends.

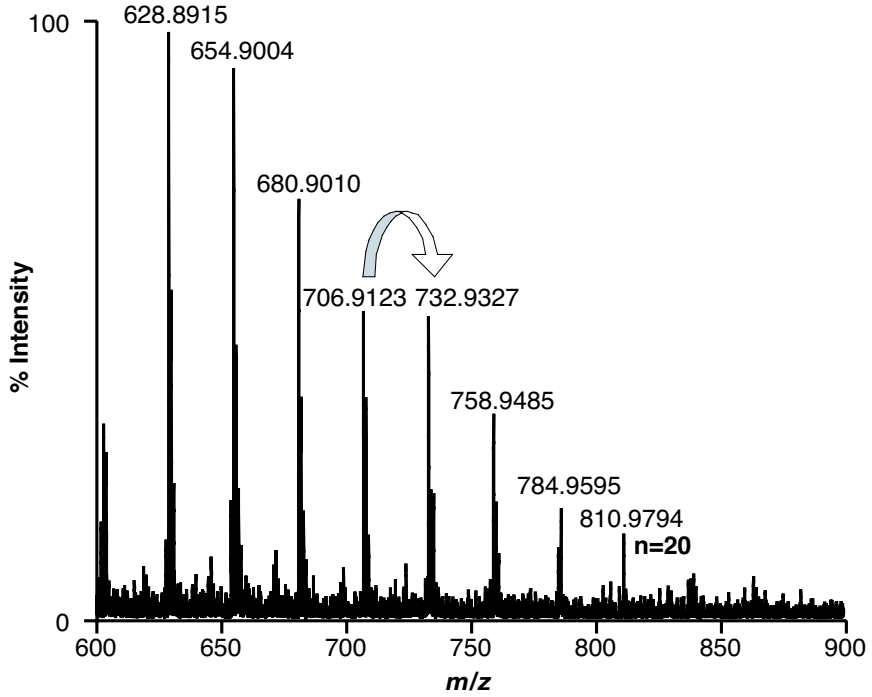

Figure 3.6: MALDI-TOF MS of polyene **6a** ionized from a dithranol matrix.

These data provide evidence for the formation of a telechelic polyene with the CTA functionality successfully placed onto both ends of each polyene chain. It also shows that catalyst **2** is capable of backbiting into a growing polyene chain in order to mediate chain transfer. Furthermore, the materials produced are completely soluble in common organic solvents and allow for much more detailed characterization of polyenes. These results encouraged us to further explore the use of CTAs as a method for producing soluble and processable PA-based materials. We anticipated difficulties, however, using telechelic PA as macroinitiators (e.g. entry 10, Table 3.1). An alternative route to PA block copolymers was therefore sought.

3.3.2 Synthesis of PA-containing Block Copolymers

CTAs containing terminal olefins have been previously used with catalyst **2** to form mixtures of monofunctionalized and difunctionalized (i.e., telechelic) polymers.[28] Furthermore, only difunctional materials result when a large excess of a CTA containing

an internal olefin is used. Extending this concept, olefin-terminated *polymers* were found to control the ROMP of COT by forming block copolymers containing PA as one of the blocks (see Equation 3). As in the case with small molecule CTAs, a polymer with an olefin in the middle of the chain should lead exclusively to triblock copolymers containing PA as the middle block. We are currently investigating this possibility, but due to difficutlties in obtaining *absolutely* pure polymers containing an internal olefin, we have limited this report to include only end-functionalized polymers.

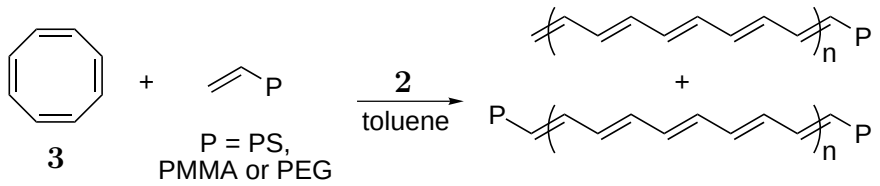

(3)

The use of olefin-terminated polymers as CTAs allows for a wide variety of block copolymer compositions, as polymers containing olefin endgroups can be prepared using numerous techniques.[33–36] Atom transfer radical polymerization (ATRP) was chosen for this work principally for its synthetic ease. Recent advances in ATRP allow these reactions to be performed without the exclusion of oxygen, and with monomers that have not been rigorously purified.[37] Allyl bromide and 5-bromo-1-pentene were convenient ATRP initiators for forming PMMA and PS functionalized with a terminal olefin.[34] ^{1}H NMR spectroscopic and MALDI-TOF MS analysis of the polymers confirmed the presence of olefin endgroups, and molecular weights were determined by GPC and NMR. As with previous reports in the literature, mass spectral analysis showed that the halogen endgroups were replaced by hydrogen atoms for many of the polymer chains after long polymerization times.[38, 39] Since ruthenium-based catalysts have been shown to successfully catalyze ATRP,[40] however, the loss of the halogen endgroup was considered advantageous, reducing the possibility of unwanted side reactions during the subsequent ROMP step. Indeed, no reaction was observed when the olefin-terminated polymer was subjected to ATRP conditions in the presence of COT.

Formation of PA block copolymers was accomplished via the ROMP of COT in the

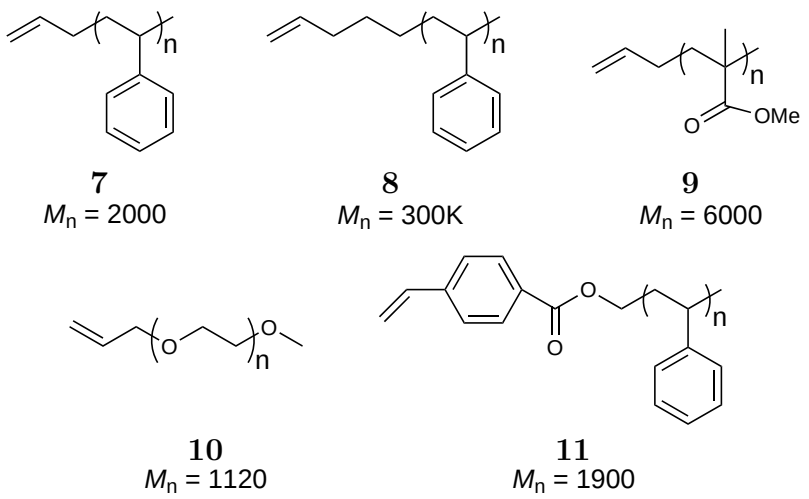

Figure 3.7: Olefin-terminated polymers.

presence of olefin-terminated polymers **7**–**11**.[41] Typically, the amount of solvent was adjusted to ensure an initial monomer concentration, $[COT]_0$, of approximately 0.2 M. When large amounts of olefin-terminated polymer were used, however, additional solvent was added to ensure complete dissolution. Monomer-to-catalyst ratios were typically maintained at 1000:1, although ratios of up to 21000:1 were found to be viable. After completely dissolving the olefin-terminated polymers in toluene, COT was added, followed by the catalyst (either in solid form or from a stock solution). Within minutes, a color appeared that varied depending on the relative proportions of COT and olefin-terminated polymer, as well as the molecular weight of the latter. For low proportions of COT, the color of the reaction was light orange, while for medium proportions it was deep orange or red and for high proportions it was deep red or black. This color was maintained throughout the reaction. Isolation of the block copolymer product was accomplished by precipitation in a non-solvent for the olefin-terminated polymer such as MeOH or hexanes. Table 3.2 shows the colors of the final polymer products from various reactions. A solution of product polymer, when left on the benchtop, became clear over the period of many weeks, indicating eventual decomposition of the conjugated structure. However, the solid polymers maintain their color for months if protected from light and oxygen.

For most block copolymer compositions, solubility of the final product was iden-

Table 3.2: Variation in composition of PA block copolymers.

CTA	[COT]/[CTA]	[COT]/[**2**]	product color	% yield[a]	polymer[b]
7	4	900	orange	18	**7a**
7	20	4000	dark rust	26	**7b**
7	100	21000	brown/black	13	**7c**[c]
8	200	800	dark grey	82	**8a**[d]
8	1000	4000	faded black	71	**8b**
9	2	1000	light orange	44	**9a**[d]
9	5	1000	orange	20	**9b**
9	20	1000	deep red	58	**9c**
9	40	1000	black	52	**9d**
10	1	500	dark red	62	**10a**
10	4	1600	brown/black	39	**10b**
10	7	1400	brown/black	28	**10c**
10	20	4000	brown/black	22	**10d**
11	20	4000	brown	36	**11a**

[a]Calculated based on total mass of reactants and recovered product. [b]All reactions were carried out in toluene with $[COT]_0$=0.2 M unless otherwise noted. [c]$[COT]_0$=1.1 M. [d]$[COT]_0$=0.03 M.

tical to that of the olefin-terminated polymer. All of the entries in Table 3.2 yielded completely soluble block copolymers. When very large amounts of COT were used in conjunction with a low molecular weight non-conjugated block (for example, samples **7c**, **9d** and **10d**), some solid product was deposited on the walls of the reaction flask. This material was redissolved upon sonication, indicating that the solubilizing effect of the nonconjugated block is sufficient to keep the block copolymers soluble, even in cases where significant crystallization of the PA blocks is possible.

Yields of the block copolymer products varied widely depending on the proportions of COT and olefin-terminated polymer, as well as the molecular weight of the latter (see Table 3.2). Yields exceeded 80% when higher molecular weight olefin-terminated polymers were used, or if lower proportions of COT were used. As the proportion of COT was increased, however, a corresponding increase in the ratio of [COT]/[**2**] led to decreased yields (see, for example, sample **7c**). Thus, as described for small molecule CTAs, the generally low yields reported in Table 3.2 are likely due to incomplete incorporation of COT. This observation is further supported by the ^{1}H NMR spectra of the block copolymers (vida infra).

3.3.2.1 Characterization of Block Copolymers

Characterization of the block copolymers by UV-vis spectroscopy provided the clearest evidence for the presence of extended PA blocks. Figure 3.8 shows the UV spectra for three types of block copolymers—PS-*b*-PA, PMMA-*b*-PA, and PEG-*b*-PA. For comparison, the absorption spectra of the homopolymers (i.e., the olefin-terminated polymer) are also shown. The absorbance bands previously seen for polyenes containing 10–15 double bonds[20] were observed in block copolymers made from small amounts of COT (e.g., sample **9a**). These details are lost, however, when larger amounts of COT are used. The smooth spectra that result indicate the presence of a wide range of conjugation lengths. In addition, as the proportion of COT is increased, the absorption region corresponding to the PA block shifts to longer wavelengths, while the absorption due to the nonconjugated block remains unchanged. These data indicate that increasing the amount of COT in the reaction produces PA blocks with longer conjugation lengths.

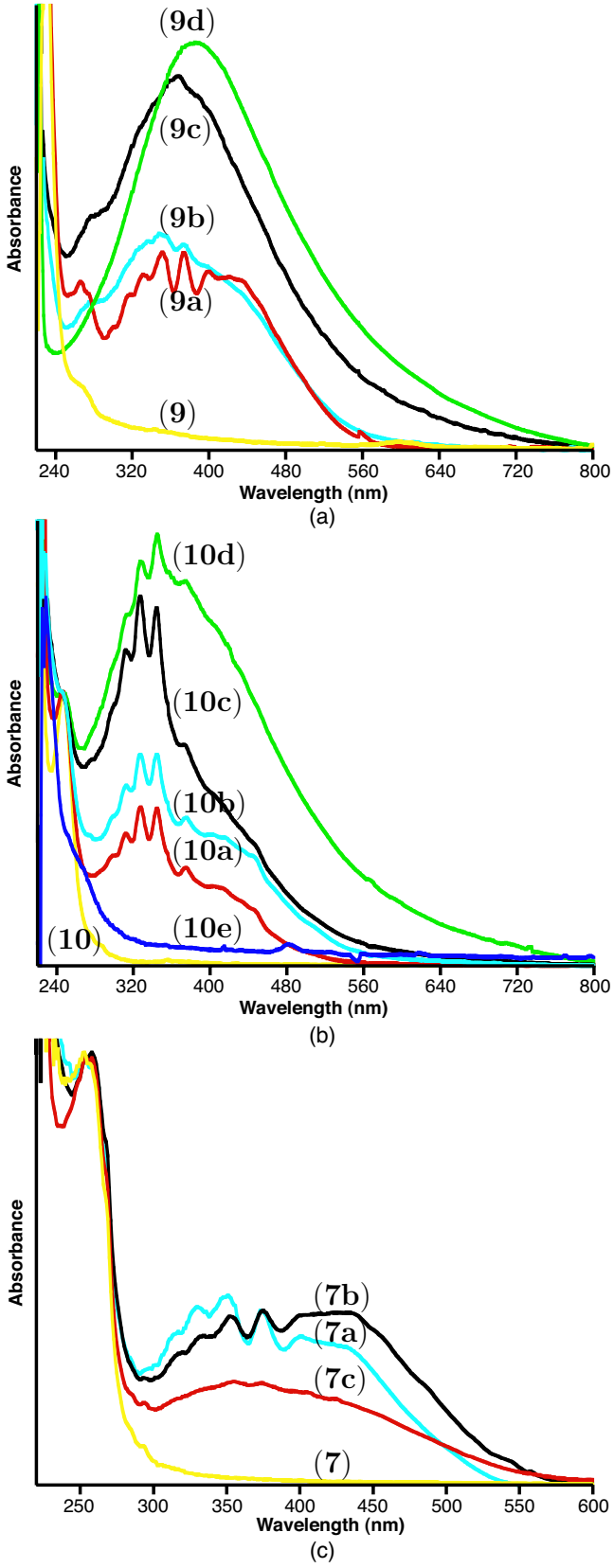

Figure 3.8: UV-vis spectra of PA-containing block copolymers in CH_2Cl_2 solution. (a) PMMA (**9**), PMMA-*b*-PA (**9a–d**). (b) PEG (**10**), PEG-*b*-PA (**10a–d**), bis(hydroxy)-terminated PEG reaction product (**10e**). (c) PS (**7**), PS-*b*-PA (**7a–c**).

To show that PA is covalently attached to the olefin terminated polymers in these reactions, the ROMP of COT was carried out in the presence of a bis(hydroxy)-teminated PEG. A significant amount of insoluble, black solid formed during the reaction. This solid was removed by filtration, and the remaining polymer product (white) was isolated by precipitation. The UV-vis spectrum of the resulting polymer is shown in Figure 3.8b (sample **10e**). The lack of absorbance above 320 nm indicates that no PA was present in the product.

Characteristic IR absorption bands of polyCOT produced with catalyst **2** include 1010, 992, 930, 773, and 745 cm^{-1}.[12] Unfortunately, absorption from the nonconjugated polymer segments often obscured these absorption bands in the PA block copolymers. For PMMA-*b*-PA, however, absorption of the PA segment at 1012 cm^{-1} is clearly visible and overlays with the absorption spectra of the olefin-terminated homopolymer (see Figure 3.9).

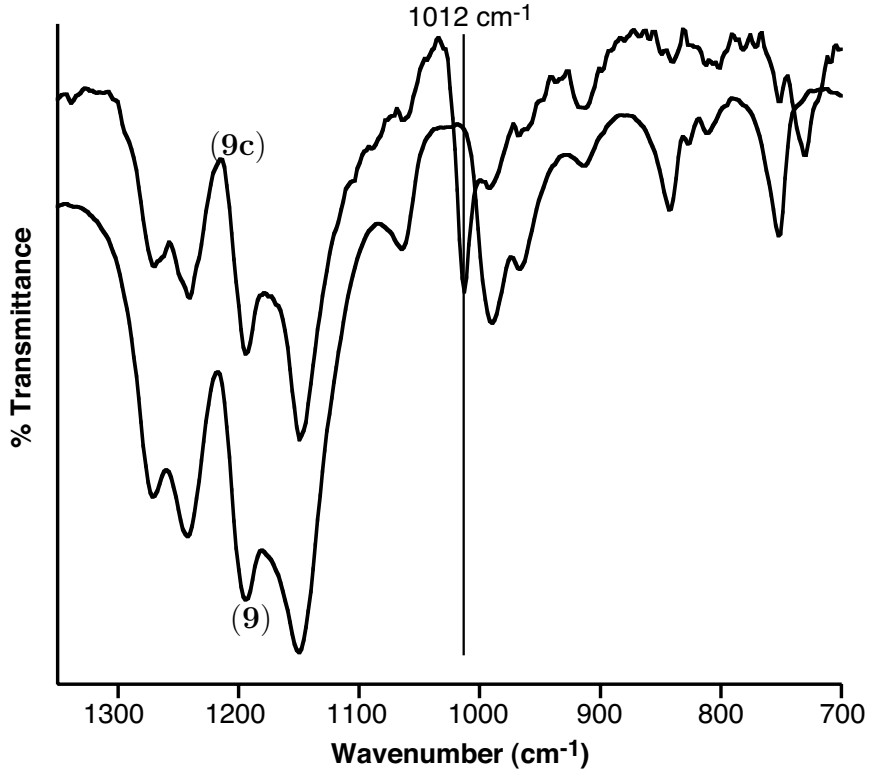

Figure 3.9: FT-IR spectra of **9** and **9c**.

For samples of PMMA-*b*-PA and PEG-*b*-PA, it was possible to observe characteristic peaks in the polyene region of the ^{1}H NMR spectra that appeared very similar to the peaks shown in Figure 3.3.[42] In general, integration of the polyene region indicated far smaller PA blocks than would be expected from the ratio of COT to olefin-terminated polymer. For example, integration for sample **9b** showed an average of four or fewer (–C=C–) units per polymer chain, whereas 20 (–C=C–) units would be expected from the initial reactant ratio. As discussed previously, this low incorporation can be attributed to two likely sources: the ROMP of COT does not reach completion, and/or benzene formed from backbiting leads to an effective loss of monomer. In all NMR spectra, however, a significant amount of unreacted olefin endgroups remained visible after block copolymer formation, indicating that some polymer chains have no attached PA blocks. This observation makes it very difficult to speculate on the average conjugation length of the PA blocks.

Along with the trends observed in UV-vis spectra, AFM afforded a method for observing changes in the relative sizes of conjugated segments between samples. Phase separation in PA-containing block copolymers has been observed previously.[19, 43–45] Tapping Mode (TM) AFM images of PS-*b*-PA films show a phase separated morphology consisting of isolated domains against a uniform background. These domains, which were absent in films formed from the olefin-terminated homopolymer, were randomly distributed in space, but fairly regular in size and shape. Furthermore, the sizes of the domains exhibited a dependency on the relative proportions of COT and olefin-terminated polymer used in the preparation of the block copolymers. Figure 3.10 shows TM AFM height images of films made by spin coating 0.4 wt% toluene solutions of **8a** and **8b**. Clearly, the domains (appearing as white spots) are larger for **8b** which contains a greater percentage of conjugated material, implying that the white spots in Figure 3.10 represent PA domains. As shown by the side views of these images (Figure 3.10b and d), the domains appear to be directed perpendicular to the film surface. These domains are highly stable: annealing the polymer films under vacuum at 130 °C for 24+ hours only reduced their height and spatial density. Furthermore, the domains could also be observed using contact mode.[46] We

believe that these images, the UV spectra of the two copolymers, and the fact that the solution of **8b** was darker in color than that of **8a** are evidence for a variation in the conjugation length of the PA blocks that relates to the relative amount of COT used in the polymerizations. It should be reiterated, however, that these polymers remained completely soluble in common organic solvents.

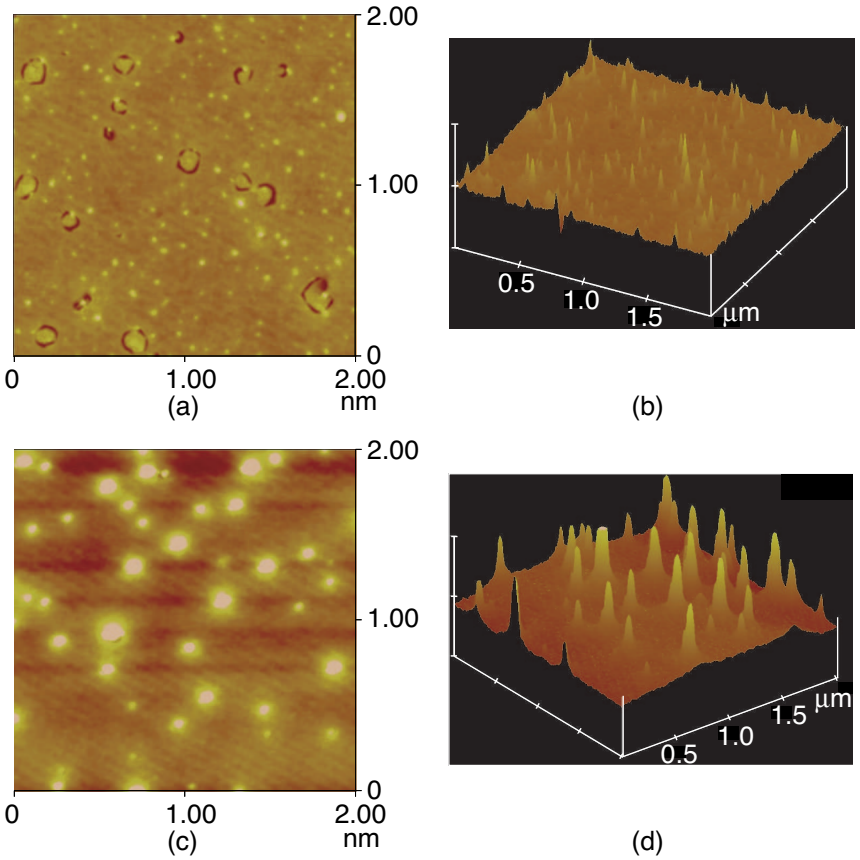

Figure 3.10: TM AFM height images. (a, b) Sample **8a**, produced from **8** and 200 equivalents of COT. (c, d) Sample **8b**, produced from **8** and 1000 equivalents of COT. In (a), (b), and (c) the same height scale applies (0–15 nm), while in (d) the height scale is 0–20 nm.

3.4 Conclusions

The synthesis of telechelic polyenes via the direct ROMP of COT in the presence of a CTA with catalyst **2** has been demonstrated. The telechelic polyenes remained

completely soluble in common organic solvents and were characterized in detail using solution and solid-state spectroscopic methods. Furthermore, PA block copolymers were synthesized in one step from olefin-functionalized commodity polymers. As a consequence of their solubility, all of these block copolymers were amenable to spin coating and subsequent AFM investigation. We hope that the tunablity and improved processability of these materials may soon lead to their commercialization; investigations of their electronic properties are currently underway.

3.5 Experimental Section

General Procedures. NMR spectra were recorded on a Varian Mercury 300 (300 MHz for ^{1}H and 75 MHz for ^{13}C). All NMR spectra were recorded in CD_2Cl_2 or $CDCl_3$ and referenced to residual proteo species. Gel permeation chromatography (GPC) was carried out on three AM GPC Gel columns, 15 μm pore size, (American Polymer Standards Corp.) connected in series with a Type 188 differential refractometer (Knauer). Molecular weights were calculated relative to polystyrene standards. MALDI-TOF mass spectra were recorded using an Applied Biosystems (ABI) Voyager DE-PRO time-of-flight mass spectrometer. A 20 Hz nitrogen laser (337 nm, 3 ns pulse width) was used to desorb the sample ions that were prepared in a dithranol matrix. Mass spectra were recorded in linear (or reflector) delayed extraction mode with an accelerating voltage of 20 kV and a delay time of 100 ns. The low mass cut-off gate was set to 500 Da to prevent the lower mass matrix ions from saturating the detector. Calibration was external using a peptide mixture provided by the instrument manufacturer covering the mass range of interest. Raw spectra were acquired with an internal 2 GHz ACQIRIS digitizer and treated with Data Explorer software provided by ABI. Tapping Mode atomic force microscopy images were obtained in air using a Nanoscope IIIa AFM (Digital Instruments, Santa Barbara, CA) with silicon cantilever probes (Veeco Metrology, Santa Barbara, CA). To improve image quality, height and amplitude images were flattened using commercial software (also from Digital Instruments). AFM samples were prepared using dilute solutions of polymer

(either 0.4 or 1 wt/wt %) in either toluene or CH_2Cl_2. A 35 μL aliquot of the solution was spin coated onto freshly cleaved mica substrates (1 cm^2) at 3000 rpm. FT-IR Spectra (KBr pellet) were recorded on a Perkin-Elmer Paragon 1000 or on a Bio-Rad Excalibur FTS 3000 spectrometer controlled by Win-IR Pro software. UV-Vis spectra were obtained on a Beckman DU 640 Spectraphotometer in either THF or CH_2Cl_2.

Materials. Toluene and CH_2Cl_2 were dried by passage through solvent purification columns.[47] 1,3,5,7-Cyclooctatetraene (COT) (**3**) (generously donated by BASF) was dried over CaH_2 and distilled prior to use. Cis-1,4-diacetoxy-2-butene (96%) (**5b**) (Aldrich) was dried over CaH_2 and distilled prior to use. Cis-2-butene-1,4-diol (95%) (**5d**) (Aldrich) was distilled prior to use. Cis-Cyclooctene (Aldrich) was degassed by freeze/pump/thaw cycles before use. Vinyl-terminated PS (**11**) (M_n = 1900, M_w/M_n = 1.11), and vinyl terminated PEG (**10**) (M_n = 1120, M_w/M_n = 1.17) were purchased from Polymer Source, Inc. $(PCy_3)_2(Cl)_2Ru$=CHPh (**1**)[48] and $(IMesH_2)(PCy_3)(Cl)_2Ru$=CHPh (**2**)[49] [Mes = 2,4,6-trimethylbenzene]as well as CTAs **5**a[50] and **5c**[51] were synthesized according to literature procedure. All other materials were used as received.

Procedure for the ROMP of COT (3) with CTA 5a (in solution). A stir bar was placed in an oven-dried small vial with a teflon screw cap. Under an argon atmosphere, 0.5 mL (4.44 mmol) of COT and 1.6 mL (4.34 mmol) of CTA **5a** were added by syringe. Subsequently 1.0 mL (8.84 x 10^{-3} mmol) of a 7.5 mg/mL solution of **2** in CH_2Cl_2 was added by syringe. The vial was placed in a 55 °C oil bath. The yellow solution turned dark orange within 5 min. After 24 h, the reaction vial was removed from the heating bath and the solution was precipitated into 100 mL of stirring MeOH and filtered through a Büchner funnel to yield a red solid. The solid was dried under reduced pressure, yielding 91 mg of polymer (20%). Alternatively, the precipitate in MeOH solution was placed in centrifuge tubes and a number of centrifuge-decant-wash with MeOH cycles were performed until the decanted liquid was colorless. The red solid was then dissolved in CH_2Cl_2, transferred to an amber vial, and the solvent was removed under reduced pressure.

Procedure for the ROMP of COT with CTA 5a (neat). An oven-dried

small vial with a teflon screw cap was charged with a stirbar and 7.3 mg (8.61 x 10^{-3} mmol) of catalyst **2**. Under an argon atmosphere, 0.5 mL (4.44 mmol) of COT and 0.55 mL (1.49 mmol) of the CTA **5a** were added by syringe. The vial was placed in an aluminum heating block set to 55 °C. The yellow solution immediately turned dark reddish-orange. After 24 h, the solution was removed from the heating block and dissolved in CH_2Cl_2. The solution was precipitated into 100 mL of stirring MeOH and filtered through a Büchner funnel to yield a purple solid. The solid was then dried under reduced pressure, yielding 124 mg of polymer (27%).

Synthesis of vinyl-terminated polystyrene (7). To a small round bottom flask containing a stirbar was added 0.365 g (4.62 mmol) 2,2'-dipyridyl, 0.299 g (4.70 mmol) copper powder, 0.114 g (0.511 mmol) $CuBr_2$, 0.4 mL (4.62 mmol) allyl bromide, and 3.0 mL (44.6 mmol) styrene. The flask was sealed with a rubber septum, purged with argon for 5 min, and heated to 110 °C. After 15 min, the reaction mixture turned bright green. The reaction was terminated after 24 h by cooling down to room temperature, dissolving the mixture in THF, and precipitating in MeOH. The resulting solid was isolated by filtration, dissolved in THF, and passed through a plug of alumina before reprecipitating in MeOH. The isolated white product was dried in vacuo.

Synthesis of vinyl-terminated polystyrene (8). As for **7**, but with 5-bromo-1-pentene as initiator.

Synthesis of vinyl-terminated polymethylmethacrylate (9). As for **7**. To maintain lower reaction viscosity, however, an amount of diphenylether equivalent to the amount of methyl methacrylate monomer (by mass) was added.

Synthesis of PA block copolymers. In a typical procedure, the olefin terminated polymer chain transfer agent was added to a small vial containing a stirbar. The vial was purged with argon for 10–15 min, toluene was added, and the mixture was stirred to completely dissolve the polymer. COT was then added, followed by the appropriate amount of a stock solution of catalyst in toluene. The solution was heated up to 55 °C and left stirring under an argon atmosphere for 24 h. The reaction mixture was cooled down to room temperature and precipitated in a nonsolvent

such as MeOH or hexane. The resulting solid was isolated by filtration, dried under reduced pressure, and stored in an amber vial under an atmosphere of argon.

3.6 Acknowledgement

MALDI-TOF analysis was carried out in a multi-user MS lab funded in part by the MRSEC. The authors thank Dr. Mona Shahgholi for assistance with MALDI analysis of the polyenes, and Dr. Brian Connell, Dr. Stuart J. Cantrill, and Daniel P. Sanders for critical reading of this manuscript. O.A.S. thanks the National Science Foundation for a graduate fellowship.

References Cited

[1] Shirakawa, H. *Angew. Chem., Int. Ed.* **2001,** *40,* 2575–2580.
[2] MacDiarmid, A. G. *Angew. Chem., Int. Ed.* **2001,** *40,* 2581–2590.
[3] Heeger, A. J. *Angew. Chem., Int. Ed.* **2001,** *40,* 2591–2611.
[4] Shirakawa, H. *Synth. Met.* **2001,** *125,* 3–10.
[5] Berets, D. J.; Smith, D. S. *Trans. Faraday Soc.* **1968,** *64,* 823.
[6] Shirakawa, H.; Ikeda, S. *Polym. J.* **1971,** *2,* 231.
[7] Edwards, J. H.; Feast, W. J. *Polymer* **1980,** *21,* 595–596.
[8] Swager, T. M.; Dougherty, D. A.; Grubbs, R. H. *J. Am. Chem. Soc.* **1988,** *110,* 2973–2974.
[9] Korshak, Y. V.; Korshak, V. V.; Kanischka, G.; Hocker, H. *Makromol. Chem., Rapid Commun.* **1985,** *6,* 685–692.
[10] Klavetter, F. L.; Grubbs, R. H. *Synth. Met.* **1989,** *28,* D99–D104.
[11] Klavetter, F. L.; Grubbs, R. H. *J. Am. Chem. Soc.* **1988,** *110,* 7807–7813.
[12] Scherman, O. A.; Grubbs, R. H. *Synth. Met.* **2001,** *124,* 431–434.
[13] Wang, X. H.; Li, J.; Zhang, J. Y.; Sun, Z. C.; Yu, L.; Jing, X. B.; Wang, F. S.; Sun, Z. X.; Ye, Z. J. *Synth. Met.* **1999,** *102,* 1377–1380.
[14] Lessner, P.; Su, T.; Melody, B.; Kinard, J.; Rajasekaran, V.; Kemet (Electronics Corp., U. "PCT Int. Appl.", 2000.
[15] Voss, K. F.; Foster, C. M.; Smilowitz, L.; Mihailovic, D.; Askari, S.; Srdanov, G.; Ni, Z.; Shi, S.; Heeger, A. J.; Wudl, F. *Phys. Rev. B* **1991,** *43,* 5109–5118.
[16] Wagaman, M. W.; Grubbs, R. H. *Macromolecules* **1997,** *30,* 3978–3985.
[17] Elsenbaumer, R. L.; Jen, K. Y.; Miller, G. G.; Shacklette, L. W. *Synth. Met.* **1987,** *18,* 277–282.
[18] Leung, L. M.; Tan, K. H.; Lam, T. S.; He, W. *React. Funct. Polym.* **2002,** *50,* 173–179.
[19] Stelzer, F.; Grubbs, R. H.; Leising, G. *Polymer* **1991,** *32,* 1851–1856.
[20] Knoll, K.; Schrock, R. R. *J. Am. Chem. Soc.* **1989,** *111,* 7989–8004.
[21] Dounis, P.; Feast, W. J.; Widawski, G. *J. Mol. Catal. A: Chem.* **1997,** *115,* 51–60.
[22] Rychnovsky, S. D. *Chem. Rev.* **1995,** *95,* 2021–2040.
[23] Jerome, R.; Henrioullegranville, M.; Boutevin, B.; Robin, J. J. *Prog. Polym. Sci.* **1991,** *16,* 837–906.
[24] Cacialli, F.; Daik, R.; Dounis, P.; Feast, W. J.; Friend, R. H.; Haylett, N. D.; Jarrett, C. P.; Schoenenberger, C.; Stephens, J. A.; Widawski, G. *Philos. Trans.*

R. Soc. London Ser. A: Math. Phys. Eng. Sci. **1997,** *355,* 707–713.

[25] Schrock, R. R.; Krouse, S. A.; Knoll, K.; Feldman, J.; Murdzek, J. S.; Yang, D. C. *J. Mol. Catal.* **1988,** *46,* 243–253.

[26] Schleyer, P. v. R.; Williams, J. E.; Blanchard, K. R. *J. Am. Chem. Soc.* **1970,** *92,* 2377–2386.

[27] Bielawski, C. W.; Scherman, O. A.; Grubbs, R. H. *Polymer* **2001,** *42,* 4939–4945.

[28] Bielawski, C. W.; Benitez, D.; Morita, T.; Grubbs, R. H. *Macromolecules* **2001,** *34,* 8610–8618.

[29] The higher reaction temperatures required for chain transfer with catalysts **1** and **2** preclude the ROMP of Durham monomers due to the instability of the PA precursor.

[30] Sanford, M. S.; Love, J. A.; Grubbs, R. H. *J. Am. Chem. Soc.* **2001,** *123,* 6543–6554.

[31] Scherman, O. A.; Kim, H. M.; Grubbs, R. H. *Macromolecules* **2002,** *35,* 5366–5371.

[32] Shibahara, S.; Yamane, M.; Ishikawa, K.; Takezoe, H. *Macromolecules* **1998,** *31,* 3756–3758.

[33] Shiono, T.; Kang, K. K.; Hagihara, H.; Ikeda, T. *Macromolecules* **1997,** *30,* 5997–6000.

[34] Nakagawa, Y.; Matyjaszewski, K. *Polym. J.* **1998,** *30,* 138–141.

[35] Manring, L. E. *Macromolecules* **1989,** *22,* 2673–2677.

[36] Kurosawa, H.; Shiono, T.; Soga, K. *Macromol. Chem. Phys.* **1994,** *195,* 1381–1388.

[37] Matyjaszewski, K.; Coca, S.; Gaynor, S. G.; Wei, M. L.; Woodworth, B. E. *Macromolecules* **1998,** *31,* 5967–5969.

[38] Bednarek, M.; Biedron, T.; Kubisa, P. *Macromol. Chem. Phys.* **2000,** *201,* 58–66.

[39] Bednarek, M.; Biedron, T.; Kubisa, P. *Macromol. Rapid Commun.* **1999,** *20,* 59–65.

[40] Simal, F.; Demonceau, A.; Noels, A. F. *Angew. Chem., Int. Ed.* **1999,** *38,* 538–540.

[41] It is evident from the characterization data that the products of these reactions contain a significant portion of unmodified polymer; however, the amount of PA that is incorporated is clearly sufficient to affect the material properties.

[42] Observance of these peaks was impossible for PS-*b*-PA samples due to the intense resonances from the phenyl protons of polystyrene.

[43] Aime, J. P.; Reibel, D.; Mathis, C. *Synth. Met.* **1993,** *55,* 127–134.

[44] Dai, L. M. *Synth. Met.* **1997,** *84,* 957–960.

[45] Stelzer, F.; Fischer, W.; Leising, G.; Heller, C. *Springer Ser. Solid-State Sci.* **1992,** *107 (Electron. Prop. Polym.),* 231–237.

[46] This morphology is possibly a result of the fast evaporation of solvent that occurs when the films are made. With films that were formed by slowly evaporating the solvent (i.e., not spin coating), the spiked morphology was not observed.

Rather, a highly disordered morphology with large, randomly placed crystal-like structures was seen.

[47] Pangborn, A. B.; Giardello, M. A.; Grubbs, R. H.; Rosen, R. K.; Timmers, F. J. *Organometallics* **1996,** *15,* 1518–1520.

[48] Schwab, P.; Grubbs, R. H.; Ziller, J. W. *J. Am. Chem. Soc.* **1996,** *118,* 100–110.

[49] Sanford, M. S.; Ulman, M.; Grubbs, R. H. *J. Am. Chem. Soc.* **2001,** *123,* 749–750.

[50] Corey, E. J.; Venkates, A. *J. Am. Chem. Soc.* **1972,** *94,* 6190–6191.

[51] Asgarzadeh, F.; Ourdouillie, P.; Beyou, E.; Chaumont, P. *Macromolecules* **1999,** *32,* 6996–7002.

Chapter 4

Formation of Covalently Attached Polymer Overlayers on Si(111) Surfaces Using Ring-Opening Metathesis Polymerization Methods

This work was done in collaboration with Agnes Juang in the Lewis group and has previously appeared as: Juang, A.; Scherman, O. A.; Grubbs, R. H.; Lewis, N. S. *Langmuir* **2001**, *17*, 1321–1323.

4.1 Abstract

We describe a method for growing uniform, covalently attached polymer onto crystalline Si(111) surfaces. H-terminated Si was first chlorinated, and the surface-bound chlorine was then replaced by a terminal olefin using a Grignard reaction. A ruthenium ring-opening metathesis polymerization catalyst was then crossed onto the terminal olefin, and the resulting surface was subsequently immersed into a solution of monomer to produce the desired surface-attached polymer. The method provides a direct linkage between the polymer and the Si without the presence of an electrically-defective oxide layer. Growth of the polymeric layer could be controlled by varying the concentration of monomer in solution, and polynorbornene films between 0.9 and 5500 nm in thickness were produced through the use of 0.01 to 2.44 M solutions of norbornene.

4.2 Introduction

The fabrication of conducting and/or nonconducting organic overlayers on crystalline Si surfaces is of interest for inhibition of surface corrosion processes,[1] for providing routes to chemical control over the electrical properties of Schottky barrier-like structures,[2] for enabling novel lithographic strategies that utilize contact printing and photopatterning,[3–5] for producing novel metal-insulator-semiconductor devices,[6] and for controlling the electrical recombination properties of Si surfaces,[7, 8] amongst other applications. To obtain acceptable electrical device properties, many of these applications require direct functionalization of the Si surface in a fashion that does not introduce significant densities of interfacial electronic defect levels. The presence of a native oxide on Si is largely unacceptable for such purposes because the resulting Si/Si oxide interface is often highly electrically defective.[9, 10] In addition, the oxide acts as a tunneling barrier for charge carriers and the uniformity of this barrier is difficult to control at the molecular level. Thermally-grown silicon oxides generally contain fixed positive charge,[9, 11–13] which also limits the types of electrical device

behavior that can be obtained from such interfaces.

It would therefore be desirable to form electrically conductive or nonconductive barrier layers of controlled thickness on Si without relying on reactions that utilize functionality arising from native and/or thermally-grown overlayers of Si oxides. Crystalline Si has recently been functionalized using a variety of approaches;[14–28] notably, alkylation of crystalline, (111)-oriented Si using a two-step chlorination/alkylation procedure can produce functionalized surfaces that have a very low surface recombination velocity, <50 cm s^{-1}, and this low defect density of < 1 active electrical surface site per 50,000 surface atoms persists in ambient atmospheric conditions.[8] We describe herein the extension of this chemistry, combined with ring-opening metathesis polymerization (ROMP) methods, to produce organic overlayers that are covalently attached to Si(111) surfaces and that provide molecular-level control over the thickness and electronic properties of the resulting Si/polymer contacts.

4.3 Results and Discussion

Scheme 4.1 depicts our methodology (i) an alkene linker of variable length is coupled to a chlorinated Si surface using a Grignard reaction; (ii) an olefin cross-metathesis reaction is used to obtain a surface-bound ruthenium ROMP catalyst, and (iii) a monomer is added to effect growth of polymer onto the surface.

To implement this approach, a (111)-oriented crystalline n-type Si substrate 7 mm x 7 mm in dimensions was first etched in 49% buffered HF(aq) for 30 s and then for 15 min in 40% NH_4F(aq).[29] The resulting H-terminated Si surface was then chlorinated by exposure to saturated PCl_5 in chlorobenzene for 45 min at 90–100 °C, with a trace of benzoyl peroxide added to serve as a radical initiator.[30, 31] This chloride-capped Si surface[32] was then exposed to allylmagnesium chloride for 14–16 hr at 75 °C in tetrahydrofuran (THF).[32] A ruthenium olefin metathesis catalyst $(Cy_3P)_2Cl_2Ru{=}CHPh$ (Cy=cyclohexyl), (**1**),[33, 34] was then reacted with the olefin-modified Si surface by immersing the Si for 3 hr into a 25 mM solution of **1** in CH_2Cl_2. The substrate was then rinsed several times with CH_2Cl_2 to remove any non-bound

Scheme 4.1: Si(111) surface modification procedure.

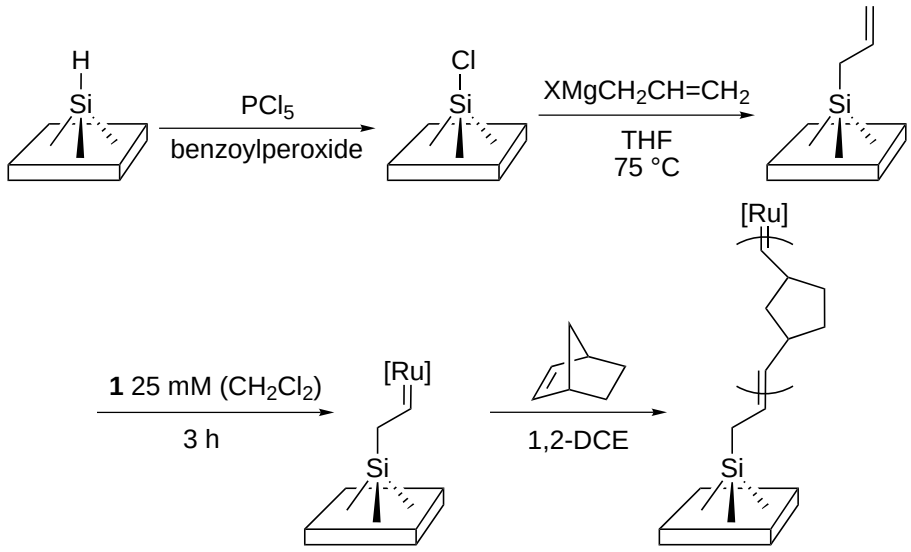

catalyst. Exposure of the surface-bound catalyst to a 0.01–2.44 M solution of the norbornene monomer, **2**, for 30 min in 1,2-dichloroethane resulted in the growth of a polymeric film on the n-Si(111) surface. The resulting films were then repeatedly washed with CH_2Cl_2 and characterized as appropriate by X-ray photoelectron (XP) spectroscopy, ellipsometry, profilometry, and scanning electron microscopy (SEM).

Figure 4.1 displays the XP spectra obtained at each step of the surface modification process. The chlorination was verified by the presence of Cl 2s and Cl 2p peaks in the XPS survey scan (Figure 4.1d).[32] Attachment of the alkene carbon linker was confirmed by the disappearance of the Cl peaks and the concomitant increase in magnitude of the C 1s peak in the XP survey spectrum (Figure 4.1c).[35] For thin polymer films, growth of polymer was evidenced by the disappearance of the Si signals and the formation of an overlayer that only displayed C peaks in the XP survey scan (Figure 4.1a) whereas thicker polymer films produced no significant XPS signals, as expected if an electrically insulating organic overlayer had been formed on the surface.

Additional experiments were performed to establish that (i) the polymerization of **2** was directly initiated by **1**, and (ii) the resulting polymer film was attached covalently to the Si surface. When an olefin-terminated alkylated Si substrate was exposed to a solution of **2**, no polymer was observed by XPS. In addition, when a H-

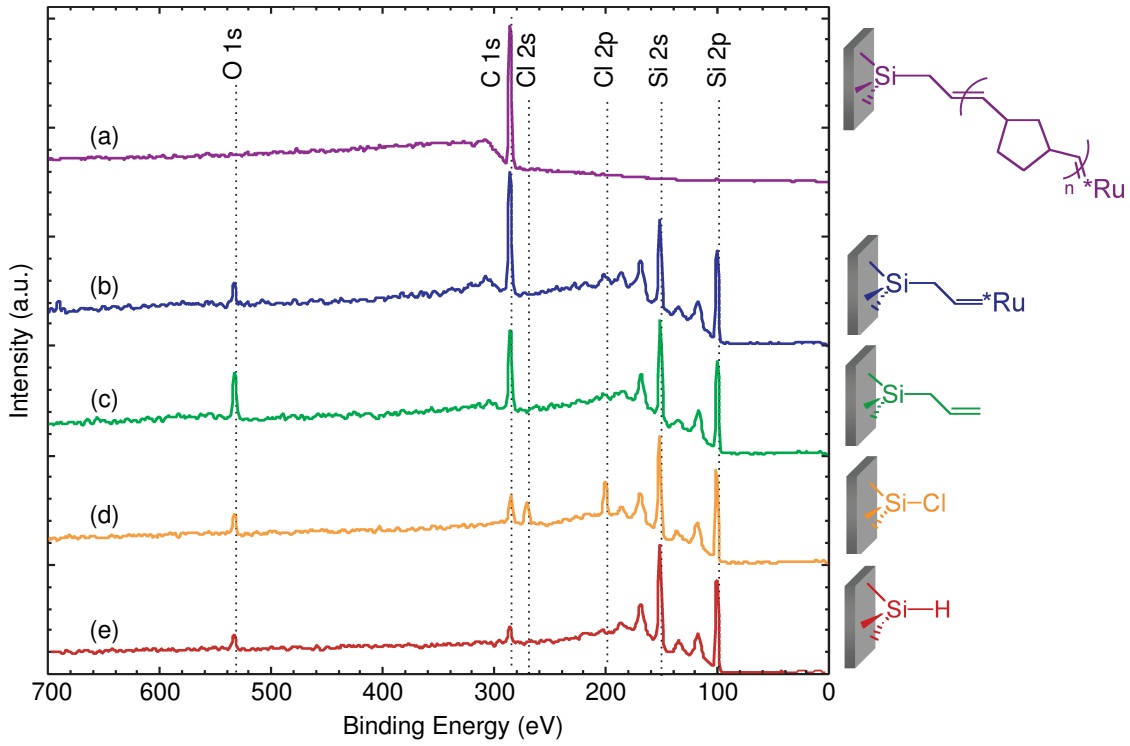

Figure 4.1: XPS survey scans. (a) covalently attached polynorbornene on Si, (b) allyl-terminated Si after immersing in a solution of **1** for 3 h, (c) allyl-terminated Si, (d) Cl-terminated Si, and (e) H-terminated Si. Spectra in a–d are normalized relative to the intensity of the Si 2p peak.

terminated Si surface was exposed to a solution of **2**, no polymer formed and the XPS signals showed only Si and a very small amount of adventitious C and O. Exposure of a H-terminated Si surface to a solution of **1** followed by exposure to a solution of **2** produced a polymer that did not persist on the Si surface after washing with CH_2Cl_2. These wet chemical experiments imply that the above technique did in fact produce covalently attached polymeric films on the Si surface, and the polymerization could not occur without the Ru initiators.

Figure 4.2 displays a SEM image of the cross section of a sample (obtained after immersion of a **1**-treated, allyl-terminated Si sample into a 2.44 M solution of norbornene in 1,2-dichloroethane for 30 min) at 1500x magnification. The SEM images indicate that the wafers were indeed covered entirely by polynorbornene. The estimated thickness of the polymer film from SEM images of two samples at 1500x magnification is 5.6±0.06 μm, which agrees with the thickness of 5.5 μm measured

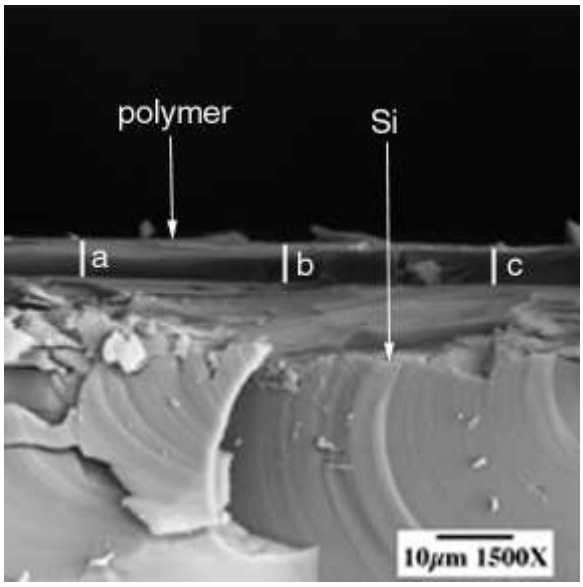

Figure 4.2: SEM of polynorbornene-modified Si(111) surface. A cross-sectional SEM image of a polynorbornene-covered Si surface at 1500x magnification. The polymer film covered the entire Si substrate, and the estimated film thickness at points a, b, and c from the SEM image are 5.0, 5.5, and 5.4 μm, respectively. These values are in good agreement with the mean polymer thickness of 5.5 μm that was determined for this same sample using profilometry.

using profilometry.

Because ROMP initiated by **1** is a controlled polymerization process,[34, 36] different film thicknesses could be obtained by varying the concentration of **2** in 1,2-dichloroethane solutions. Table 4.1 summarizes the thicknesses of several polymer films produced at a fixed reaction time (30 min) in response to variation in the concentration of monomer in the solution. The standard deviation in the ellipsometrically derived thickness measured at six different spots for each sample was usually $< \pm 10\%$ of the mean thickness value, indicating that the polymer film covered the entire Si substrate. Consistently, the SEM image of Figure 4.2 yielded a film thickness of 5.3 ± 0.2 μm over a distance of 75 μm.

The method would appear to be general in that a wide range of monomers can be polymerized with **1**[36, 38–40] and could be used to form overlayers of controlled thickness on Si surfaces. When the first polymer layer is electrically insulating (as in the present case), this should allow formation of metal-insulator-semiconductor

Table 4.1: Dependence of the polymer film thickness on the concentration of norbornene in solution.

Monomer Concentration (M)	Thickness[a] (Å)
0.01	9±1
0.09	120±14
0.18	420±140
0.27	1280±660

[a]Each thickness value is an average of measurements on at least four samples, with six different locations measured on each sample.[37]

structures or of capacitors of controlled thickness, whereas when the first polymer is metallic or semiconducting in nature (e.g., when cyclooctatetraenes, phenylenevinylenes, etc., are used as feedstocks),[41] the process should provide a route to formation of semiconductor/metal or semiconductor heterojunction structures. Langmuir-Blodgett techniques[42] have been used to synthesize organic thin films with controlled structure and composition; however, the fragility of the resulting films represents a major obstacle to practical implementation. More robust films have been obtained using polymers with functionalities appropriate for covalent attachment to surfaces.[43] The significant improvement in physical properties, however, generally is accompanied by a loss of control over the order and composition of the overlayer. Weck *et al.* reported the ROMP of substituted norbornenes from a modified gold surface, but only small amounts of polymer were formed.[40] The procedure described herein is analogous to that reported recently by Kim *et al.*, who used ROMP to produce substituted norbornenes from a self-assembled monolayer of 5-(bicycloheptenyl)trichlorosilane formed on a silicon wafer bearing a native oxide (Si/SiO_2),[39] followed by opening of the olefin and exchange with the catalyst. Our approach is complementary to this work in that the present method allows for the formation of covalently attached interfacial polymeric layers in situations in which the presence of an intervening Si oxide layer is undesirable.

4.4 Conclusions

In conclusion, we have demonstrated the growth of polymer films that are covalently attached to Si surfaces via a Si-C linkage. The thickness of the linker unit can be controlled at the molecular level, and the thickness of the polymer can be independently controlled by varying the concentration of monomer, so that polymer thicknesses between 0.9 and 5500 nm can be obtained.

References Cited

[1] Bansal, A.; Lewis, N. S. *J. Phys. Chem. B* **1998,** *102,* 4058.

[2] Sailor, M. J.; Klavetter, F. L.; Grubbs, R. H.; Lewis, N. S. *Nature* **1990,** *346,* 155.

[3] Huck, W. T. S.; Yan, L.; Stroock, A.; Haag, R.; Whitesides, G. M. *Langmuir* **1999,** *15,* 6862.

[4] Clark, S. L.; Montague, M.; Hammond, P. T. *Supramol. Sci.* **1997,** *4,* 141.

[5] Whidden, T. K.; Ferry, D. K.; Kozicki, M. N.; Kim, E.; Kumar, A.; Wilbur, J.; Whitesides, G. M. *Nanotechnology* **1996,** *7,* 447.

[6] Sailor, M. J.; Ginsburg, E. J.; Gorman, C. B.; Kumar, A.; Grubbs, R. H.; Lewis, N. S. *Science* **1990,** *249,* 1146.

[7] Bansal, A.; Lewis, N. S. *J. Phys. Chem. B* **1998,** *102,* 1067.

[8] Royea, W. J.; Juang, A.; Lewis, N. S. *Appl. Phys. Lett.* **2000,** *77,* 1988.

[9] Sze, S. *The Physics of Semiconductor Devices;* Wiley: New York, 2nd ed.; 1981.

[10] Royea, W. J.; Michalak, D. J.; Lewis, N. S. *Appl. Phys. Lett.* **2000,** *77,* 2566.

[11] Eades, W. D.; Swanson, R. M. *J. Appl. Phys.* **1985,** *58,* 4267.

[12] Yablonovitch, E.; Gmitter, T. J. *Sol. St. Electron.* **1992,** *35,* 261.

[13] Aberle, A. G.; Glunz, S.; Warta, W. *J. Appl. Phys.* **1992,** *71,* 4422.

[14] Boukherroub, R.; Morin, S.; Bensebaa, F.; Wayner, D. D. M. *Langmuir* **1999,** *15,* 3831.

[15] Sieval, A. B.; Vleeming, V.; Zuilhof, H.; Sudholter, E. J. R. *Langmuir* **1999,** *15,* 8288.

[16] Boukherroub, R.; Wayner, D. D. M. *J. Am. Chem. Soc.* **1999,** *121,* 11513.

[17] Sieval, A. B.; Demirel, A. L.; Nissink, J. W. M.; Linford, M. R.; van der Mass, J. H.; de Jeu, W. H.; Zuilhof, H.; Sudholter, E. J. R. *Langmuir* **1998,** *14,* 1759.

[18] Linford, M. R.; Chidsey, C. E. D. *J. Am. Chem. Soc.* **1993,** *115,* 12631.

[19] Linford, M. R.; Fenter, P.; Eisenberger, P. M.; Chidsey, C. E. D. *J. Am. Chem. Soc.* **1995,** *117,* 3145.

[20] Zazzera, L. A.; Evans, J. F.; Deruelle, M.; Tirrell, M.; Kessel, C. R.; McKeown, P. *J. Electrochem. Soc.* **1997,** *144,* 2184.

[21] Feng, W. J.; Miller, B. *Langmuir* **1999,** *15,* 3152.

[22] Effenberger, F.; Gotz, G.; Bidlingmaier, B.; Wezstein, M. *Angew. Chem., Int. Ed.* **1998,** *37,* 2462.

[23] Allongue, P.; de Villeneuve, C. H.; Pinson, J.; Ozanam, F.; Chazalviel, J. N.; Wallart, X. *Electochim. Acta* **1998,** *43,* 2791.

[24] He, J.; Patitsas, S. N.; Preston, K. F.; Wolkow, R. A.; Wayner, D. D. M. *Chem. Phys. Lett.* **1998,** *286,* 508.

[25] de Villeneuve, C. H.; Pinson, J.; Bernard, M. C.; Allongue, P. *J. Phys. Chem. B* **1997,** *101,* 2415.

[26] Wagner, P.; Nock, S.; Spudich, J. A.; Volkmuth, W. D.; Chu, S.; Cicero, R. L.; Wade, C. P.; Linford, M. R.; Chidsey, C. E. D. *J. Struct. Biol.* **1997,** *119,* 189.

[27] Hamers, R. J.; Coulter, S. K.; Ellison, M. D.; Hovis, J. S.; Padowitz, D. F.; Schwartz, M. P.; Greenlief, C. M.; Russell, J. *Accts. Chem. Res.* **2000,** *33,* 617.

[28] Schwartz, M. P.; Ellison, M. D.; Coulter, S. K.; Hovis, J. S.; Hamers, R. J. *J. Am. Chem. Soc.* **2000,** *122,* 8529.

[29] Higashi, G. S.; Becker, R. S.; Chabal, Y. J.; Becker, A. J. *Appl. Phys. Lett.* **1991,** *58,* 1656.

[30] Hassler, K.; Koll, W. *J. Organomet. Chem.* **1995,** *487,* 223.

[31] Wyman, D. P.; Wang, J. Y. C.; Freeman, W. R. *J. Org. Chem.* **1963,** *28,* 3173.

[32] Bansal, A.; Li, X.; Lauermann, I.; Lewis, N. S.; Yi, S. I.; Weinberg, W. H. *J. Am. Chem. Soc.* **1996,** *118,* 7225.

[33] Schwab, P.; France, M. B.; Ziller, J. W.; Grubbs, R. H. *Angew. Chem., Int. Ed.* **1995,** *34,* 2039.

[34] Schwab, P.; Grubbs, R. H.; Ziller, J. W. *J. Am. Chem. Soc.* **1996,** *118,* 100.

[35] No Ru signal was observed in the XPS data, however, the intensity of this signal is expected to be very low. Assuming that reagent **1** has bound onto 50% of the total available groups in a monolayer of olefin on the Si surface implies a 1:41 Ru/C ratio for the atoms in the overlayer. With the atomic sensitivity factors of Ru $3d_{5/2}$ and C 1s being 1.55 and 0.205, respectively,[44] the area of the Ru $3d_{5/2}$ peak is calculated to be 18% of the C 1s signal. Because both the Ru $3d_{5/2}$ and Ru $3d_{3/2}$ peak positions are within 5 eV of the C 1s peak, observation of such small Ru peaks in the presence of these C 1s signals is not readily possible with our XPS instrument (VG Instruments M-probe Spectrometer, with a full width at half maximum of 1.50±0.01 eV for the Au $4f_{7/2}$ peak in survey scan mode). Additionally, the Ru $3p_{3/2}$ peak is about 1/3 as intense as the Ru $3d_{5/2}$ peak, so the estimated relative peak area of the Ru $3p_{3/2}$ would be only 6% of the C 1s peak area.

[36] Amir-Ebrahimi, V.; Corry, D. A.; Hamilton, J. G.; Thompson, J. M.; Rooney, J. J. *Macromolecules* **2000,** *33,* 717.

[37] The standard deviation between measurements at six separate locations on each sample was usually less than ±10% of the mean film thickness value on that sample; thus, the quoted standard deviation in film thickness for the thicker films predominantly reflects the differences in polymer film thickness between the different experimental trials.

[38] Maughon, B. R.; Morita, T.; Bielawski, C. W.; Grubbs, R. H. *Macromolecules* **2000,** *33,* 1929.

[39] Kim, N. Y.; Jeon, N. L.; Choi, I. S.; Takami, S.; Harada, Y.; Finnie, K. R.; Girolami, G. S.; Nuzzo, R. G.; Whitesides, G. M.; Laibinis, P. E. *Macromolecules* **2000,** *33,* 2793.

[40] Weck, M.; Jackiw, J. J.; Rossi, R. R.; Weiss, P. S.; Grubbs, R. H. *J. Am. Chem. Soc.* **1999,** *121,* 4088.

[41] Scherman, O. A.; Grubbs, R. H. *Synth. Met.* **2001,** *124,* 431–434.

[42] Ulman, A. *An Introduction to Ultrathin Organic Films;* Academic Press: Boston, 1991.

[43] Lenk, T. J.; Hallmark, V. M.; Rabolt, J. F.; Haussling, L.; Ringsdorf, H. *Macromolecules* **1993,** *26,* 1230.

[44] Wagner, C. D.; Riggs, W. M.; Davis, L. E.; Moulder, J. F.; Muilenberg, G. E. *Handbook of X-Ray Photoelectron Spectroscopy;* Perkin-Elmer Corporation Physical Electronics Division: Eden Prairie, Minnesota, 1979.

Chapter 5

Synthesis of Polymer Dielectric Layers for Organic Thin-Film Transistors via Surface-Initiated Ring-Opening Metathesis Polymerization

5.1 Abstract

Polymer-based dielectric layers for use in electronic devices such as thin-film transistors (TFTs), capacitors, and other logic elements have attracted much attention for their low cost, processability, and tunable properties. Current methods for incorporating organic materials into these devices are either not ideal or not possible when applied to the deposition of polymer dielectric materials. The living ring-opening metathesis polymerization (ROMP) of strained, cyclic olefins can provide a method for growing organic polymers from a surface. ROMP would allow for pinhole-free dielectrics with controlled layer thickness and tunable electronic and surface properties by growing a covalently attached polymer from the surface. Furthermore, ROMP from surfaces is unique in its ability to polymerize monomers from either solution or vapor phase and can be performed under mild ambient conditions, afford polymer growth in minutes, and allow for flexibility in polymer structure and dielectric layer composition. We have shown the feasibility of producing TFTs and capacitors using surface attached ROMP polymers as a layer of dielectric material. Preliminary results indicate that this method will allow for highly tunable materials with desired properties. The ability to grow conformal polymer layers on any topology will be very important as device dimensions and applications change.

5.2 Introduction

The use of organic materials in electronic devices such as field effect transistors (FETs) and light emitting diodes (LEDs) has become an attractive approach toward decreasing weight and cost, simplifying production, and increasing versatility of these devices. Electronic devices containing polymer layers have been incorporated into applications such as active-matrix displays[1–3] and integrated circuits.[4, 5]

For optimal FET performance, a polymer dielectric layer should be chemically and electrically compatible, with the organic semiconductor facilitating a smooth interface between adjacent layers.[6] Low leakage and tunable dielectric properties are

also desirable. This requires that the layer be pinhole-free, with controlled thickness and composition.

Current methods for depositing polymer layers include spin-coating, ink-jet printing, and screen printing.[7–9] Unlike these methods, surface-initiated polymerizations can produce densely packed, conformal layers over any surface topology. Compared with other surface-initiated polymerization methods, ring-opening metathesis polymerization (ROMP) allows mild conditions and short reaction times. Therefore, we have chosen to investigate surface-initiated ROMP (SI-ROMP) as a method for forming polymer dielectric layers.

SI-ROMP has been demonstrated from Au, Si, and Si/SiO_2 surfaces using catalyst **1** and a variety of linking molecules.[10–12] Conformal block copolymers grown on Au nanoparticles demonstrated the living nature of SI-ROMP with catalyst **1**.[13] We report here that SI-ROMP polymer layers can be used as the dielectric layer in electronic devices, either alone or in tandem with an inorganic dielectric layer. We also report that, as with solution-phase ROMP,[14] catalyst **2** is more active than catalyst **1** in SI-ROMP (Figure 5.1).

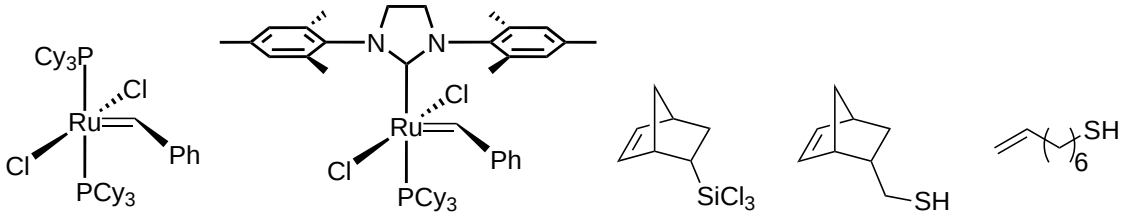

1 **2** **3** **4** **5**

Figure 5.1: Catalysts and linking molecules employed in SI-ROMP.

Polymer dielectric layers covalently attached to Au or Si/SiO_2 surfaces were formed via ROMP from surface-tethered metathesis catalysts (Scheme 5.1). Exposure of a self-assembled monolayer (SAM) of a linking molecule (**3**, **4** or **5**)[15] (Figure 5.1) to a solution of catalyst (**1** or **2**), followed by subsequent exposure to a solution of monomer, generated the polymer film. Between each of these steps, the surfaces were extensively rinsed with solvent to remove chemically unbound material.

Many variables were found to significantly affect the thickness and uniformity

Scheme 5.1: Construction of an FET using a SI-ROMP polymer dielectric layer (**4** shown as example linker).

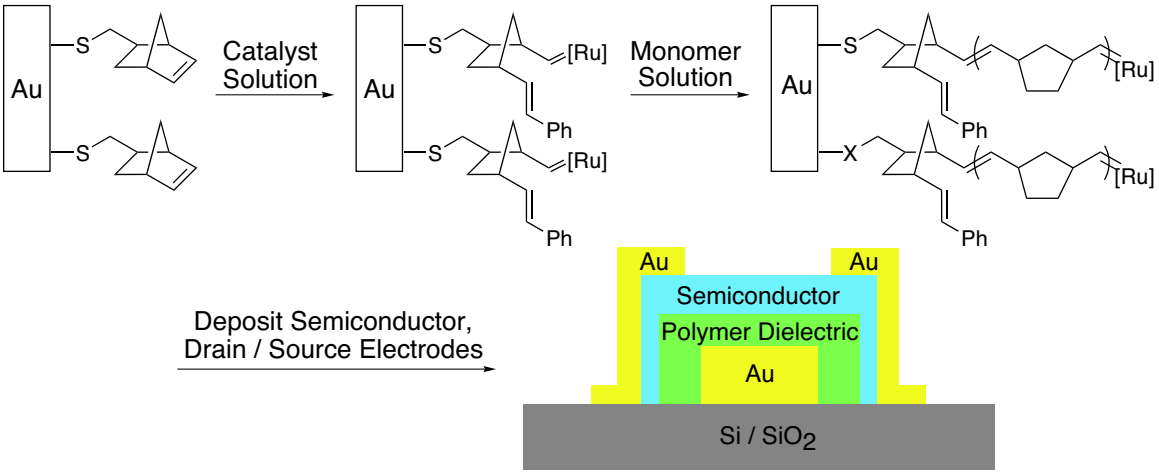

of SI-ROMP polymer films. Most importantly, catalyst **2** is far more active than catalyst **1**. Given identical reaction conditions, films produced from catalyst **2** are up to 10 times thicker than those produced from catalyst **1**. For example, using **4** as the linker, films produced after 15 min of exposure to a 3 M solution of norbornene at room temperature (rt) are nearly 2.5 μm in thickness using catalyst **2**, versus 250 nm with catalyst **1**. Furthermore, catalyst **2** produces polymer films greater than 300 nm thick from 1 M monomer solutions, whereas catalyst **1** requires concentrations in excess of 3 M to produce equivalent films.

Polymerization conditions were also found to affect SI-ROMP films. Decreased thicknesses result for polymerizations conducted above rt, or for prolonged periods of time ($>$ 1 h). Almost no film remains after 24 h of polymerization time, suggesting that, as in solution-phase ROMP, secondary metathesis (chain transfer) reactions are occurring between growing chains. Slower than ROMP, and promoted by elevated temperature,[16] secondary metathesis in SI-ROMP would lead to chain termination and generation of polymer fragments that are no longer covalently attached to the substrate.

Smooth, pinhole-free dielectric films are important, since the overlaying semiconductor layer of an FET must continuously bridge the source and drain contacts.[17]

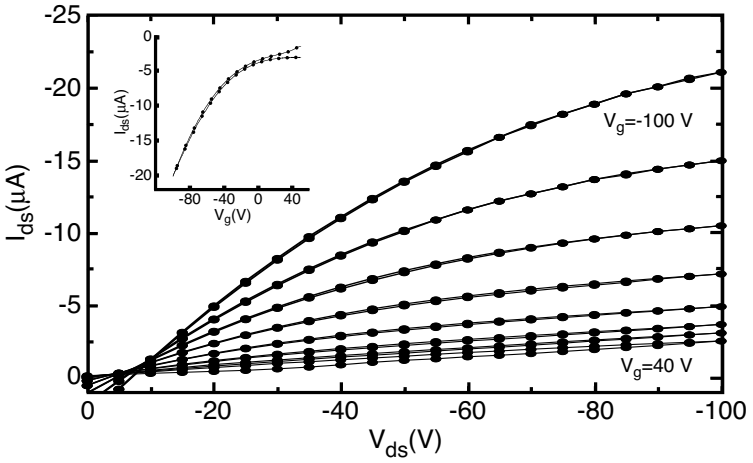

Figure 5.2: Current-voltage characteristics of an FET produced by lamination, containing a SI-ROMP polynorbornene dielectric layer. The drain bias was swept from 0 to -100 V and back at gate biases between 40 and -100 V in 20 V steps. Inset shows drain current as gate voltage was swept from 40 to -100 V and back.

Electrical shorting between the gate and drain and/or source electrodes was observed due to pinholes present in untreated SI-ROMP polynorbornene films. Annealing at 135 °C for 15 min densifies the films and significantly reduces the number of pinholes, resulting in relatively smooth, unshorted films.

Construction of FETs (as shown in Scheme 5.1) was demonstrated using the lamination method.[18] A SI-ROMP polymer dielectric layer was grown on a Au strip gate electrode (1000 Å thick, 1 mm wide) using linker **4**, catalyst **2**, and a 3 M norbornene solution. The thickness of the resulting polynorbornene film was 1.2 μm with a capacitance of 3 nF cm^{-2} measured at 20 Hz. After annealing, a 400 Å layer of pentacene was vapor deposited over the polymer dielectric. This was pressed against a separate PDMS substrate containing parallel Au strips as drain and source electrodes spaced 240 μm apart. A representative current-voltage (I/V) diagram for the resulting FETs is shown in Figure 5.2. Ranges for mobility and on/off ratio were 0.1–0.3 cm^2 V^{-1} s^{-1} and 10–100, respectively.[6] Little to no hysteresis was observed for these devices (see inset of Figure 5.2), indicating minimal charge buildup between the dielectric and semiconducting layers.

In addition to the lamination method, direct deposition of Au drain/source elec-

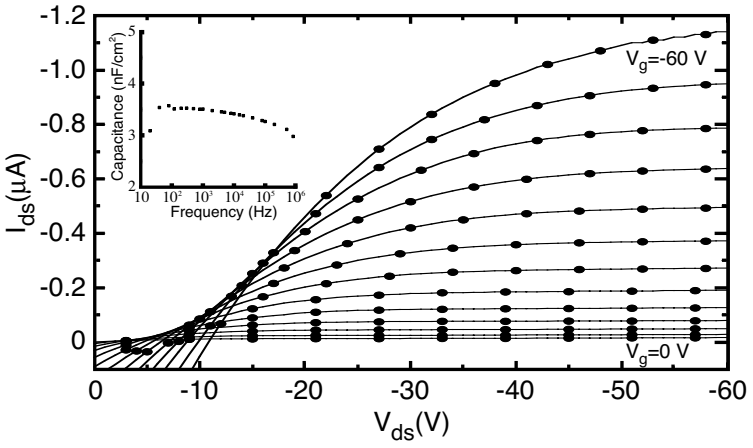

Figure 5.3: Current-voltage characteristics of an FET produced by direct deposition of the semiconductor layer and Au drain/source electrodes over a SI-ROMP polynorbornene dielectric layer grown from a Au gate electrode. The drain bias was swept from 0 to -60 V at gate biases between 0 and -60 V in 5 V steps. Inset shows capacitance of a polynorbornene capacitor as a function of frequency. The leakage current is due to the unpatterned gate and organic semiconducting layers.

trodes over the pentacene semiconducting layer also produced functioning FETs. Example I/V characteristics for these devices are shown in Figure 5.3. As seen in previous studies, mobilities and on/off ratios (up to 10^{-2} cm^2 V^{-1} s^{-1} and 100, respectively) were lower than those for the laminated devices due to partial degradation of the pentacene layer by the metal deposition.[18] The capacitance of the SI-ROMP dielectric films for these devices was found to have no significant frequency dependence down to 20 Hz (see inset of Figure 5.3).

Finally, FETs were constructed using a SI-ROMP polymer dielectric layer covalently bound to a Si/SiO_2 (either native or thermally grown oxide) surface. Working devices were constructed using either catalyst (**1** or **2**), linker **3**, and 2 M norbornene solutions.

Apart from washing extensively with solvent, no effort was made to remove residual (covalently bound or imbedded) catalyst from the polymer films. Rutherford backscattering spectroscopy (RBS) and medium energy ion scattering (MEIS) measurements, however, indicated exceptionally low surface concentrations of Ru for catalyst-functionalized SAMs as well as the washed films. Increasing the concen-

tration of ruthenium bonded to the SAM may result in denser films and less leakage.

These devices demonstrate that surface-initiated polymer dielectric layers are both chemically and electrically compatible with other FET component layers. In general, a high yield ($> 90\%$) of working TFTs was obtained only with annealed dielectric films at least 1 μm thick. Further optimization of polymer growth conditions, yielding higher graft densities and reduced surface roughness, should allow the use of thinner films as well as improve the compatibility between the polymer film and organic semiconductor.[19]

For devices using patterned (e.g., striped Au) substrates, the SI-ROMP polymer grows conformally over the gate electrode, eliminating the need to pattern the dielectric. Furthermore, spin-coated dielectric layers tend to be thinner at the edges of the electrode, leading to a lower breakdown voltage. In contrast, the thickness of the surface-grown polymer layer can be about the same at the edges as for the flat surface, illustrating a clear advantage of SI-ROMP.

In conclusion, construction of FETs using SI-ROMP polymer dielectric layers has been demonstrated. Mild reaction conditions, short reaction times, and simple solution processing methods make SI-ROMP an attractive method for constructing polymer dielectric layers. Layer thicknesses ranging from below 100 nm to above 2 μm are accessible simply by varying the polymerization conditions. Research is underway in optimizing FET device characteristics, as well as incorporating SI-ROMP block copolymers into organic-based FETs.

5.3 Experimental Section

Materials. Acetone, isopropyl alcohol, ethanol, 8-bromo-1-octene, tetrahydrofuran (anhydrous), hexamethyldisilathiane, tetrabutylammoniumfluoride (1.0 M in THF with 5% H_2O), and bicyclo[2.2.1]hept-2-ene (norbornene) were used as received from Aldrich. Dichloromethane (Aldrich, anhydrous) was degassed prior to use by sparging with argon. 1,2-dichloroethane (Aldrich, anhydrous) was first filtered through a plug of neutral alumina (Brockman Grade I; this procedure is necessary in

order to have film growth), and then degassed by sparging with argon. 5-(Bicycloheptenyl)trichlorosilane (**3**) was purchased from Gelest, Inc., and used as received. Bicyclo[2.2.1]hept-5-ene-2-methanethiol (**4**) was prepared as described in the literature.[20] Catalysts **1**[21] and **2**[22]were prepared as described in the literature. 7-Octene-1-thiol (**5**) was prepared according to a literature procedure,[23] with 8-bromo-1-octene as starting material.

Substrate Preparation and Metal/Organic Semiconductor Deposition. Silicon wafers containing a 3000 Å thermally grown oxide layer were obtained from Silicon Quest International. Gold substrates (typically composed of a 500 or 1000 Å layer of gold over a 50 or 100 Å layer of titanium, both vacuum deposited in an e-beam evaporator) were prepared on silicon wafers containing a native oxide layer (Silicon Quest International). Substrates were cut into 1 cm^2 squares, individually cleaned by sequential washings with acetone, deionized water, and ^{i}PrOH, and dried in a stream of dry nitrogen (N_2). The substrates were then soaked in a boiling solution of $H_2O/H_2O_2/NH_4OH$ (5:1:1) for 30 min, washed with water and ^{i}PrOH, and dried with dry N_2.

Surface Functionalization. In a typical procedure using gold substrates, self-assembled monolayers (SAMs) were formed by submerging freshly cleaned substrate squares in a filtered solution of thiol in absolute EtOH (typically 0.5 or 0.75 mM) for 24 h. The squares were then removed and washed, first with EtOH, then with ^{i}PrOH before being dried in a stream of dry N_2. Using Si/SiO_2 substrates, freshly cleaned squares were submerged for 6 h in a 0.5 wt% solution of trichlorosilane in pentane in a N_2 glovebox. The squares were then removed, sonicated for 5 min each in toluene (2 times), 50/50 toluene/acetone, and acetone, and dried in a stream of dry N_2.

Reaction of the olefin-functionalized substrates with catalyst was done in dichloromethane solutions of catalyst **1** or **2** (typically 13 or 25 mM) at room temperature (rt) or 40 °C. After the prescribed length of time, the squares were removed from solution, washed thoroughly with dichloromethane, and dried under N_2. They were then immediately placed in a fresh, filtered solution of norbornene in 1,2-dichloroethane and allowed to react for a prescribed length of time at rt or 40 °C. The squares were

then washed thoroughly with dichloromethane and dried under vacuum.

Device Construction. For the FETs using a gold strip as the gate electrode deposited on SiO_2 (both lamination and direct deposition methods), linker **4** and catalyst **2** were used. Catalyst attachment and norbornene polymerization were done at rt for 10 min and 15 min, respectively. The thickness of the polynorbornene film was 1.2 μm for the lamination devices, and ranged from 800 to 1100 nm for the direct deposition samples. In mobility calculations, a width (W) of 2–3 mm and length (L) of 1 mm were used for the laminated devices. A width of 940 μm and length of 240 μm were used for the direct deposition devices.

For the FETs using Si/SiO_2 as gate electrode, catalyst attachment was done with dichloromethane solutions of catalyst **1** or **2** at rt for 10 min, and the polymerizations were carried out with 1,2-dichloroethane solutions of norbornene (between 2 and 4 M) at rt, times varying between 15 and 40 min. The thickness of the polynorbornene films, which were very smooth and did not require annealing, ranged between 230 and 800 nm, but only those films thicker than 600 nm were used to make TFTs.

The organic semiconducting layer of pentacene (Aldrich) was deposited by thermal evaporation under vacuum (typically to a thickness of 300 Å). Gold overlayers were deposited in an e-beam evaporator under vacuum.

Characterization. Ellipsometric measurements were performed on a Rudolph Ellipsometer AutoEL. Profilometric measurements were measured using a Dektak 3030. Current-voltage characteristics were obtained with a Hewlett-Packard (HP) 4155A semiconductor parameter analyzer. AFM Tapping Mode data was acquired on a JEOL JSPM-4210 scanning probe microscope in a nitrogen environment. "NON-CONTACT ULTRASHAR" silicon cantilevers were purchased from NT-MDT, Ltd. Rutherford backscattering spectroscopy (RBS) and medium energy ion scattering (MEIS, a low energy ultrahigh resolution variant of RBS) were performed at the Rutgers University ion scattering facility. 1.5 MeV He ions (in RBS) and 100 keV protons (in MEIS) were used to quantify film composition and thickness.

5.4 Acknowledgements

The authors thank the National Science Foundation, Office of Naval Research, NJCOOE, and Lucent Technologies for financial support, and Dr. Brian Connell and Daniel P. Sanders for advice on this manuscript.

References Cited

[1] Rogers, J. A.; Bao, Z. *J. Polym. Sci. Part A: Polym. Chem.* **2002,** *40,* 3327–3334.

[2] Sheraw, C. D.; Zhou, L.; Huang, J. R.; Gundlach, D. J.; Jackson, T. N.; Kane, M. G.; Hill, I. G.; Hammond, M. S.; Campi, J.; Greening, B. K.; Francl, J.; West, J. *Appl. Phys. Lett.* **2002,** *80,* 1088–1090.

[3] Huitema, H. E. A.; Gelinck, G. H.; van der Putten, J. B. P. H.; Kuijk, K.; Hart, C. M.; Cantatore, E.; Herwig, P. T.; van Breemen, A. J. J. M.; de Leeuw, D. M. *Nature* **2001,** *414,* 599.

[4] Gelinck, G. H.; Geuns, T. C. T.; de Leeuw, D. M. *Appl. Phys. Lett.* **2000,** *77,* 1487–1489.

[5] Crone, B. K.; Dodabalapur, A.; Sarpeshkar, R.; Filas, R. W.; Lin, Y. Y.; Bao, Z.; O'Neill, J. H.; Li, W.; Katz, H. E. J. *Appl. Phys.* **2001,** *89,* 5125–5132.

[6] Performance as measured by mobility and on/off ratio. See Katz, H. E.; Bao, Z. J. *Phys. Chem. B* **2000**, *104*, 671–678.

[7] Halik, M.; Klauk, H.; Zschieschang, U.; Schmid, G.; Radlik, W.; Weber, W. *Adv. Mater.* **2002,** *14,* 1717–1721.

[8] Bao, Z. N.; Feng, Y.; Dodabalapur, A.; Raju, V. R.; Lovinger, A. *J. Chem. Mat.* **1997,** *9,* 1299–1301.

[9] Kawase, T.; Sirringhaus, H.; Friend, R. H.; Shimoda, T. *Adv. Mater.* **2001,** *13,* 1601–1604.

[10] Weck, M.; Jackiw, J. J.; Rossi, R. R.; Weiss, P. S.; Grubbs, R. H. *J. Am. Chem. Soc.* **1999,** *121,* 4088–4089.

[11] Juang, A.; Scherman, O. A.; Grubbs, R. H.; Lewis, N. S. *Langmuir* **2001,** *17,* 1321–1323.

[12] Kim, N. Y.; Jeon, N. L.; Choi, I. S.; Takami, S.; Harada, Y.; Finnie, K. R.; Girolami, G. S.; Nuzzo, R. G.; Whitesides, G. M.; Laibinis, P. E. *Macromolecules* **2000,** *33,* 2793–2795.

[13] Watson, K. J.; Zhu, J.; Nguyen, S. T.; Mirkin, C. A. *J. Am. Chem. Soc.* **1999,** *121,* 462–463.

[14] Bielawski, C. W.; Grubbs, R. H. *Angew. Chem., Int. Ed.* **2000,** *39,* 2903–2906.

[15] In general, films produced with linker **4** were thicker than those produced with linker **5**. Catalyst attachment is likely more efficient with **4**; the reasons for this are currently under investigation.

[16] Choi, T. L.; Grubbs, R. H. *Angew. Chem., Int. Ed.* **2003,** *42,* 1743–1746.

[17] Bao, Z. N.; Rogers, J. A.; Katz, H. E. *J. Mater. Chem.* **1999,** *9,* 1895–1904.
[18] Loo, Y. L.; Someya, T.; Baldwin, K. W.; Bao, Z.; Ho, P.; Dodabalapur, A.; Katz, H. E.; Rogers, J. A. *Proc. Natl. Acad. Sci. USA* **2002,** *99,* 10252–10256.
[19] Increased grain-size was observed when pentacene was deposited over SI-ROMP polymer layers that had been annealed.
[20] Inokuma, S.; Sugie, A.; Moriguchi, K.; Shimomura, H.; Katsube, J. *Heterocycles* **1982,** *19,* 1909–1913.
[21] Schwab, P.; Grubbs, R. H.; Ziller, J. W. *J. Am. Chem. Soc.* **1996,** *118,* 100–110.
[22] Sanford, M. S.; Ulman, M.; Grubbs, R. H. *J. Am. Chem. Soc.* **2001,** *123,* 749–750.
[23] Hu, J.; Fox, M. A. *J. Org. Chem.* **1999,** *64,* 4959–4961.

Chapter 6

Ring-Opening Metathesis Polymerization of Functionalized-Low-Strain Monomers with Ruthenium-Based Catalysts

6.1 Abstract

A detailed study of the ring-opening metathesis polymerization of low-strain monomers with ruthenium catalysts is reported. The effects of monomer concentration, reaction temperature, and catalyst dependence are described for unsubstituted cycloolefins. The ROMP of low-strain olefins with polar substituents is also examined with ruthenium olefin metathesis catalysts and a predictive model for ROMP feasibility is proposed.

6.2 Introduction

Functionalized linear polymers represent an important class of materials. Several methods have been established to prepare functionalized polymers such as ionic and free radical polymerization of vinyl monomers, group transfer polymerization (GTP), and, more recently, ring-opening metathesis polymerization (ROMP).[1–3] ROMP is an attractive method to synthesize functional polymers as it is robust, produces absolutely linear material, and is amenable to forming various copolymers of controlled architecture.[4, 5] Substituted cyclobutenes and cyclooctenes have been used extensively to prepare linear polymers with a wide range of functionality.[6, 7] With these monomers it is difficult (or in the case of mono-substitution, impossible) to control the regioregularity of functionalities along the polymer backbone. Symmetrically substituted 5- and 7-membered ring monomers provide access to a range of regioregular polymers. Few examples, however, are reported in the literature.[8–11] The low ring strains inherent to 5-, 6-, and 7-membered cycloalkenes[12] make them more challenging substrates for ROMP.

The driving force behind the ROMP of cyclic olefins is the release of strain energy,[2] encompassed by the enthalpic term, ΔH, in the equation below.

$$\Delta G = \Delta H - T\Delta S$$

Monomer concentration and reaction temperature are intimately associated with thermodynamics of ROMP. For every cyclic olefin monomer, there exists a critical

monomer concentration below which no polymerization will occur at a given temperature. Performing the ROMP at low temperatures can mitigate the entropic loss inherent to all polymerizations and drive the reaction to high molecular weight polymer. Lower reaction temperatures, however, require catalysts with higher activities. As a result, ROMP of low-strain monomers has traditionally been performed with highly active early transition metal catalysts.[2, 9] Unfortunately, these catalysts are not tolerant of many polar functionalities. It is well established that ruthenium-based olefin metathesis catalysts, such as **1**, demonstrate significantly more tolerance towards polar functionality.[13, 14] It was recently demonstrated that catalyst **2** was capable of performing the ROMP of cyclopentene at 25 °C.[15] We now report that ruthenium catalysts **1**, **2**, and **3** (Figure 6.1) are all capable of polymerizing low-strain cycloolefins, so that the ROMP of 5- and 7-membered cycloalkenes with polar substituents can now be realized.

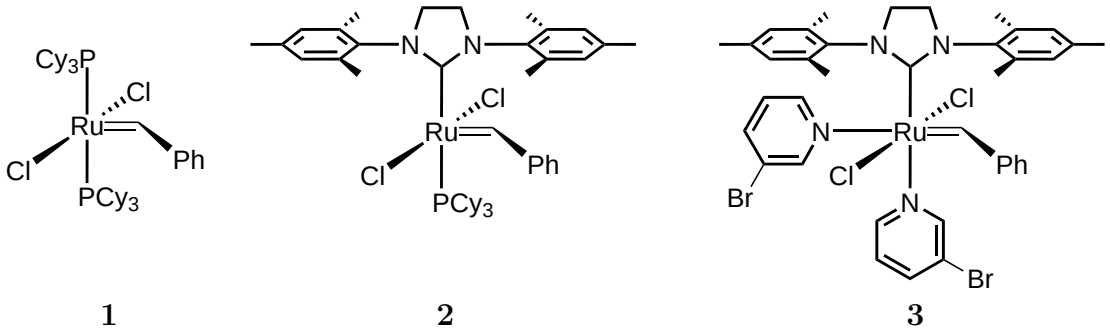

1 **2** **3**

Figure 6.1: Ruthenium olefin metathesis catlaysts.

6.3 Results and Discussion

6.3.1 ROMP of Unsubstituted Monomers

The ROMP of the low-strain monomers cyclopentene (**4**) and cycloheptene (**5**) was investigated with ruthenium catalysts **1**–**3** (Scheme 6.1). Polymerization behavior of **4** and **5** was studied with respect to catalyst loading, monomer concentration, and reaction temperature. The experimental strain energy for **4** and **5** are 6.8 and

Scheme 6.1: ROMP of cyclopentene and cycloheptene with ruthenium catalysts.

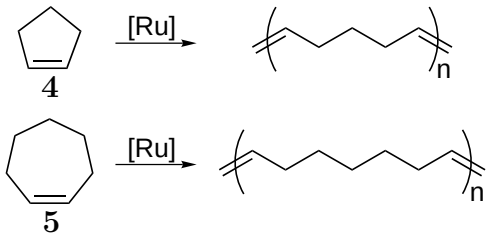

6.7 kcal/mol, respectively,[12] suggesting they should behave similarly with the olefin metathesis catalysts. Indeed, this appeared to be the case with a few notable exceptions (Table 6.1).

In agreement with previous reports that utilized early transition metal catalysts, relatively high yields of polymer could be obtained for neat polymerization with the ruthenium catalysts at 25 °C.[9] Entries 1–4 in Table 6.1 illustrate that yields of 80% and greater are obtained by the neat ROMP of **4** with ruthenium catalysts **1** and **2**, however, a low yield is obtained for neat ROMP of **4** and **5** with catalyst **3**. This is due to the sparing solubility of the bromo-pyridine catalyst in neat hydrocarbon monomers. In solution studies, where catalyst solubility is not a factor, the yields of polymer are all similar as expected. This can be seen in entries 6–8 in Table 6.1 which all produce polymer in comparable yield with catalyst **3** giving the best molecular weight control. By increasing the monomer to catalyst ratio, ([M]/[cat]), the yields remain constant with a commensurate increase in the molecular weights, M_{n}, for ROMP of monomer **4**. In the case of monomer **5**, however, the yields drop off as the monomer to catalyst ratio increases (entries 13–15). In all cases, yields decrease with a lower monomer concentration as expected with the thermodynamic constraints discussed previously for low-strain monomer.

6.3.2 ROMP of Substituted Monomers

After successfully demonstrating that catalysts **1**–**3** could ROMP monomers **4** and **5** to high molecular weight polymer, we decided to explore derivatives of these low-strain monomers bearing polar substituents. These functionalities are incompatible

Table 6.1: Results for the ROMP of **4** and **5** with ruthenium catalysts at 25 °C.

Entry	Monomer ([M])	Catalyst	[M]/[cat]	% yield	M_n ($\times 10^{-3}$) GPC[a]	PDI
1[c]	**4** (11.3)[a]	**1**	250	80	15.2	1.5
2[c]	**4** (11.3)[a]	**1**	500	92	27.1	1.6
3[c]	**4** (11.3)[a]	**1**	1000	84	75.4	1.6
4[c]	**4** (11.3)[a]	**2**	500	87	19.9	1.3
5[c]	**4** (11.3)[a]	**3**	500	38[f]	28.5	1.6
6[c]	**4** (5)[b]	**1**	500	64	22.1	1.5
7[c]	**4** (5)[b]	**2**	500	68	15.7	1.5
8[c]	**4** (5)[b]	**3**	500	67	13.3	1.3
9[c]	**4** (4)[b]	**1**	500	48	13.6	1.5
10[c]	**4** (4)[b]	**2**	500	51	38.4	1.5
11[c]	**4** (4)[b]	**3**	500	41	12.2	1.5
12[d]	**5** (8.6)[a]	**1**	250	84	23.7	1.3
13[d]	**5** (8.6)[a]	**2**	250	85	116	1.7
14[d]	**5** (8.6)[a]	**2**	500	67	160	1.7
15[d]	**5** (8.6)[a]	**2**	1000	23	191	1.6
16[d]	**5** (8.6)[a]	**3**	250	41[f]	50.2	1.6
17[d]	**5** (5)[b]	**1**	250	87	39.2	1.5
18[d]	**5** (5)[b]	**2**	250	86	53.9	1.5
19[d]	**5** (5)[b]	**3**	250	72	43.7	1.4
20[d]	**5** (2)[b]	**1**	250	64	24.8	1.6
21[d]	**5** (2)[b]	**2**	250	44	103	1.5
22[d]	**5** (2)[b]	**3**	250	64	35.6	1.4

[a]ROMP of neat monomer. [b]Polymerizations carried out in in CH_2Cl_2. [c]Polymerization time of 24 h. [d]Polymerization time of 30 min. [e]Samples run in THF; molecular weight values obtained using MALLS. [f]Low yields due to sparing solubility of **3** in neat monomers.

with early transition metal catalysts, but present no difficulty for the ruthenium systems.[5, 14, 15] This would allow for the direct preparation of polar functionalized linear polymers without the need for subsequent polymer modification.[4, 13] Furthermore, as we have previously demonstrated, ROMP of a symmetric monomer will ensure an absolutely regioregular polymer,[13, 16] thus providing new materials for detailed structure–property studies.

The addition of substituents to monomers **4** and **5** will certainly make the ROMP of these low-strain monomers more challenging.[2] This can be explained by the "*gem*-

dialkyl effect" whereby substituents on a ring serve to stabilize the ring-closed system relative to its linear counterpart.[17] As ROMP is a process governed by thermodynamic equilibrium, this effect results in a lower concentration of the linear polymer.

The polar monomers employed in this study, and shown in Scheme 6.2, possess ester, silyl ether, and ketone functionalities. The ROMP of monomers **6**, **7**, **8**, **9** provide a synthetic route for oxygen containing materials such as ethylene vinyl alcohol (EVOH) and ethylene carbon monoxide (E/CO) copolymers. These materials have been demonstrated to have useful properties in commercial applications.[13, 18, 19]

Scheme 6.2: ROMP of substituted low-strain monomers.

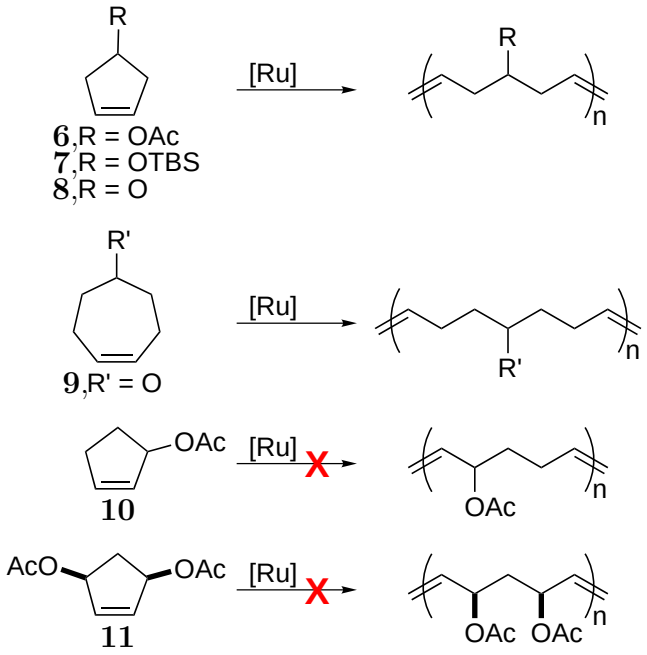

ROMP of the substituted monomers was successfully carried out neat at 25 °C with catalysts **1**–**3**, as illustrated in Table 6.2. Entries 1–6 in Table 6.2 illustrate that the ROMP of symmetric monomers **6** and **7** could be carried out in high yield and with controlled molecular weights with all three ruthenium catalysts. Moreover, no significant difference was observed in the ROMP of **6** and **7** as expected for structurally similar monomers. Monomer **8** does not undergo polymerization with catalysts **1** or **2**, indicating a low ring strain. Catalyst **3**, however, allows for the formation of **poly**(**8**) which is an insoluble material. This suggests that **poly**(**8**) is

trapped through a kinetic process.[1, 20, 21] Catalyst **3** is known to initiate much faster than either **1** or **2**, and may allow for rapid polymerization of **8** to high molecular weight insoluble polymer. No conditions were found under which monomers **10** and **11** would successfully polymerize.

Table 6.2: Results for the ROMP of **6**–**11** with ruthenium catalysts at 25 °C.

Entry	Monomer	Catalyst	[M]/[cat]	% yield	M_n ($\times 10^{-3}$) GPC[e]	PDI
1[c]	**6**	**1**	500	75	36.9	1.4
2[c]	**6**	**2**	500	66	28.9	1.3
3[c]	**6**	**3**	500	65	28.0	1.5
4[c]	**7**	**1**	150	72	18.7	1.7
5[c]	**7**	**2**	150	66	17.0	1.3
6[c]	**7**	**3**	150	71	16.6	1.3
7[c]	**8**	**1**	250	0	—	—
8[c]	**8**	**2**	250	0	—	—
9[c]	**8**	**3**	250	24	—	—
10[c]	**8**	**3**	500	63	5.6	1.8
11[d]	**10**	**1**	500	0	—	—
12[d]	**10**	**2**	500	0	—	—
13[d]	**10**	**3**	500	0	—	—
14[d]	**11**	**3**	250	0	—	—

[a]ROMP of neat monomer. [b]Polymerizations carried out in in CH_2Cl_2. [c]Polymerization time of 24 h. [d]Polymerization time of 30 min. [e]Samples run in THF; molecular weight values obtained using MALLS. [f]Low yields due to sparing solubility of **3** in neat monomers.

6.3.3 Model for Low-Strain ROMP

By varying the placement and nature of the substituents, we observed a marked effect on a monomer's potential to undergo ROMP. A method to predict whether or not ROMP of a particular monomer is feasible would be very helpful for the design of new functionalized monomers. The ease of ROMP is reflected by the strain energy of each monomer.[2, 13] Therefore, a model to predict strain energy should correlate to ROMP feasibility as well.

We chose to model the strain energy of a cyclic olefin with the enthalpic terms

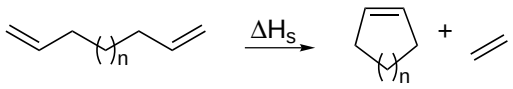

Figure 6.2: Isodesmic reaction used to calculate the strain energy released by ROMP.

of a ring-closing metathesis reaction (Figure 6.2). Our model reaction is isodesmic, having the same number and type of bonds in both reactants and products,[22] so that the change in energy is solely due to the strain inherent in the cycle form. The ring strain for the cyclic olefin is the difference in energy between the products and the reactant.

In order to validate our model, un-substituted, cyclic olefins ranging from cyclopropene to cyclooctene were calculated and compared with their experimentally determined strain energies. The calculations were carried out using DFT with a B3LYP functional and a 6-31G** basis set. As can be seen by the graph in Figure 6.3, the correlation of calculated values with experiment is quite good. Slightly larger deviations are observed for cycloheptene and cyclooctene as a result of a natural distribution of several conformers at 298 K for these larger rings that are not reflected in our calculations. We also carried out these calculations at a semi-empirical level of theory with AM1, PM3 and PM5 parameterization schemes; however, all of these resulted in poor agreement with experimental results.

Satisfied with our method, we proceeded to calculate the strain energies for the substituted monomers described above. The calculated values are shown in Table 6.3. Again, the experimental results we observe in this study appear to correlate with our model. Under our polymerization conditions, it appears that the minimal strain energy necessary for successful ROMP lies between 3.4 and 4.4 kcal/mol. The successful development of this model should allow for the evaluation of a new monomer's ability to undergo ROMP.

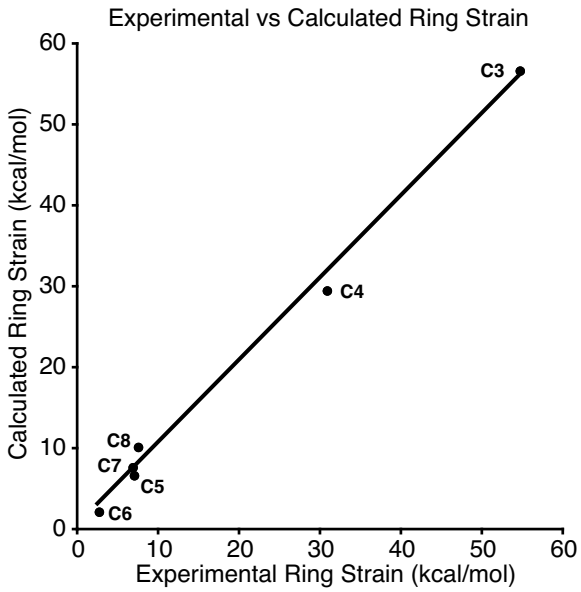

Figure 6.3: Graph depicting the correlation between calculated[12] and experimental strain energies.

Table 6.3: Calculated strain energies and "ROMP-ability" for several low-strain monomers.

Monomer	E_s(calc)[a]	ROMP[b]
5	7.84	yes
9	7.44	yes
4	6.84	yes
7	4.99	yes
6	4.47	yes
8	4.45	yes
10	3.36	no
11	2.29	no

[a]Strain energy in kcal/mol, calculated at DFT B3LYP/6-31G**. [b]Neat monomer, rt. [c]Only polymerizes with catalyst **3**.

6.4 Conclusions

The ROMP of cyclopentene and cycloheptene has been investigated with several ruthenium olefin metathesis catalysts. All of the catalysts employed afforded reasonable to high yields of ROMP polymer and demonstrated molecular weight control. As previously demonstrated, the polymer behavior is extremely dependent on the

monomer concentration. This is consistent with the thermodynamic governance of the ROMP process. The use of functional group tolerant ruthenium catalysts has also allowed for the incorporation of polar substituents pendent from the linear polymer backbone. When symmetrically substituted 5- and 7-membered ring monomers are polymerized, the resulting materials possess an absolutely linear structure with a perfectly regioregular distribution of functionality. In order to better understand the relationship between substitution patterns and ring strain of a cyclic olefin monomer, a simple model for predicting ring strains was developed. A high degree of correlation was found between experimental and calculated data for both substituted and unsubstituted cycloolefins. This model could be generally applied as a predictive tool for rational monomer design.

6.5 Experimental Section

Materials. Toluene and CH_2Cl_2 were dried by passage through solvent purification columns.[23] $(PCy_3)_2(Cl)_2Ru{=}CHPh$ (**1**),[24] $(H_2IMes)(PCy_3)(Cl)_2Ru{=}CHPh$ (**2**),[25] $(H_2IMes)(3\text{-Br-py})_2(Cl)_2Ru{=}CHPh$ (**3**),[26] 4-acetoxycyclopentene (**6**),[27, 28] 4-*tert*-butyldimethylsilyloxycyclopentene (**7**),[28] 4-cyclohepten-1-one (**9**),[29] and 3-acetoxycyclopentene (**10**)[30] were synthesized according to literature procedures. Cyclopentene (98%) (**4**) (TCI America), 3-cyclopenten-1-one (98%) (**8**) (Astatech), cycloheptene (97%) (**5**) (Pfaltz & Bauer), and *cis*-3,5-diacetoxycyclopentene (98%) (**11**) (Fluka) were used as received.

Methods and procedures. NMR spectra were recorded on either a Varian Mercury 300 (299.87 MHz for ^{1}H and 75.41 MHz ^{13}C) or a Varian Inova 500 (500.62 MHz for ^{1}H and 125.89 MHz ^{13}C). All NMR spectra were recorded in $CDCl_3$ and referenced to residual protio species. Gel permeation chromatography (GPC) was carried out in THF on two PLgel 5 μm mixed-C columns (Polymer Labs) connected in series with a DAWN EOS multiangle laser light scattering (MALLS) detector and an Optilab DSP differential refractometer (both from Wyatt Technology). No calibration standards were used, and dn/dc values were obtained for each injection assuming 100% mass

elution from the columns.

Computational methodology. All calculations were performed using the hybrid DFT functional B3LYP as implemented by the Jaguar 4.0 program package.[31] A 6-31G** basis set was used for all compounds.

Polymerization procedure, neat monomer. In a typical experiment, a small vial was charged with catalyst **1** (11.1 mg, 0.0135 mmol) and a stirbar under a flow of argon. Next, monomer **4** (0.30 mL, 0.231 g, 3.39 mmol, 251 equiv) was added via syringe at room temperature and the reaction was allowed to stir. The reaction mixture gelled within 1 min. After 24 h, the polymerization was quenched with 0.1 mL ethyl vinyl ether and then dissolved in 1 mL dichloromethane. The polymer solution was then precipitated into 75 mL of MeOH at 0 °C. The polymer precipitate was washed several times with MeOH and dried under vacuo overnight; yield 0.185 g (80%).

Polymerization procedure, in solution. In a typical experiment, a small vial was charged with monomer **5** (0.30 mL, 0.249 g, 2.59 mmol, 259 equiv) and a stirbar under a flow of argon. Next, 0.20 mL (0.01 mmol) of a catalyst **3** stock solution (0.05 M) was added via syringe at room temperature and the reaction was allowed to stir. The reaction mixture gelled within 1 min. After 30 min, the polymerization was quenched with 0.1 mL ethyl vinyl ether and then dissolved in 1 mL dichloromethane. The polymer solution was then precipitated into 75 mL of MeOH at 0 °C. The polymer precipitate was washed several times with MeOH and dried under vacuo overnight; yield 0.180 g (72%).

Polymer characterization. For **poly**(**4**): ^{1}H NMR (500.62 MHz, $CDCl_3$, δ): 5.42–5.33 (m, 2H, H_a), 2.08–1.90 (m, 4H, H_b), 1.39 (quint, J = 7.5 Hz, 2H, H_c). $^{13}C\{^1H\}$ NMR (125.89 MHz, $CDCl_3$, δ): 130.45 (C1 *t*), 129.94 (C1 *c*), 32.51 (C2 *tc*), 32.37 (C2 *tt*), 30.01 (C3 *ct/tc*), 29.86 (C3 *tt*), 27.06 (C2 *ct*).

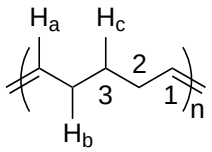

poly(4)

For **poly**(**5**): ^{1}H NMR (299.87 MHz, $CDCl_3$, δ): 5.41–5.31 (m, 2H, H_a), 2.08–1.90 (m, 4H, H_b), 1.40–1.22 (m, 6H, H_c/H_d). $^{13}C\{^{1}H\}$ NMR (75.41 MHz, $CDCl_3$, δ): 130.53 (C1 *t*), 130.07 (C1 *c*), 32.99 (C2 *t*), 30.08 (C3 *cc*), 30.04 (C3 *ct*), 29.97 (C3 *tc*), 29.93 (C3 *tt*), 29.38 (C4 *cc*), 29.26 (C4 *ct/tc*), 29.13 (C4 *tt*), 27.60 (C2 *c*).

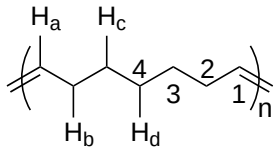

poly(5)

For **poly**(**6**): ^{1}H NMR (299.87 MHz, $CDCl_3$, δ): 5.5–5.3 (br m, 2H, H_a), 4.82 (br m, 1H, H_c), 2.3–2.15 (br m, 4H, H_b), 1.99 (s, 3H, OAc). $^{13}C\{^{1}H\}$ NMR (75.41 MHz, $CDCl_3$, δ): 170.82 (OAc–C=O), 128.68 (C1 *t*), 127.41 (C1 *c*), 73.20 (C3), 73.04 (C3), 37.09 (C2), 31.91 (C2), 21.44 (OAc–CH_3).

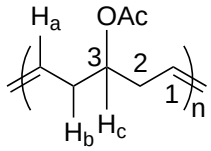

poly(6)

For **poly**(**7**): ^{1}H NMR (299.82 MHz, $CDCl_3$, δ): 5.56–5.31 (br m, 2H, H_a), 3.74–3.55 (br m, 1H, H_c), 2.30–1.98 (br m, 4H, H_b), 0.88 (s, 9H, Si–*t*Bu), 0.03 (s, 6H, Si–Me_2). $^{13}C\{^{1}H\}$ NMR (75.40 MHz, $CDCl_3$, δ): 129.36 (C1 *t*), 127.87 (C1 *c*), 72.91 (C3), 40.81 (C2), 35.61 (C2), 26.24 (Si–C(**C**H_3)$_3$), 18.49 (Si–**C**(CH_3)$_3$), -4.12 (Si–(**C**H_3)$_2$).

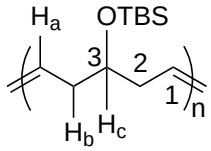

poly(7)

For **poly**(**8**): **poly**(**8**) is an intractable solid and solution phase characterization has been unsuccessful to date.

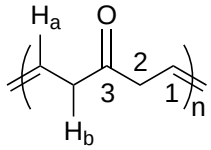

poly(8)

For **poly**(**9**):^{1}H NMR (299.82 MHz, $CDCl_3$, δ): 5.42–5.28 (m, 2H, H_a), 2.48–2.38 (m, 4H, H_c), 2.32–2.18 (m, 4H, H_b). $^{13}C\{^{1}H\}$ NMR (75.40 MHz, $CDCl_3$, δ): 209.92 (C4), 129.80 (C1 *t*), 129.37 (C1 *c*), 42.80 (C3 *c*), 42.76 (C3 *t*), 26.90 (C2 *t*), 21.81 (C2 *c*).

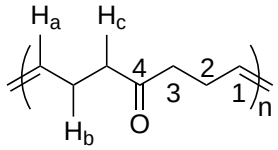

poly(9)

6.6 Acknowledgements

The authors thank Daniel P. Sanders and Professor Dennis A. Dougherty for helpful discussions. This work was supported by the National Science Foundation.

References Cited

[1] Grubbs, R. H., Ed.; *Handbook of Metathesis;* Wiley-VCH: Weinheim, 2003.

[2] Ivin, K. J.; Mol, J. C. *Olefin Metathesis and Metathesis Polymerization;* Academic Press: London, 1997.

[3] Odian, G. *Principles of Polymerization;* Wiley & Sons: New York, 3rd ed.; 1991.

[4] Lynn, D. M.; Kanaoka, S.; Grubbs, R. H. *J. Am. Chem. Soc.* **1996,** *118,* 784–790.

[5] Choi, T. L.; Grubbs, R. H. *Angew. Chem., Int. Ed.* **2003,** *42,* 1743–1746.

[6] Maughon, B. R.; Grubbs, R. H. *Macromolecules* **1997,** *30,* 3459–3469.

[7] Hillmyer, M. A.; Laredo, W. R.; Grubbs, R. H. *Macromolecules* **1995,** *28,* 6311–6316.

[8] Dounis, P.; Feast, W. J.; Kenwright, A. M. *Polymer* **1995,** *36,* 2787–2796.

[9] Schrock, R. R.; Yap, K. B.; Yang, D. C.; Sitzmann, H.; Sita, L. R.; Bazan, G. C. *Macromolecules* **1989,** *22,* 3191–3200.

[10] Trzaska, S. T.; Lee, L. B. W.; Register, R. A. *Macromolecules* **2000,** *33,* 9215–9221.

[11] Patton, P. A.; Lillya, C. P.; Mccarthy, T. J. *Macromolecules* **1986,** *19,* 1266–1268.

[12] Schleyer, P. v. R.; Williams, J. E.; Blanchard, K. R. *J. Am. Chem. Soc.* **1970,** *92,* 2377–2386.

[13] Scherman, O. A.; Kim, H. M.; Grubbs, R. H. *Macromolecules* **2002,** *35,* 5366–5371.

[14] Hillmyer, M. A.; Lepetit, C.; McGrath, D. V.; Novak, B. M.; Grubbs, R. H. *Macromolecules* **1992,** *25,* 3345–3350.

[15] Bielawski, C. W.; Grubbs, R. H. *Angew. Chem., Int. Ed.* **2000,** *39,* 2903–2906.

[16] Wagener, K. B.; Patton, J. T.; Forbes, M. D. E.; Myers, T. L.; Maynard, H. D. *Polym. Int.* **1993,** *32,* 411-415.

[17] Allinger, N. L.; Zalkow, V. *J. Org. Chem.* **1960,** *25,* 701–704.

[18] Drent, E.; van Broekhoven, J. A. M.; Budzelaar, P. H. M. *Recl. Trav. Chim. Pays-Bas* **1996,** *115,* 263–270.

[19] Sen, A. *Chemtech* **1986,** *16,* 48–51.

[20] Scherman, O. A.; Rutenberg, I. M.; Grubbs, R. H. *J. Am. Chem. Soc.* **2003,** *125,* 8515–8522.

[21] Scherman, O. A.; Grubbs, R. H. *Synth. Met.* **2001,** *124,* 431–434.

[22] Lewis, L. L.; Turner, L. L.; Salter, E. A.; Magers, D. H. *J. Mol. Struct., Theochem.* **2002,** *592,* 161–171.

[23] Pangborn, A. B.; Giardello, M. A.; Grubbs, R. H.; Rosen, R. K.; Timmers, F. J. *Organometallics* **1996,** *15,* 1518–1520.
[24] Schwab, P.; Grubbs, R. H.; Ziller, J. W. *J. Am. Chem. Soc.* **1996,** *118,* 100–110.
[25] Sanford, M. S.; Ulman, M.; Grubbs, R. H. *J. Am. Chem. Soc.* **2001,** *123,* 749–750.
[26] Sanford, M. S.; Love, J. A.; Grubbs, R. H. *Organometallics* **2001,** *20,* 5314–5318.
[27] Goering, H. L.; Seitz, Jr., E. P.; Tseng, C. C. *J. Org. Chem.* **1981,** *46,* 5305–5308.
[28] Buckley, S. L. J.; Drew, M. G. B.; Harwood, L. M.; Macias-Sanchez, A. J. *Tetrahedron Lett.* **2002,** *43,* 3593–3596.
[29] Marshall, J. A.; Royce, R. D. *J. Org. Chem.* **1982,** *47,* 693–698.
[30] Goering, H. L.; Kantner, S. S.; Seitz, Jr., E. P. *J. Org. Chem.* **1985,** *50,* 5496–5499.
[31] Jaguar 4.0, Schrodinger, Inc., Portland, Oregon, 2000.

Chapter 7

Synthesis of Well-Defined Poly(vinylalcohol$_2$-*alt*-methylene) via Ring-Opening Metathesis Polymerization

This chapter has previously appeared as: Scherman, O. A.; Kim, H. M.; Grubbs, R. H. *Macromolecules* **2002**, *35*, 5366–5371.

7.1 Abstract

The synthesis of a new methylene-(vinyl alcohol) copolymer, poly((vinyl alcohol)$_2$-*alt*-methylene) (MVOH), by ring-opening metathesis polymerization with ruthenium catalysts is reported. Unsaturated cyclic 1,3-diols were protected with a di-*tert*-butylsilyl group to form strained cyclic olefins. The molecular weights of the polymers were controlled by varying the monomer-to-catalyst ratios or by the addition of a chain transfer agent. Hydrogenation and subsequent deprotection of the ROMP polymers yield the MVOH copolymer structure which was confirmed by ^{1}H NMR and ^{13}C NMR spectroscopies. Thermal properties of the corresponding MVOH copolymer are reported.

7.2 Introduction

Interest in making well-defined linear polymers with alcohol functionalities is spurred by the commercial utility of ethylene-(vinyl alcohol) (EVOH) copolymers. EVOH copolymers are a class of materials that exhibit excellent barrier properties towards gases and hydrocarbons[1] and have found use in the food packaging and in biomedical and pharmaceutical industries.[1, 2] Furthermore, the lack of understanding of the property–structure relationships in these materials has fueled academic interest in the microstructure of EVOH copolymers.[2–5] The most widely employed synthetic route to EVOH copolymers is the free radical polymerization of ethylene and vinyl acetate, followed by saponification.[3] These EVOH copolymers contain a degree of branching, much like low-density polyethylene (LDPE), and have a random distribution of alcohol functionality along the polymer backbone[2, 4] both of which limit the elucidation of the structure–property relationships in these materials.

The direct incorporation of polar functional groups along the backbone of linear polymers made via ring-opening metathesis polymerization (ROMP) is now possible due to the development of functional group tolerant late transition metal olefin metathesis catalysts. Recently, Hillmyer *et al.* reported the ROMP of cyclooctenes

bearing an alcohol-, ketone-, halogen-, or acetate substituent with a ruthenium olefin metathesis catalyst.[6] However, the asymmetry of the substituted cyclooctene allowed for head-to-head (HH), head-to-tail (HT), and tail-to-tail (TT) coupling, yielding polymer with regiorandom placement of the functional groups.[6] A similar problem was encountered by Chung *et al.*, who reported the ROMP of a borane-substituted cyclooctene with an early transition metal catalyst followed by oxidation to yield an alcohol functionalized linear polymer.[3] A solution to this regiorandom distribution of functional groups was reported by Valenti *et al.* using the acyclic diene metathesis (ADMET) polymerization of an alcohol-containing symmetric diene.[4, 7] However, the molecular weights of these polymers are restricted to $< 3 \times 10^4$ by ADMET,[4] and their rich hydrocarbon content limits the barrier properties of the final EVOH copolymers.[1]

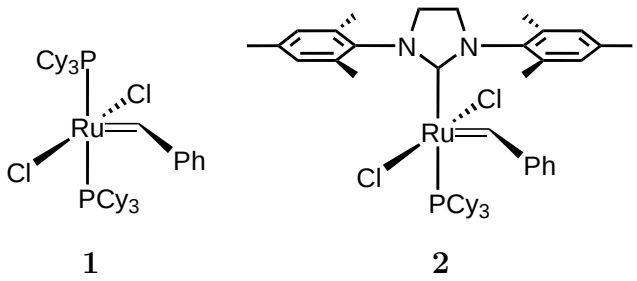

1 **2**

Figure 7.1: Ruthenium olefin metathesis catalysts (Cy=cyclohexyl).

To produce copolymers with a high content of precisely spaced alcohol functionalities, we favor a polymerization scheme involving the ROMP of a symmetric alcohol-containing monomer with functional group tolerant ruthenium catalysts, $(PCy_3)_2(Cl)_2Ru{=}CHPh$ (**1**)[8] and $(IMesH_2)(PCy_3)(Cl)_2Ru{=}CHPh$ (**2**)[9] (Figure 7.1).

Catalysts **1** and **2** have been shown to afford the ROMP of many substituted cyclic olefins.[10–13] Recent development of ruthenium catalysts, such as **2**, coordinated with an N- heterocyclic carbene has allowed for the ROMP of low-strain cyclopentene and substituted cyclopentene.[10] The ROMP of a symmetric cyclopentene yields a regioregular polyalkene as no difference exists between HH, HT, and TT couplings. Hence, the ROMP of alcohol- or acetate-disubstituted cyclopentene monomers was

Scheme 7.1: Attempt to ROMP cyclopentene monomers **3** and **4**.

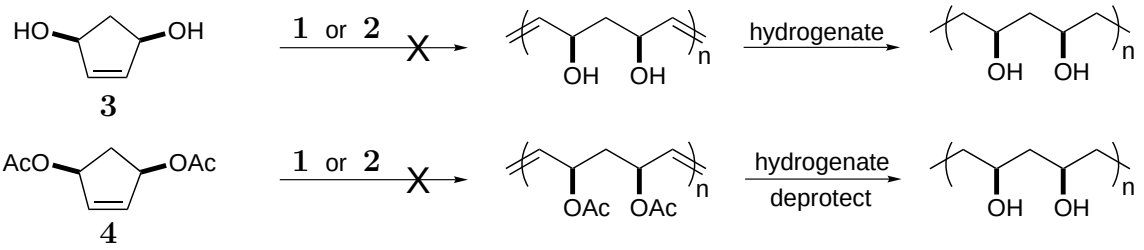

attempted (Scheme 7.1).

Unfortunately, neither catalyst **1** nor the more active **2** could afford the ROMP of these cyclopentene monomers, most likely due to their low ring strain. In addition, the oxygen-containing substituents may coordinate to the olefin metathesis catalysts or sterically inhibit catalyst coordination with the olefin. Therefore, a different protection strategy was employed in an effort to maintain the 1,3-substituted cyclopentene structure while temporarily increasing monomer ring strain and moving the oxygen functionalities further from the olefin to facilitate ROMP.

A general synthetic route to a linear polymer with precisely-spaced alcohol functionalities is displayed in Scheme 7.2. In this paper, we describe a method to produce a new vinyl alchol copolymer, poly((vinyl alcohol)$_2$-*alt*-methylene) (MVOH). This alternating MVOH copolymer has a high content of precisely-spaced vinyl alcohol functionalities which are *cis* within each monomer repeat unit and, depending upon the relative orientation between adjacent monomer units, may provide for tacticity in the MVOH material.

Scheme 7.2: A bicyclic protection strategy enroute to MVOH through a temporarily strained, symmetric monomer.

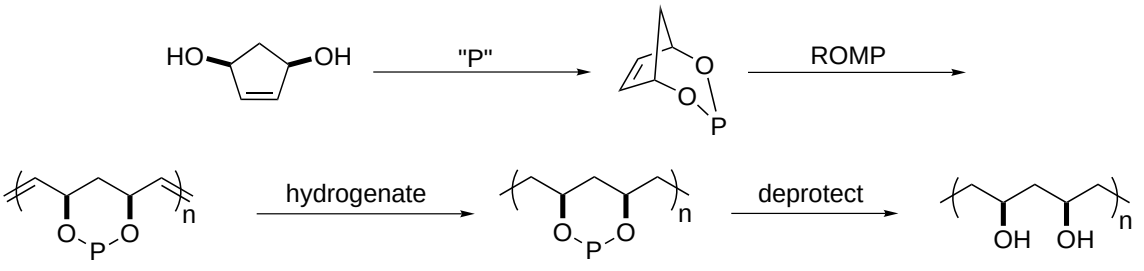

7.3 Results and Discussion

7.3.1 Monomer Design and Synthesis

We believe the ROMP of monomers **3** and **4** was not successful due to low ring strain,[10] to possible heteroatom coordination with catalysts **1** and **2**, or by steric hinderance of the olefin. Hence, a highly strained, bicyclic monomer, 3,3-di-*tert*-butyl-2,4-dioxa-3-sila-bicyclo[3.2.1]oct-6-ene, (**5**) was readily synthesized[14] to overcome these problems. Monomer **5** maintains symmetry and a 1,3-diol relationship that, upon hydrogenation and silane deprotection, ensures an alternating copolymer with two successive vinyl alcohol units followed by a methylene unit (Scheme 7.3). Also, the symmetry of a five-member ring with 1,3-substitution dictates a regioregular polymer as head-to-head and head-to-tail connections are equivalent. Furthermore, by tying up the heteroatoms with the silane, a *cis* relationship in each repeat unit between the vinyl alcohols is maintained. Depending on the *cis*/*trans* ratio of the ROMP polymer, tacticity in the final MVOH copolymer may be affected.[12, 13]

Scheme 7.3: Synthetic route to MVOH through a temporarily strained, symmetric bicyclic monomer.

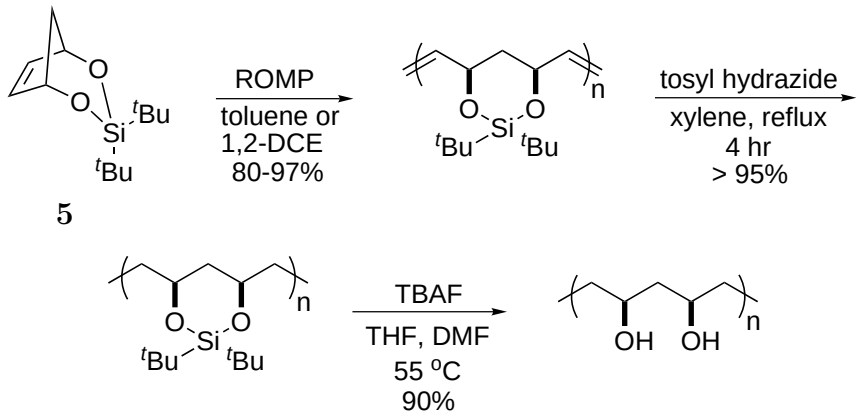

7.3.2 ROMP of Bicyclic Silicon-Protected Diol with 1

Previous results have demonstrated that the ROMP of norbornene and oxanorbornenes with **1** is a controlled polymerization.[15, 16] It is therefore reasonable to believe that the ROMP of **5** with catalyst **1** might also be a controlled polymerization.

Upon exposure to catalyst **1**, monomer **5** undergoes ROMP and gels quickly (Figure 7.2). Therefore, polymerizations were carried out in solution (1:1 vol) with either toluene or 1,2-dichloroethane (1,2-DCE) to ensure a homogeneous polymerization. Monomer **5** was polymerized with varying amounts of **1** at 55 °C (Table 7.1). All polymerizations reached high conversion ($\geq$ 80%) in approximately 1 day and were fully characterized by ^{1}H/^{13}C NMR (Figure 7.5a and c) and MALLS/SEC. Over the molecular weight range 2 x 10^4–2.2 x 10^5 g/mol, PDI values were relatively low and constant for polymers produced in both chlorinated and aromatic solvents. Also, it is evident that the [**5**]/[**1**]ratio is reflected in the M_{n} of each polymer in a linear fashion.

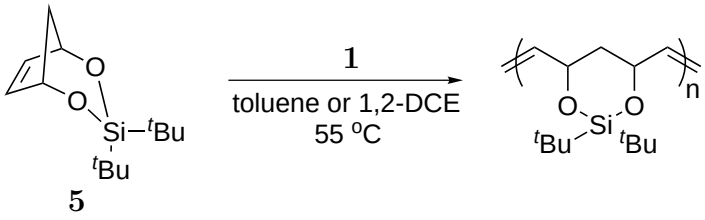

Figure 7.2: ROMP of monomer **5** with catalyst **1**.

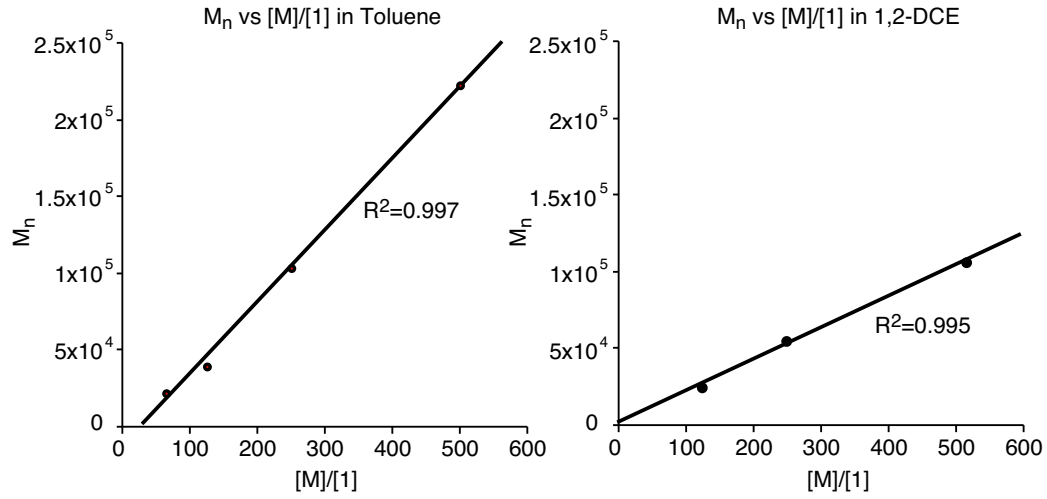

Figure 7.3: Graphs of M_{n} vs [monomer]/[catalyst]ratio for the ROMP of **5** with **1** in toluene and 1,2-DCE.

The graphs in Figure 7.3 display the molecular weight vs [monomer]/[catalyst]ratios for the series **P1**–**4**, carried out in toluene, and **P5**–**7**, carried out in 1,2-DCE. The

slopes of the graphs in Figure 7.3 differ by a factor of approximately 2, which indicates a difference in the initiation rates of catalyst **1** in toluene and 1,2-DCE. Catalyst **1** appears to be initiating more readily in 1,2-DCE (**P5**–**7**), as the slope of roughly 1 is obtained when plotting DP vs. [monomer]/[catalyst].[17] A difference in initiation rates for **1** has been previously observed by Sanford *et al.*,[11] and these data are consistent with faster initiation in chlorinated vs aromatic solvents. Low PDI's and the linear relationship between molecular weight vs [monomer]/[catalyst]are characteristic of a controlled polymerization.

Table 7.1: ROMP of **5** with **1**

Polymer	[**5**]/[**1**]	time (h)	% yield	M_n ($\times 10^{-3}$) GPC[a]	M_w ($\times 10^{-3}$) GPC[a]	PDI
P1[b]	63	21	90	21.8	28.4	1.3
P2[b]	130	17	97	39.3	51.7	1.3
P3[b]	250	24	95	103.4	139.2	1.3
P4[b]	510	18	95	222.3	309.1	1.4
P5[c]	120	21	84	24.2	33.7	1.4
P6[c]	250	27.5	77	55.3	73.9	1.3
P7[c]	510	27.5	80	105.8	131.6	1.2

[a]Samples run in THF; molecular weight values obtained using MALLS with an average dn/dc value of 0.108 mL/g. [b]Polymerizations run in toluene. [c]Polymerizations run in 1,2-DCE.

7.3.3 ROMP of Bicyclic Silicon-Protected Diol with 2 and a Chain Transfer Agent

Telechelic polymers can be made readily via ROMP of a cylic olefin with a symmetric chain transfer agent (CTA).[18–21] With the more active catalyst **1**, the molecular weight of the resulting polymer is controlled solely by the [monomer]/[CTA]ratio at thermodynamic equilibrium; furthermore, much lower catalyst loadings can be employed, thereby reducing costs considerably. When the ROMP of **5** with CTA **6** is carried out in toluene (Figure 7.4), the M_n is controlled by the ratio of [**5**]/[**6**], and high conversions are obtained with a catalyst loading up to 4 x 10^4.

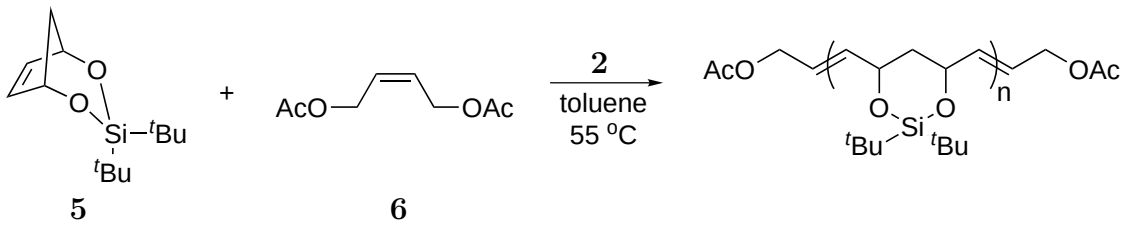

Figure 7.4: ROMP of monomer **5** with catalyst **2** and chain transfer agent **6**.

Entries **P8–10** in Table 7.2 indicate that thermodynamic equilibrium is reached within 24 h, after which the molecular weight and conversion remain constant. As expected, as the [monomer]/[CTA]ratio is doubled, the M_{n} increases by a factor of two (**P8** & **P11**).

Table 7.2: ROMP of **5** with **2** and CTA **6**

Polymer[b]	[**5**]/[**2**]	[**5**]/[**6**]	time (h)	% yield	M_{n} ($\times 10^{-3}$) GPC[a]	M_{w} ($\times 10^{-3}$) GPC[a]	PDI
P8	20000	100	23	84	57.4	57.4	2.5
P9	20000	100	70	82	58.3	58.3	2.3
P10	20000	100	113	80	57.1	151.1	2.6
P11	40000	200	22	87	120.2	278.7	2.3

[a]Samples run in THF; molecular weight values obtained using MALLS with an average dn/dc value of 0.110 mL/g. [b]All polymerizations run in toluene.

7.3.4 Hydrogenation of Polymers

Hydrogenation of the polymer backbone was carried out in high yield by tosyl hydrazide reduction in refluxing xylenes.[22–26] The saturated polymers were fluffy white solids and were characterized by ^{1}H and ^{13}C NMR as well as MALLS/SEC. Figure 7.5a displays the ^{13}C NMR spectrum of the unsaturated polymer backbone made with catalyst **1**. Upon hydrogenation, the loss of olefinic carbons is clearly evident in Figure 7.5b as the carbon, 1, in the sp^2 region at 131–132 ppm has disappeared and a new carbon, 1', appears in the sp^3 region at 34 ppm. Figure 7.5c displays the ^{1}H NMR spectrum prior to saturation of the backbone. The four peaks between 4 and 6 ppm

in Figure 7.5c represent the two sets of *cis* and *trans* olefin protons, H_a, and methine protons, H_b. For polymers made with catalyst **1** (**P1**–**7**), integration is consistent between the two sets with a 1.4/0.6 *trans*/*cis* ratio or 70% *trans* olefins along the polymer backbone, while the polymers made with catalyst **2** (**P8**–**11**) consisted of 50% *trans* olefins.[27] These sets of peaks disappear (Figure 7.5d) upon hydrogenation as the *cis* and *trans* methine protons collapse to a singe peak, H_f, at 4 ppm and new methylene protons, H_e + $H_{g/h}$, appear between 1.4 and 1.6 ppm.

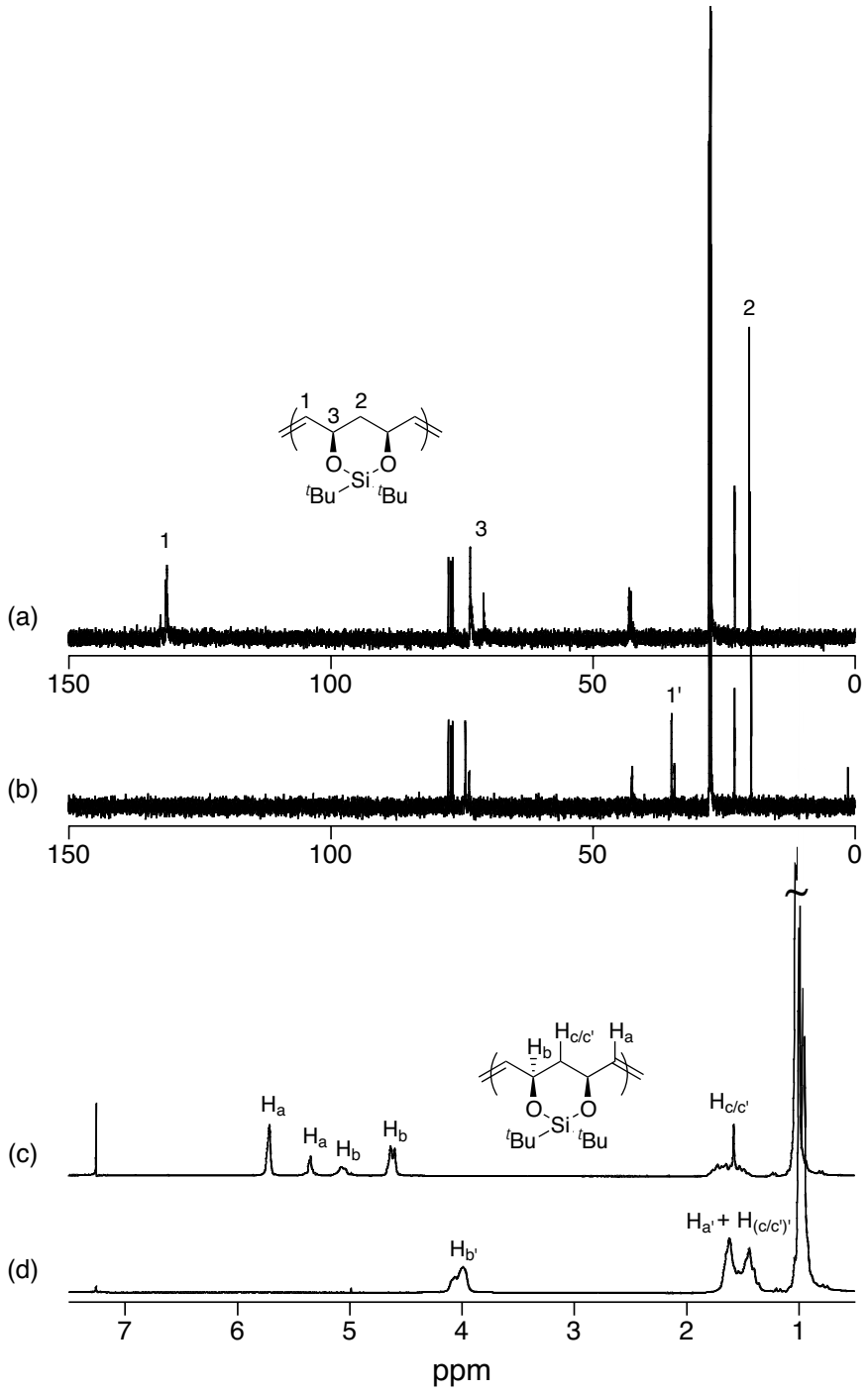

Figure 7.5: (a) ^{13}C NMR spectrum of ROMP polymer from monomer **5** with catalyst **1**. (b) ^{13}C NMR spectrum of polymer after hydrogenation. (c) ^{1}H NMR spectrum of ROMP polymer from monomer **5** with catalyst **1**. (d) ^{1}H NMR spectrum of polymer after hydrogenation.

7.3.5 Deprotection of Polymers

Deprotection of the saturated polymer was accomplished with tetrabutylammonium fluoride (TBAF) in (3:1 v/v) THF:DMF to produce the new alternating MVOH copolymer. It was necessary to use DMF as a cosolvent in the deprotection step so that the polymeric material would remain soluble throughout the entire reaction. Reactions carried out solely in THF resulted in incomplete deprotection. MVOH copolymers could then be obtained as a whitish, stringy solid by precipitation from the THF/DMF solution into a MeOH:CH_2Cl_2 (1:1 v/v) solution. Once dried, the MVOH copolymers were readily soluble in DMSO (at room temperature), but not in DMF, water, THF, or MeOH. MALLS/SEC characterization was not carried out on the final product due to the insolubility of MVOH copolymer in THF.

Only three sets of carbon resonances are observed in the ^{13}C NMR spectrum of poly((vinyl alcohol)$_2$-*alt*-methylene) (originating from the ROMP polymer produced with catalyst **1**) in DMSO-d_6, as shown in Figure 7.7a. The peaks labeled 1 and 3 in Figure 7.7a consist of two peaks as shown in the insets. Recent research has elucidated the tacticity of poly(vinyl alcohol) (PVA) homopolymer with high field NMR spectrometers.[28, 29] Nagara *et al.* report that the chemical shift data for the methine carbon (carbon 3 in Figure 7.7a) follows the trend for triads: $\delta_{mm} > \delta_{rm/rm} > \delta_{rr}$.[29] By analogy, the methine region in Figure 7.7a is suggestive of a higher m dyad tacticity for MVOH produced with catalyst **1**. In contrast, the equal intensities of these peaks in the material produced with catalyst **2** suggest equal m and r dyad distributions; the m and r dyads are shown in (Figure 7.6). The carbon assigned as 2 can only exist in one local environment as the two alcohol functionalities that surround it must always be in a *cis* relationship.

The ^{1}H NMR spectra in Figure 7.7b shows complete removal of the silane protect-

Figure 7.6: Structures of the m and r dyads in the MVOH polymer.

ing group, as no signals are present around 1.0 ppm. The peak at 4.5 ppm, H_d, was assigned to the alcohol protons as it disappeared upon addition of D_2O, leaving the peak at 3.6 ppm, H_a, to be assigned to the methine protons. The remaining peaks between 1.2 and 1.6 ppm, $H_{b/b'} + H_{c/c'}$, are assigned as the 6 methylene protons. All of these assignments are in good agreement with the similar EVOH copolymers previously prepared,[2, 30] and the ^{1}H NMR spectra for MVOH made with catalysts **1** and **2** are the same.

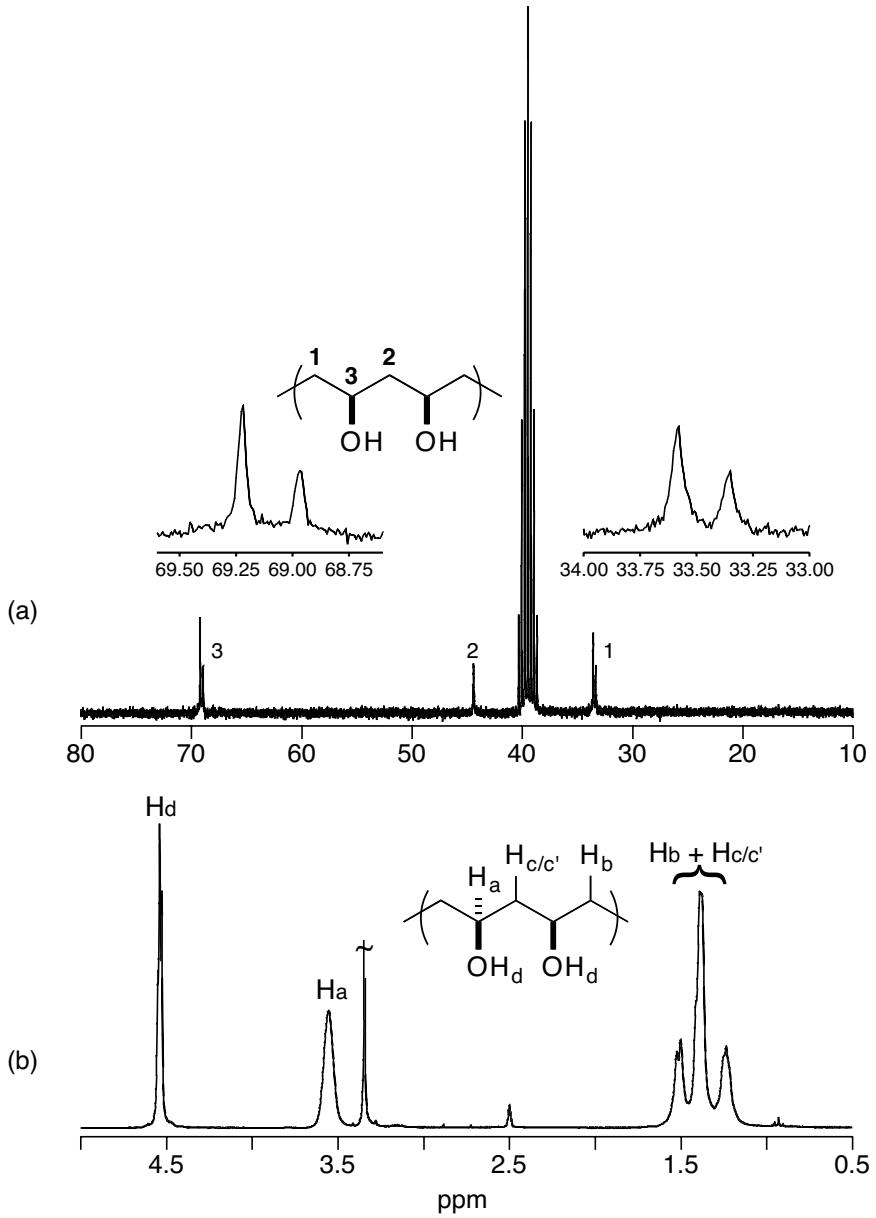

Figure 7.7: ^{13}C NMR spectrum (a) ^{1}H NMR spectrum (b) of unprotected MVOH polymer (originating from the ROMP of monomer **5** with catalyst **1**.

7.3.6 Thermal Analysis

Figure 7.8a shows the DSC thermogram of the MVOH copolymer, originating from catalyst **1**, with a clear melting transition at 193 °C (peak, 180 °C onset; a T_{m} of 180 °C was observed for the MVOH originating from catalyst **2**). This high T_{m} is consistent with a higher vinyl alcohol content in the copolymer as Mori *et al.* have shown that the T_{m} of EVOH copolymers varies over the range of ca.120–200 °C with increasing vinyl alcohol content.[30] The TGA curve displayed in Figure 7.8b shows an onset to decomposition at 360 °C. The thermal stability of the MVOH copolymer is substantially better than PVA homopolymer which displays thermal weight loss slightly below 300 °C.[3] A small decrease in weight is observed in the TGA curve around 60 °C and coincides with a large peak in the DSC thermogram. This is consistent with elimination of methanol, likely trapped in the MVOH copolymer upon precipitation. The melting temperature and increased thermal stability relative to PVA are comparable with structurally similar EVOH materials.[3, 30–32]

7.4 Conclusions

The successful ROMP of temporarily strained cyclopentene derivatives with ruthenium olefin metathesis catalysts **1** and **2** has been demonstrated. The symmetry of the monomer allowed for the placement of precisely defined alcohol functionality along the polymer backbone. Hydrogenation of the polymers followed by silane deprotection allowed for the synthesis of a new methylene-(vinyl alcohol) polymer which is similar to EVOH copolymers in structure and properties. Polymers were isolated in high yield and characterized by ^{1}H and ^{13}C NMR spectroscopies. Molecular weight of the polymers could be controlled over a large range by varying the monomer-to-catalyst ratio as well as by addition of chain transfer agents to the polymerization. Thermal properties of the new copolymer was determined by DSC and TGA analysis and showed a higher thermal stability than PVA. To our knowledge, these MVOH copolymers represent the first vinyl alcohol–hydrocarbon materials that can be syn-

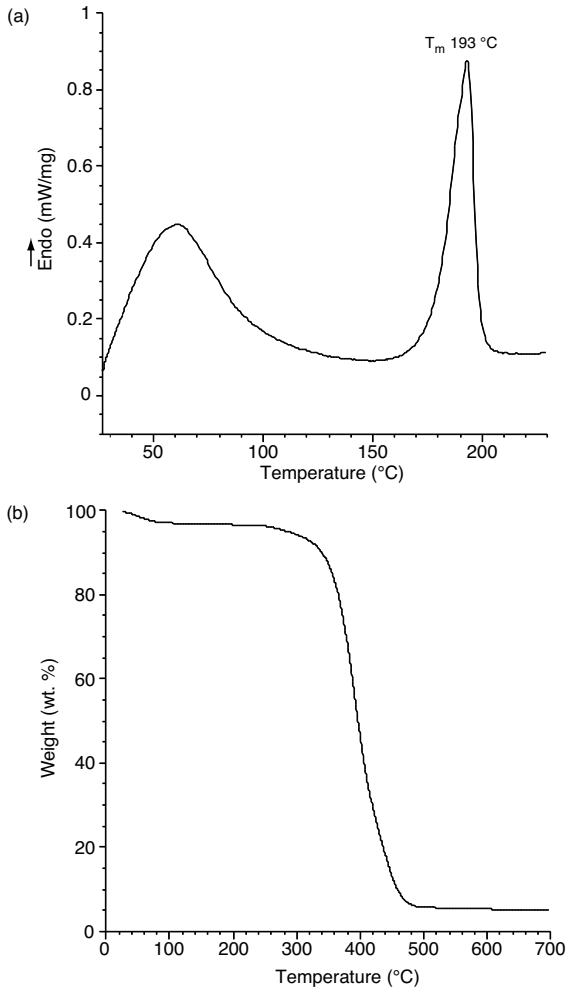

Figure 7.8: (a) DSC heating scan of deprotected MVOH polymer at a scan rate of 10 °C/min. (b) Thermogravimetric analysis of deprotected MVOH polymer at a scan rate of 10 °C/min under N_2 purge.

thesized in a controlled fashion over a large molecular weight range, are completely regioregular, and contain a desirable high alcohol percentage. This should allow for a more detailed understanding of the structure–property relationship in EVOH-type materials and aid in studies of grafting materials such as lactic acid[33] and/or functional groups[5] from the alcohol functionalities. Finally, this methodology is currently being applied toward other heteroatom-containing, temporarily strained cycloolefin monomers.

7.5 Experimental Section

General Procedures. NMR spectra were recorded on a Varian Mercury 300 (300 MHz for ^{1}H and 74.5 MHz for ^{13}C). All NMR spectra were recorded in $CDCl_3$ or DMSO-d_6 and referenced to residual proteo species. Gel permeation chromatography (GPC) was carried out on two PLgel 5 μm mixed-C columns (Polymer Labs) connected in series with a DAWN EOS multi angle laser light scattering (MALLS) detector and an Optilab DSP differential refractometer (both from Wyatt Technology). No calibration standards were used, and dn/dc values were obtained for each injection assuming 100% mass elution from the columns. Differential scanning calorimetry (DSC) and thermogravimetric analysis (TGA) was carried out simultaneously on a Netzsch STA 449C under a flow of N_2 at a heating rate of 10 °C/min.

Materials. Toluene was dried by passage through solvent purification columns.[34] *cis*-4-Cyclopentene-1,3-diol (> 99%) was obtained from Fluka and used as received. *cis*-1,4-Diacetoxy-2-butene (95+%) (**6**) was obtained from TCI America and degassed by an argon purge prior to use. *N*,*N*-Dimethylformamide (anhydrous) (DMF), 1,2-dichloroethane (anhydrous), 2,6-lutidine (99+%, redistilled) and di-*tert*-butylsilyl-bis(trifluoromethanesulfonate) (97%) were obtained from Aldrich and used as received. $(PCy_3)_2(Cl)_2Ru{=}CHPh$ (**1**),[8] $(IMesH_2)(PCy_3)(Cl)_2Ru{=}CHPh$ (**2**),[35] and 3,3-di-*tert*-butyl-2,4-dioxa-3-sila-bicyclo[3.2.1]oct-6-ene[14] (**5**) were synthesized according to the literature.

Polymerization of 3,3-Di-*tert*-butyl-2,4-dioxa-3-sila-bicyclo[3.2.1]oct-6-ene (5) via ROMP with Catalyst 1. In a typical experiment, a small vial was charged with 0.25 g (1.0 mmol) of monomer and a stirbar. The monomer was degassed by three freeze–pump–thaw cycles. 3.4 mg (4.13 x 10^{-6} mol) of catalyst **1** was added as a solution in 1,2-dichloroethane or toluene (1 mL of solvent). The vial was placed in a 55 °C aluminium heating block stirring under argon for approximately 20 h. The reaction mixture was dissolved in 3 mL dichloromethane and precipitated into 50 mL of stirring MeOH. The white polymer precipitate was washed several times with MeOH and dried in vacuo overnight; yield (77–95%). See Table 7.1 for molecular

weight data. ^{1}H NMR (300 MHz, $CDCl_3$): 5.75 *trans* (bs, 2H), 5.38 *cis* (d, $J = 4.0$ Hz, 2H), 5.08 *cis* (d, $J = 8.8$ Hz, 2H), 4.62 *trans* (d, $J = 10.2$ Hz, 2H), 1.4–1.8 (m, 2H), 1.0 (18H). ^{13}C NMR (75 MHz, $CDCl_3$): 132.3, 131.4, 131.1, 73.3, 70.7, 42.9, 42.6, 27.6, 27.5, 27.3, 22.8, 20.0,19.9.

Polymerization of 3,3-Di-*tert*-butyl-2,4-dioxa-3-sila-bicyclo[3.2.1]oct-6-ene (5) with CTA 6 via ROMP with Catalyst 2. In a typical experiment, a small vial was charged with 0.25 g (1.0 mmol) of monomer and a stirbar. The monomer was degassed by three freeze–pump–thaw cycles. Under an argon atmosphere, 0.25 mL (1.0×10^{-2} mmol) of a 6.90 mg/mL CTA in toluene solution was added via a syringe. Then 0.75 mL (5.3×10^{-5} mmol) of a 0.0595 mg/mL solution of **2** in toluene was added via a syringe. The vial was placed in a 55 °C heating apparatus and left stirring under argon for 23–113 h. The reaction mixture was dissolved in 2 mL of dichloromethane and precipitated into 50 mL of stirring MeOH. The white polymer precipitate was washed several times with MeOH and dried in vacuo overnight; yield (82–90%). See Table 7.2 for molecular weight data. ^{1}H NMR (300 MHz, $CDCl_3$): 5.73 *trans* (m, 2H), 5.35 *cis* (m, 2H), 5.06 *cis* (m, 2H), 4.62 *trans* (d, $J = 10.2$ Hz, 2H), 1.4–1.8 (m, 2H), 1.0 (18H). ^{13}C NMR (75 MHz, $CDCl_3$): 131.6, 131.3, 73.5, 43.2, 27.7, 27.6, 23.0, 20.2, 20.1.

Hydrogenation of Polymers after ROMP. In a typical experiment, a dry flask was charged with 0.35 g of polymer (M_n = 80360 g/mol, PDI = 1.3), 1.80 g of tosyl hydrazide (9.4 mmol, 6.5 equiv per double bond), 15 mL of xylenes, and a trace of BHT. The mixture was degassed by three freeze–pump–thaw cycles, and a reflux condenser was attached to the flask under argon. The reaction was heated to reflux for 4 h. The solution was cooled to room temperature and then precipitated into 125 mL of stirring MeOH. The white polymer precipitate was washed several times with MeOH and then dried in vacuo overnight; yield 0.34 g (99%). M_n = 75140 g/mol, PDI = 1.2, dn/dc = 0.076. ^{1}H NMR (300 MHz, $CDCl_3$): 3.9–4.1 (2H), 1.4–1.7 (6H), 1.0 (18H). $_{13}$C NMR (75 MHz, $CDCl_3$): 74.1, 73.5, 73.4, 42.4, 42.3, 34.8, 34.3, 27.8, 27.7, 27.3, 22.8, 19.7.

Desilation of Saturated Polymers. In a typical experiment, a dry flask was

charged with 0.1952 g of polymer and a stirbar. A reflux condenser was attached and the system was purged with argon. 20 mL of dry THF was added followed by 10 mL of dry DMF, at which point the solution became cloudy white. 8 mL of tetrabutylammonium fluoride (TBAF) 1.0 M in THF was added via a syringe. The reaction was brought to reflux (75 °C) for 40 h. It was then cooled to room temperature and precipitated into 400 mL of 1:1 MeOH:CH_2Cl_2 stirring at room temperature. A stringy precipitate was observed; it was vacuum filtered and washed with copious amounts of both MeOH and CH_2Cl_2 and dried under dynamic high vacuum overnight; yield 0.0713 g (87%). ^{1}H NMR (300 MHz, DMSO-d_6): 4.53 (s, 2H), 3.56 (bs, 2H), 1.2–1.6 (6H). ^{13}C NMR (75 MHz, DMSO-d_6): 69.3, 69.0, 44.4, 33.6, 33.3.

7.6 Acknowledgment

The authors would like to thank John P. Morgan, Isaac M. Rutenberg, and Daniel P. Sanders for critical reading of this manuscript. O.A.S. thanks the National Science Foundation for a graduate fellowship. H.M.K thanks the National Institute of Health for a postdoctoral fellowship. This work was supported by the National Science Foundation.

References Cited

[1] Lagaron, J. M.; Powell, A. K.; Bonner, G. *Polym. Testing* **2001,** *20,* 569–577.
[2] Ramakrishnan, S. *Macromolecules* **1991,** *24,* 3753–3759.
[3] Ramakrishnan, S.; Chung, T. C. *Macromolecules* **1990,** *23,* 4519–4524.
[4] Valenti, D. J.; Wagener, K. B. *Macromolecules* **1998,** *31,* 2764–2773.
[5] Bruzaud, S.; Levesque, G. *Macromol. Chem. Phys.* **2000,** *201,* 1758–1764.
[6] Hillmyer, M. A.; Laredo, W. R.; Grubbs, R. H. *Macromolecules* **1995,** *28,* 6311–6316.
[7] Schellekens, M. A. J.; Klumperman, B. *J. Macromol. Sci., Rev. Macromol. Chem. Phys.* **2000,** *C40,* 167–192.
[8] Schwab, P.; Grubbs, R. H.; Ziller, J. W. *J. Am. Chem. Soc.* **1996,** *118,* 100–110.
[9] Scholl, M.; Ding, S.; Lee, C. W.; Grubbs, R. H. *Org. Lett.* **1999,** *1,* 953–956.
[10] Bielawski, C. W.; Grubbs, R. H. *Angew. Chem., Int. Ed.* **2000,** *39,* 2903–2906.
[11] Sanford, M. S.; Love, J. A.; Grubbs, R. H. *J. Am. Chem. Soc.* **2001,** *123,* 6543–6554.
[12] Amir-Ebrahimi, V.; Corry, D. A.; Hamilton, J. G.; Thompson, J. M.; Rooney, J. J. *Macromolecules* **2000,** *33,* 717–724.
[13] Hamilton, J. G.; Frenzel, U.; Kohl, F. J.; Weskamp, T.; Rooney, J. J.; Herrmann, W. A.; Nuyken, O. *J. Organomet. Chem.* **2000,** *606,* 8–12.
[14] Lang, H.; Moser, H. E. *Helv. Chim. Acta* **1994,** *77,* 1527–1540.
[15] Lynn, D. M.; Kanaoka, S.; Grubbs, R. H. *J. Am. Chem. Soc.* **1996,** *118,* 784–790.
[16] Lynn, D. M.; Mohr, B.; Grubbs, R. H. *J. Am. Chem. Soc.* **1998,** *120,* 1627–1628.
[17] The molecular weight of the monomer is 240.41 g/mol. Dividing the M_n values by 240.41 g/mol yields a slope of 2.0 in toluene and 0.9 in 1,2-DCE.
[18] Hillmyer, M. A.; Grubbs, R. H. *Macromolecules* **1993,** *26,* 872–874.
[19] Hillmyer, M. A.; Grubbs, R. H. *Macromolecules* **1995,** *28,* 8662–8667.
[20] Hillmyer, M. A.; Nguyen, S. T.; Grubbs, R. H. *Macromolecules* **1997,** *30,* 718–721.
[21] Bielawski, C. W.; Scherman, O. A.; Grubbs, R. H. *Polymer* **2001,** *42,* 4939–4945.
[22] Wu, Z.; Grubbs, R. H. *Macromolecules* **1994,** *27,* 6700–6703.
[23] Hahn, S. F. *J. Polym. Sci., Part A: Polym. Chem.* **1992,** *30,* 397–408.
[24] Harwood, H. J.; Russell, D. B.; Verthe, J. J. A.; Zymonas, J. *Makromol. Chem.* **1973,** *163,* 1–12.
[25] Mango, L. A.; Lenz, R. W. *Makromol. Chem.* **1973,** *163,* 13–36.

[26] Nakagawa, T.; Okawara, M. *J. Polym. Sci., Part A-1* **1968,** *6,* 1795–1807.
[27] The *trans* and *cis* peaks were determined by coupling constants.
[28] Katsuraya, K.; Hatanaka, K.; Matsuzaki, K.; Amiya, S. *Polymer* **2001,** *42,* 9855–9858.
[29] Nagara, Y.; Nakano, T.; Okamoto, Y.; Gotoh, Y.; Nagura, M. *Polymer* **2001,** *42,* 9679–9686.
[30] Mori, Y.; Sumi, H.; Hirabayashi, T.; Inai, Y.; Yokota, K. *Macromolecules* **1994,** *27,* 1051–1056.
[31] Lommerts, B. J.; Sikkema, D. J. *Macromolecules* **2000,** *33,* 7950–7954.
[32] Yokota, K. *Prog. Polym. Sci.* **1999,** *24,* 517–563.
[33] Carlotti, S. J.; Giani-Beaune, O.; Schue, F. *J. Appl. Polym. Sci.* **2001,** *80,* 142–147.
[34] Pangborn, A. B.; Giardello, M. A.; Grubbs, R. H.; Rosen, R. K.; Timmers, F. J. *Organometallics* **1996,** *15,* 1518–1520.
[35] Sanford, M. S.; Ulman, M.; Grubbs, R. H. *J. Am. Chem. Soc.* **2001,** *123,* 749–750.

Chapter 8

Synthesis and Characterization of Stereoregular Ethylene-Vinyl Alcohol Copolymers Made by Ring-Opening Metathesis Polymerization

8.1 Abstract

The synthesis of regioregular as well as stereoregular ethylene vinyl alcohol (EVOH) copolymers by ring-opening metathesis polymerization (ROMP) with ruthenium catalysts is reported. Symmetric cyclooctene-diol monomers were protected as acetates, carbonates, or acetonides to temporarily add ring strain as well as impart solubility to the monomer. Polymer molecular weights could be easily controlled by either varying the monomer-to-catalyst ratio or by the addition of a chain transfer agent. Hydrogenation and subsequent deprotection of the ROMP polymers afforded the EVOH materials in high yields and the structures were confirmed by ^{1}H NMR and ^{13}C NMR spectroscopies. Thermal properties of the corresponding EVOH copolymers are reported and suggest that differences in diol stereochemistry drastically affect the polymer morphology.

8.2 Introduction

Ethylene vinyl alcohol (EVOH) copolymers have found commercial utility in food packaging as well as in the biomedical and pharmaceutical industries as a result of their excellent barrier properties toward gases and hydrocarbons.[1–7] The structure of EVOH copolymers affects the material's ability to limit gas or hydrocarbon diffusion through a membrane.[8, 9] Unfortunately, the current commercial route to these materials involves the free-radical polymerization of vinyl acetate and ethylene monomers followed by saponification.[10] The overall architecture is impossible to control and EVOH produced in this fashion contains a degree of branching similar to low-density polyethylene (LDPE).[11, 12] Furthermore, while the relative amount of vinyl alcohol can be controlled in the feed ratio of the two monomers, exact placement of alcohol functionality along the polymer backbone cannot be controlled.[9] This has resulted in a poor understanding of structure–property relationships in EVOH.

It has been demonstrated that the incorporation of polar functional groups pendent from a linear polymer backbone can be readily accomplished through ring-

opening metathesis polymerization (ROMP) with functional group-tolerant late transition metal catalysts.[9, 10, 13–17] Polar, substituted cyclic olefins such as alcohol-, ketone- or even halogen-substituted cyclooctenes undergo ROMP to form absolutely linear polymer bearing pendent functional groups.[13] The asymmetric monomer, however, prevents absolute control over the placement of the polar group along the polymer backbone. Head-to-head (HH), head-to-tail (HT), and tail-to-tail (TT) couplings are all possible, leading to a regiorandom distribution of functionality.[13] This problem has been addressed by two different olefin metathesis polymerization techniques, displayed in Figure 8.1.[9, 12, 18]

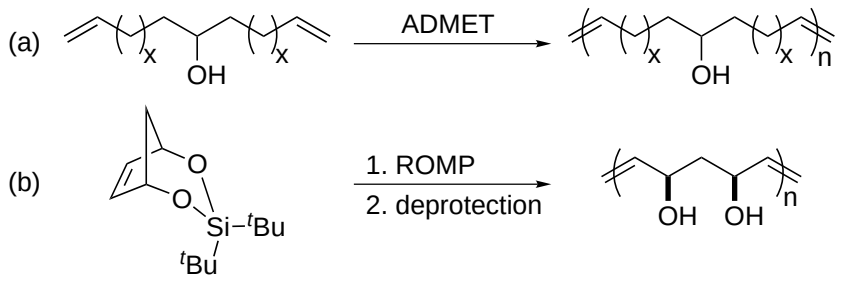

Figure 8.1: (a) ADMET of symmetric alcohol-containing monomer to produce a regioregular EVOH copolymer. (b) ROMP of a temporarily strained, symmetric monomer to produce a regioregular EVOH material with a higher vinyl alcohol content.

Valenti *et al.* reported the acyclic diene metathesis polymerization (ADMET) of a symmetric alcohol-containing monomer (Figure 8.1a).[12] The molecular weights, however, are restricted to $< 3 \times 10^4$ g/mol when employing ADMET and the relatively high hydrocarbon to alcohol ratio limits the overall barrier properties of these EVOH materials.[1, 12] More recently, we illustrated that ROMP of a symmetric monomer could be carried out in high yield to afford a linear EVOH type material (Figure 8.1b) with controlled placement of the alcohol functionality, molecular weight control over a wide range, and a much higher incorporation of alcohol groups.[9] Functional group-tolerant ruthenium catalysts **1**[19] and **2**[20] (Figure 8.2) were necessary to carry out the ROMP of the polar monomer.

While ROMP is capable of producing linear high molecular weight polymer, the amount of ring strain inherent in the cyclic olefin monomer plays a critical role in the

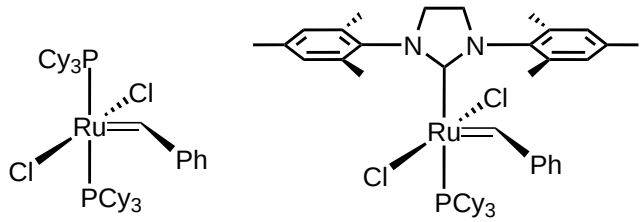

1 **2**

Figure 8.2: Ruthenium olefin metathesis catalysts.

polymerizability of each monomer.[21, 22] The addition of substituents to monocyclic olefins serves to lower the ring strain and can render a monomer non-polymerizable via ROMP.[21] Therefore, we introduced a method to temporarily add ring strain through carefully chosen protecting groups while keeping the monomers symmetric to avoid issues of regiorandom monomer addition.[9] While ROMP of symmetric monomers resolves the problems of branching and regiocontrol of functional groups, the effect of stereochemistry between neighboring alcohols has yet to be addressed. We would like to report our attempts to separately gauge the effect of relative stereocontrol on material properties. This allowed for a more detailed structure–property study with respect to barrier properties of architecture-controlled EVOH materials.

Scheme 8.1: ROMP of *trans*-diol **3**.

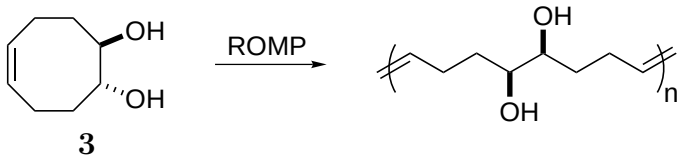

3

The direct ROMP of cyclooctene-*trans*-diol (**3**) was afforded by the addition of ruthenium catalyst **1** to monomer **3** as depicted in Scheme 8.1.[3] Unfortunately, this polymerization could only be carried out in neat monomer, as solubility of the unprotected diol **3** in common organic solvents suitable for ROMP was minimal.[3] Moreover, the molecular weight of the resulting ROMP polymer was limited to *ca.* 20000 g/mol due to diffusion in the highly viscous polymerization mixture.[3–5] All attempts to ROMP cyclooctene-*cis*-diol (**4**) failed as **4** is a crystalline solid with a melting point

well above the temperature range useful for catalysts **1** and **2**. Again, the lack of solubility of **4** in organic solvents suitable for ROMP prevented solution polymerization of the unprotected diol monomer. In order to produce perfectly linear EVOH materials that differed only in the relative stereochemistry between the neighboring 1,2-diols along the polymer backbone, protection of the diols was used to enhance the solubility of monomers **3** and **4**.

8.3 Results and Discussion

8.3.1 Monomer Design and Synthesis

In order to compare the effect that relative stereochemistry has on EVOH material properties, two monomers differing only in diol stereochemistry were selected: cyclooctene-*trans*-diol **3** and cyclooctene-*cis*-diol **4**. Due to the limited solubility of the diols in organic solvents,[3] the free alcohols were protected prior to polymerization. Considerations of monomer symmetry as well as ring strain were taken into account so that the resulting ROMP polymers would retain regioregular placement of alcohol groups along the polymer backbone and that high yields could be achieved.

Acetate protection afforded both the *trans* and *cis* monomers **5** and **6**, respectively (Scheme 8.2a). Both of these monomers underwent ROMP to yield the acetate-protected polymers, although higher monomer concentrations were necessary to achieve reasonable yields of polymer due to a decrease in ring strain relative to un-substituted cyclooctene. Both ROMP polymers, however, formed gels and did not dissolve in common organic solvents. Therefore, another protection strategy was employed. In an attempt to increase polymer yields at low monomer concentrations, carbonate protection was chosen to make bicyclic (8,5-fused) monomers that would retain symmetry as illustrated in Scheme 8.2b. While both the *trans*-carbonate **7** and *cis*-carbonate **8** did undergo ROMP, the resulting ROMP polymers were intractable in CH_2Cl_2, toluene, and THF and were only mildly soluble in DMF. A different bicyclic protection was carried out to form the *trans*-acetonide **9** and *cis*-acetonide **10** as shown

in Scheme 8.2c. The ROMP of these monomers produced polymers that remained soluble in common organic solvents and allowed for subsequent hydrogenation and deprotection steps to arrive at EVOH copolymers differing only in relative stereochemistry between neighboring alcohol functionalities.

Scheme 8.2: Protection strategies for *trans* and *cis* cyclooctene-diol monomers.

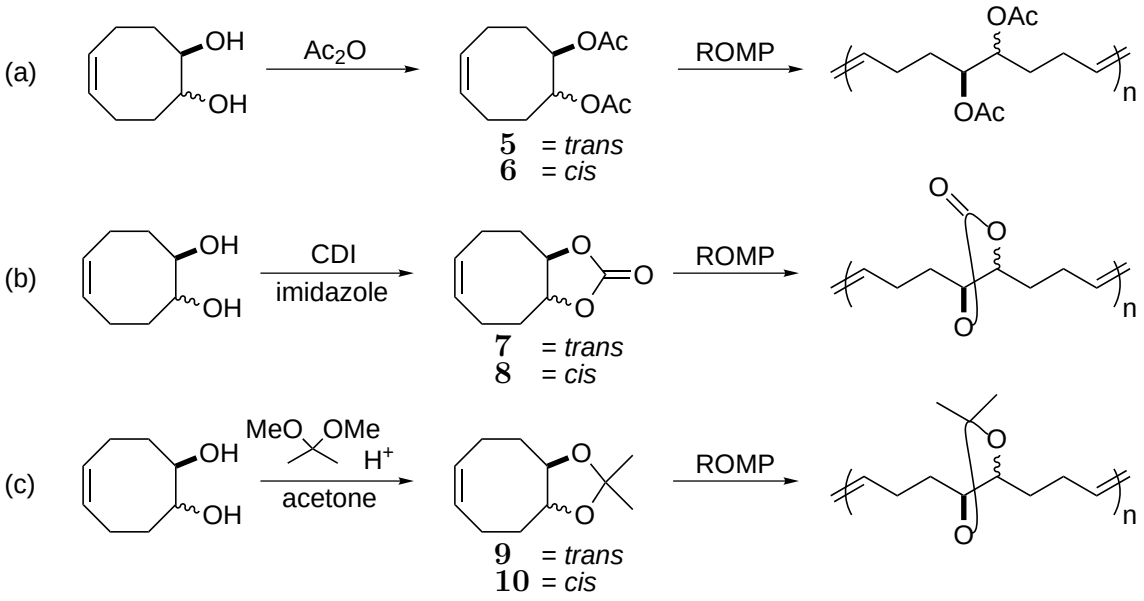

8.3.2 ROMP of Acetonide Monomers with Catalyst 1

It has been previously demonstrated that ROMP of strained cyclic olefins with catalyst **1** occurs in a controlled and living fashion.[23, 24] Therefore, ROMP of monomers **9** and **10** was expected to yield polymers in which the molecular weight could be controlled by setting the monomer to catalyst ratio, $[M]_0/[\mathbf{1}]$. ROMP polymer **11**

Scheme 8.3: ROMP of **9** with catalyst **1** yields acetonide-protected polymer **11**.

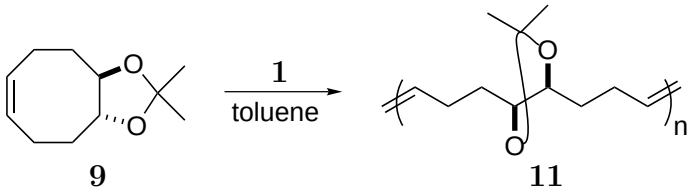

forms upon introduction of catalyst **1** to a solution of *trans* monomer **9**, as shown in Scheme 8.3. Product yield, however, greatly depends on the monomer concentration, as shown in Figure 8.3a. Polymer yields are poor when $[M]_0 < 2$ M, although yields are reasonable and MW control is dictated by [M]/[**1**]ratio when the polymerization is carried out at 3 or 4 M (Figure 8.3b). The low yields of polymer produced from polymerizations below $[M]_0 = 2$ M are likely due to low ring strain as a result of the *trans*-8,5-ring fusion in **9**.[21] This has been observed before with *trans*-8,6-ring fusions by Miller *et al.*[25] Miller noted that the ring-closing metathesis (RCM) of acyclic dienes to produce *trans*-8,6-fused bicyclic compounds afforded higher yields than for the corresponding RCM of *cis*-8,6-fused compounds.[25] This suggests that *trans*-8,5 fused materials like **9** might also prefer the ring-closed form while the opposite might be true for *cis*-8,5 fused materials such as **10**. In fact, this trend holds for the ROMP of monomers **9** and **10**, as the ability for these two monomers to undergo ROMP is markedly different.

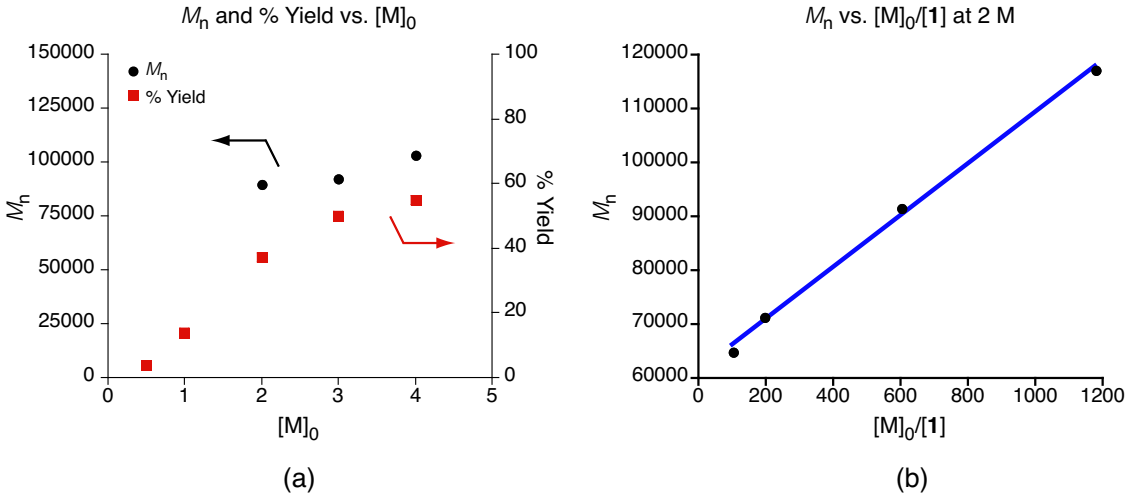

Figure 8.3: (a) ROMP of **9** with catalyst **1** at 55 °C, $[M]_0$/[**1**]= 400 at varying $[M]_0$. (b) Molecular weight control is achieved by varying $[M]_0$/[**1**]ratio.

As illustrated in Scheme 8.4, when catalyst **1** is introduced to a solution of monomer **10** ROMP polymer **12** is formed in high yield at much lower initial monomer concentrations. Reasonable yields (50-60%) can be achieved at $[M]_0 = 0.25$ M and

Scheme 8.4: ROMP of **10** with catalyst **1** yields acetonide-protected polymer **12**.

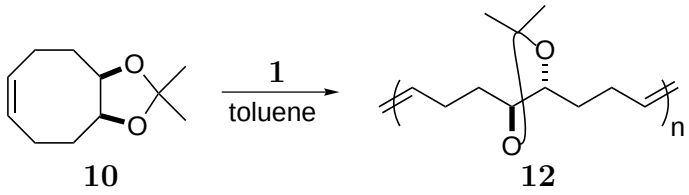

10 **12**

yields exceed 75% at $[M]_0 = 1$ M. Figure 8.4 shows excellent molecular weight control over a wide range for the ROMP of **10** with catalyst **1** at 1 M. As indicated by the data in Table 8.1, M_n is directly related to the [monomer]/[catalyst]ratio in a linear manner, and the polymerizations reach high yields within 24 h with relatively narrow PDIs.

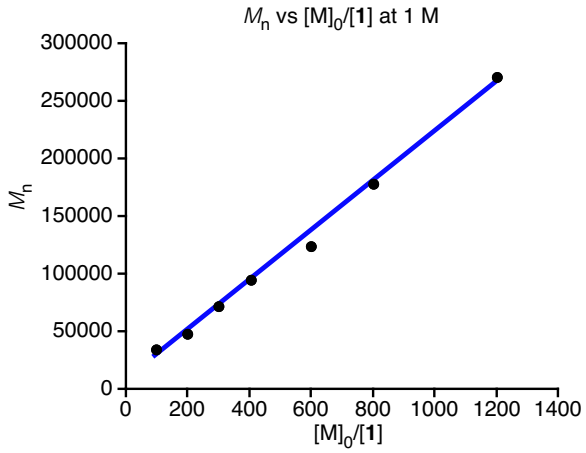

Figure 8.4: ROMP of **10** carried out at 1 M and 55 °C with catalyst **1** to produce polymer **12**; molecular weight control is achieved by varying the $[M]_0$/[**1**]ratio.

8.3.3 ROMP of Acetonide Monomers with Catalyst 2

While controlling the polymer molecular weight by adjusting the monomer to catalyst ratio is straightforward, the amount of catalyst employed directly affects the polymer produced. In an effort to reduce the amount of catalyst necessary to carry out the ROMP of monomers **9** and **10**, the use of highly active catalyst **2** was investigated.[14] It has been shown previously that the use of catalyst **2** with an acyclic chain transfer agent (CTA) affords telechelic polymers of controlled molecular

Table 8.1: ROMP of **10** ($[M]_0$=1 M) with **1** at 55 °C for 24 h.

[**10**]/[**1**]	M_n ($\times 10^{-3}$) GPC[a]	PDI	% yield
100	34.4	1.3	79
200	47.7	1.7	81
300	72.4	1.6	78
400	94.7	1.6	80
600	124	1.5	76
800	178	1.5	72
1200	271	1.3	73

[a]Samples run in THF; molecular weight values obtained using MALLS.

weight.[9, 26–29] The addition of a CTA such as **13** to the ROMP of **10** yielded telechelic polymer **14** as depicted in Scheme 8.5.

Scheme 8.5: ROMP of **10** with catalyst **2** in the presence of chain transfer agent **13** to yield telechelic acetonide-protected polymer **14**.

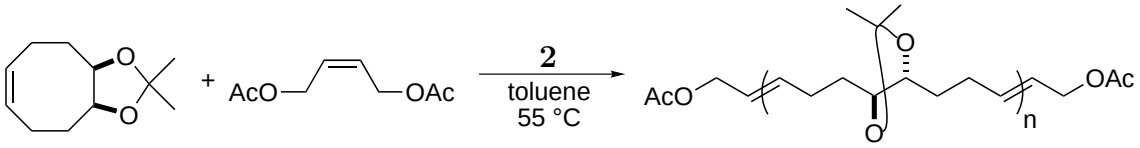

10 **13** **14**

Polymers **12** and **14** differ only by the functional groups at the termini of the latter. Moreover, the molecular weight of **14** can be easily controlled by the ratio of monomer to CTA, [**10**]/[**13**],[9, 27–29] thereby reducing the amount of catalyst needed for polymerization and simultaneously removing effect of catalyst in determining polymer molecular weight.[26]

Through the use of catalyst **2** and a CTA, much higher monomer-to-catalyst ratios can be employed allowing access to a large range of polymer molecular weights. The plot in Figure 8.5 and the data in Table 8.2 show excellent molecular weight control for the ROMP of **10** with CTA **13** at 1 M with $[M]_0$/[**2**]ratio of 5000.

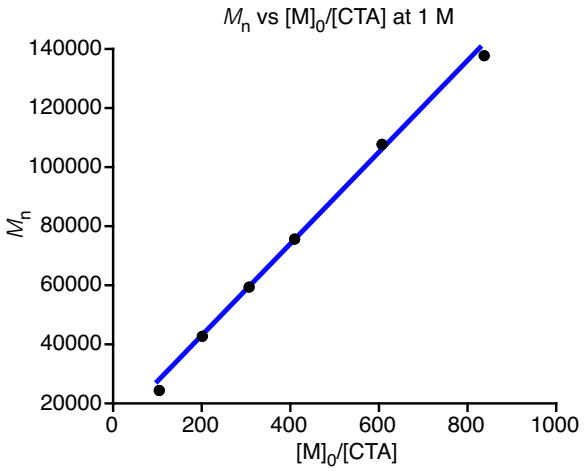

Figure 8.5: ROMP of **10** carried out at 1 M and 55 °C with catalyst **2** and CTA **13** to produce telechelic polymer **14**; molecular weight control is achieved by varying the $[M]_0/[CTA]$ratio.

8.3.4 Hydrogenation of Acetonide-Protected ROMP Polymers

While polymers resulting from the ROMP of monomers **5**–**8** led to gelled or intractable materials, polymers **11** and **12** were soluble in common organic solvents, allowing for mild hydrogenations to be carried out. Direct formation of diimide in situ[9, 30–34] afforded complete hydrogenation of the olefins without removing the acetonide protecting group as depicted in Scheme 8.6. After 5–6 h in refluxing xylenes, hydrogenation of the ROMP polymers was complete as evidenced by the lack of olefin signals in both the ^{1}H and ^{13}C NMR spectra. The hydrogenation reaction was carried out with 1 equiv of tri-propylamine (per tosylhydrazide) in order to keep the acetonides from catalytically deprotecting with the formation of tosic acid.[9] Saturated polymers **15** and **16** remained soluble in organic solvents, allowing for characterization by ^{1}H and ^{13}C NMR, gel permeation chromatography (GPC), as well as thermal analysis by differential scanning calorimetry (DSC).

Table 8.2: ROMP of **10** ($[M]_0$=1 M) with **2** at 55 °C for 24 h, [**10**]/[**2**]=5000.

[**10**]/[**13**]	M_n ($\times 10^{-3}$) GPC[a]	PDI	% yield
100	24.5	1.9	70
200	43.0	1.6	74
300	59.8	1.6	74
400	75.7	1.6	75
600	108	1.6	76
800	138	1.5	76

[a]Samples run in THF; molecular weight values obtained using MALLS.

Scheme 8.6: Hydrogenation of ROMP polymers by *in situ* diimide formation.

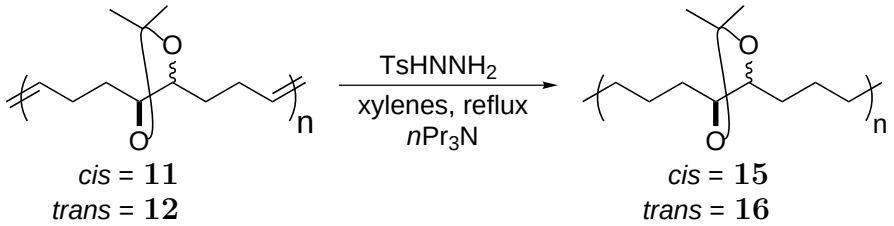

cis = **11**
trans = **12**

cis = **15**
trans = **16**

8.3.5 Deprotection of Acetonide Groups

In order to arrive at the final EVOH structure, deprotection of the acetonide groups was necessary. As shown in Scheme 8.7, removal of the acetonides was accomplished by extended heating at 80 °C in 1,4-dioxane with a catalytic amount of trifluoroacetic acid (TFA) and water. This reaction proved quite challenging as polymers **15** and **16** are hydrophobic and possess a very different solubility profile than the hydrophilic EVOH copolymers **17** and **18**.[9] While the formation of EVOH **17** occurred readily, the transformation of **16** to **18** required 10–20% DMSO as a co-solvent in order to keep the polymer soluble throughout the entire reaction.[9] In the absence of DMSO, the reaction resulted in incomplete deprotection and undesired product which precipitated from solution.

Scheme 8.7: Deprotection of acetonides.

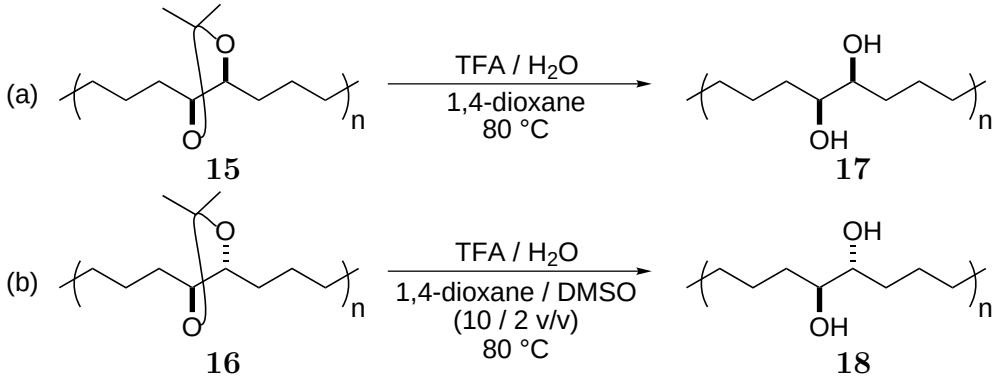

8.3.6 Thermal Analysis of ROMP, Hydrogenated, and Deprotected Polymers

Thermal analysis was carried out on polymers **11** and **12** and **15**–**18** by DSC. Glass transition temperatures, T_g, as well as the relevant melting transition temperatures, T_m, are listed in Table 8.3. Only glass transitions are observed for the amorphous

Table 8.3: Thermal analysis of ROMP, hydrogenated, and deprotected EVOH polymers.

Polymer	T_g, onset (°C)	T_m, onset (°C)
11	-12.4	—
12	-6.6	—
15	-14.1	—
16	-2.7	—
17	34.4	111
18	50	157

acetonide-protected ROMP polymers **11** and **12**. While both T_g values are sub-ambient, they differ by nearly 6 °C, suggesting that the syn and anti diols impose a slightly different packing in the solid state. This difference is even more pronounced (11.4 °C) in the hydrogenated forms, **15** and **16**. Finally, the fully deprotected EVOH copolymers **17** and **18** show a clear difference in both the T_g and T_m values with a nearly 40 °C increase in the melting transition temperature between the syn and anti 1,2-diols. Moreover, the ΔH for the melting transition observed for the syn 1,2-diol

EVOH **17** was 21.17 J/g, while the ΔH for the anti 1,2-diol EVOH **18** nearly doubled, with a value of 42.12 J/g. This indicates that the anti stereochemical relationship between the diols along the polymer backbone allowed for more crystalline regions in the EVOH material relative to the syn stereochemical relationship. In addition, the T_g for **17** was much easier to observe in the DSC trace relative to **18**. Previously, it has been observed that higher melting transitions in EVOH copolymers arise from higher alcohol content.[9, 35] The dramatic increase in T_m between **17** and **18**, however, suggests that the relative stereochemistry between the pendent alcohol groups can also have a remarkable effect on material morphology and crystalline packing of the polymer chains.

8.4 Conclusions

The successful ROMP of symmetric cyclooctene diol monomers that differ only in the relative stereochemistry between the alcohols has been demonstrated with the functional group-tolerant ruthenium catalysts **1** and **2**. In order to obtain molecular weight control over the polymers, a protection strategy was needed due to the lack of solubility of cyclooctene diol in common organic solvents. Acetonide protection for the diols provided the necessary solubility as well as enhanced ring strain for the *cis* diol (**4**) in the form of a bicyclic 8,5-fused system while keeping the symmetry of the monomer. Hydrogenation and subsequent deprotection afforded regioregular EVOH copolymers with 1,2-diols along the polymer backbone differing only in a syn and anti relationship. This allowed for direct probing of the effect of relative stereochemistry on EVOH copolymer properties. Thermal analysis indicated that a mere change in the relative stereochemistry greatly affects both the glass and melting transitions of the EVOH materials without requiring an increase in overall alcohol content. The ability to modify the properties of a material by simply imposing regularity on the structure of a polymer chain is evident. Finally, the use of ROMP with late transition metal ruthenium catalysts combined with rational monomer design has allowed us to elucidate the effects of polymer architecture on the material properties of EVOH

copolymers.

8.5 Experimental Section

General Procedures. NMR spectra were recorded on a Varian Mercury 300 (300 MHz for ^{1}H and 74.5 MHz for ^{13}C). All NMR spectra were recorded in $CDCl_3$, DMSO-d_6, or 1,4-Dioxane-d_8 and referenced to residual proteo species. Gel permeation chromatography (GPC) was carried out on two PLgel 5 μm mixed-C columns (Polymer Labs) connected in series with a DAWN EOS multi angle laser light scattering (MALLS) detector and an Optilab DSP differential refractometer (both from Wyatt Technology). No calibration standards were used, and dn/dc values were obtained for each injection assuming 100% mass elution from the columns. Differential scanning calorimetry (DSC) and thermogravimetric analysis (TGA) was carried out simultaneously on a Netzsch STA 449C under a flow of N_2 at a heating rate of 10 °C/min or on a Perkin Elmer Pyris1 under a flow of He at a heating rate of 10 °C/min.

Materials. Toluene and CH_2Cl_2 were dried by passage through solvent purification columns.[36] *cis*-1,4-Diacetoxy-2-butene (95+%) (**13**) was obtained from TCI America and degassed by an argon purge prior to use. 1,5-Cyclooctadiene (redistilled, 99+%), 9-Oxabicyclo[6.1.0]non-4-ene (95%), *N,N*-Dimethylformamide (anhydrous, 99.8%) (DMF), 1,1'-Carbonyldiimidazole, *p*-Toluene sulfonhydrazide (97%), Pyridinium *p*-toluene sulfonate (98%), Tripropylamine (99+%), 1,4-Dioxane (99+%), Xylenes (98.5+%), Trifluoroacetic acid (99+%), Acetic anhydride (99+%), and 2,2'-Dimethoxypropane (98%) were obtained from Aldrich as used as received. Potassium osmate (VI) dihydrate (99%) was obtained from Strem and used as received. Dimethylsulfoxide was obtained from ACROS Organics and used as received. Imidazole (99%) was obtained from EM Science and used as received. Acetone (technical grade) was dried over calcium sulfate and filtered prior to use as a solvent. Ruthenium catalysts $(PCy_2)(Cl)_2Ru{=}CHPh$ (**1**)[19] and $(H_2IMes)(PCy_2)(Cl)_2Ru{=}CHPh$ (**2**)[37] as well as organic compounds Cyclooctene-*trans*-diol (**3**),[38] Cyclooctene-*cis*-diol (**4**),[39]

Cyclooctene-*trans*-diacetate (**5**),[40, 41] Cyclooctene-*cis*-diacetate (**6**),[40, 41] Cyclooctene-*trans*-carbonate (**7**),[40] Cyclooctene-*cis*-carbonate (**8**),[40] Cyclooctene-*trans*-acetonide (**9**),[42] and Cyclooctene-*cis*-acetonide (**10**)[43] were all synthesized according to literature procedures.

Polymerization procedure for acetonide-protected monomers with catalyst 1. In a typical experiment, a small vial was charged with 0.185 g (1.0 mmol) of monomer **10** and a stirbar. Under an argon atmosphere, 0.6 mL of degassed toluene was added via syringe. In a separate vial, a 21.2 mg/mL catalyst **1** solution in toluene was prepared. 0.4 mL of the catalyst solution was then added to the monomer solution via syringe under argon. The reaction vial was placed in a 55 °C aluminum heating block stirring under argon for 24 h. The reaction mixture was then quenched with 0.1 mL ethyl vinyl ether and then dissolved in 1 mL CH_2Cl_2 and precipitated into 50 mL of stirring MeOH. A light brown ppt. was washed several times with MeOH and dried in vacuo overnight; yield (79%). See Table 8.1 for molecular weight data. ^{1}H NMR (300 MHz, $CDCl_3$): 5.5 *trans* 5.4 *cis* (two br s, 2H), 4.05 (br s, 2H), 1.95–2.35 (m, 4H), 1.3–1.65 (m, 10H). ^{13}C NMR (75 MHz, $CDCl_3$): 130.2, 129.8, 107.6, 77.5, 30.1, 29.9, 29.4, 29.0, 26.4, 24.2.

Polymerization procedure for acetonide-protected monomers with catalyst 2 and CTA 13. In a typical experiment, a small vial was charged with 0.185 g (1.0 mmol) of monomer **10** and a stirbar. Under an argon atmosphere, 0.8 mL of a 2.2 mg/mL solution of **13** in toluene was added. Next 0.2 mL of a 0.9 mg/mL solution of catalyst **2** in toluene was added via syringe. The reaction vial was placed in a 55 °C aluminum heating block stirring under argon for 24 h. The reaction mixture was then dissolved in 1 mL CH_2Cl_2 and precipitated into 50 mL of stirring MeOH. A white ppt. was washed several times with MeOH and dried in vacuo overnight; yield (75%). See Table 8.2 for molecular weight data. ^{1}H NMR (300 MHz, $CDCl_3$): 5.5 *trans* 5.4 *cis* (two br s, 2H), 4.05 (br s, 2H), 1.95–2.35 (m, 4H), 1.3–1.65 (m, 10H). ^{13}C NMR (75 MHz, $CDCl_3$): 130.1, 129.7, 107.5, 77.6, 30.1, 29.9, 29.4, 28.9, 26.3, 24.2.

Hydrogenation procedure for acetonide-protected polymers. In a typical

experiment, an oven-dried 500 mL round bottom flask was charged with a stirbar, 1.0 g of polymer **15**, 6.83 g of tosyl hydrazide (35.6 mmol, 6.5 equiv per double bond) 125 mL of xylenes, and a trace of BHT. The mixture was degassed by pulling high vacuum on the solution for about 45 s. Under an argon atmosphere, a flask was fitted with a reflux condenser. The reaction was heated to reflux for 7 h. It was then cooled to room temperature and then precipitated into 700 mL of stirring ice-cold stirring MeOH. The white ppt. was washed several times with MeOH and then dried in vacuo overnight; yield 1.01 g (99%). ^{1}H NMR (300 MHz, $CDCl_3$): 3.58 (br s, 2H), 1.25–1.6 (m, 18 H). ^{13}C NMR (75 MHz, $CDCl_3$): 107.9, 81.2, 33.3, 30.0, 27.7, 26.5.

Deprotection of 15. In a typical experiment, a 25 mL round bottom flask was charged with a stirbar and 0.25 g polymer. The polymer was then dissolved in 10 mL of 1,4-dioxane. A reflux condenser was attached to the flask and the reaction was stirred at 80 °C for 10 min under argon. 1 mL of H_2O and 1 mL of TFA were added via syringe and the reaction was allowed to stir at 80 °C under argon. An additional 2.5 mL of H_2O was added to the reaction over the course of 72 h, after which the reaction was allowed to cool to room temperature and precipitated into 200 mL of acetone stirring at room temperature. A fluffy white solid was obtained through several centrifugation, decant, rinse cycles and dried under vacuum overnight; yield 0.19 g (99%). ^{1}H NMR (300 MHz, DMSO-d_6, 85 °C): 3.55 (br s, 2H), 1.22–1.62 (br m, 12H). ^{13}C NMR (75 MHz, DMSO-d_6, 85 °C): 76.0, 32.9, 29.2, 25.4.

Deprotection of 16. In a typical experiment, a 25 mL round bottom was charged with a stirbar and 255.9 mg of polymer. It was first dissolved in 8 mL of 1,4-dioxane and then under an argon atmosphere 1 mL of DMSO was slowly added to the solution over the course of 30 min. A reflux condenser was attached and the reaction was heated to 80 °C for 2 h. Next 0.2 mL of TFA was added and the reaction was stirred overnight under argon at 80 °C. After 24 h, an additional 0.2 mL of TFA and 1 mL of DMSO were added and the reaction was kept at 80 °C. After 72 h, an additional 1 mL of DMSO and 0.1 mL TFA and 0.2 mL H_2O were added to the reaction. 1 mL of DMSO was also added after 96 h as well as 0.2 mL TFA. Finally, after 144 h, the reaction was stopped and precipitated into 100 mL of acetone stirring at room

temperature. A whitish ppt. was obtained through several centrifugation, decant, rinse cycles and dried under vacuum overnight; yield 200.0 mg (99%). ^{1}H NMR (300 MHz, DMSO-d_6, 85 °C): 3.18 (br s, 2H), 1.05–1.58 (br m, 12H).

8.6 Acknowledgements

The authors thank Isaac M. Rutenberg, Daniel P. Sanders, and Brian Connell for both helpful discussions and critical reading of this manuscript. O.A.S. thanks the National Science Foundation for a graduate fellowship. This work was supported by the National Science Foundation and Kuraray Co., LTD (Japan).

References Cited

[1] Lagaron, J. M.; Powell, A. K.; Bonner, G. *Polym. Testing* **2001,** *20,* 569–577.

[2] Lopez-Rubio, A.; Lagaron, J. M.; Gimenez, E.; Cava, D.; Hernandez-Munoz, P.; Yamamoto, T.; Gavara, R. *Macromolecules* **2003,** *36,* 9467–9476.

[3] Banslaben, D. A.; Huynh-Tran, T. C.; Blanski, R. L.; Hughes, P. A.; Roberts, W. P.; Grubbs, R. H.; Hatfield, G. R. Regio-Regular Functionalized Polymeric Packaging Material. US Patent 6,203,923, March 20, 2001.

[4] Banslaben, D. A.; Huynh-Tran, T. C. T.; Blanski, R. L.; Hughes, P. A.; Roberts, W. P.; Grubbs, R. H.; Hatfield, G. R. Regio-Regular Copolymer and Methods of Forming Same. US Patent 6,506,860, January 14, 2003.

[5] Banslaben, D. A.; Huynh-Tran, T. C. T.; Blanski, R. L.; Hughes, P. A.; Roberts, W. P.; Grubbs, R. H.; Hatfield, G. R. Regio-Regular Copolymer and Methods of Forming Same. US Patent 6,153,714, November 28, 2000.

[6] Lagaron, J. M.; Powell, A. K.; Bonner, G. *Polym. Testing* **2001,** *20,* 569–577.

[7] Ramakrishnan, S. *Macromolecules* **1991,** *24,* 3753–3759.

[8] Greenfield, M. L.; Theodorou, D. N. *Macromolecules* **1993,** *26,* 5461–5472.

[9] Scherman, O. A.; Kim, H. M.; Grubbs, R. H. *Macromolecules* **2002,** *35,* 5366–5371.

[10] Ramakrishnan, S.; Chung, T. C. *Macromolecules* **1990,** *23,* 4519–4524.

[11] Ramakrishnan, S. *Macromolecules* **1991,** *24,* 3753–3759.

[12] Valenti, D. J.; Wagener, K. B. *Macromolecules* **1998,** *31,* 2764–2773.

[13] Hillmyer, M. A.; Laredo, W. R.; Grubbs, R. H. *Macromolecules* **1995,** *28,* 6311–6316.

[14] Bielawski, C. W.; Grubbs, R. H. *Angew. Chem., Int. Ed.* **2000,** *39,* 2903–2906.

[15] Sanford, M. S.; Love, J. A.; Grubbs, R. H. *J. Am. Chem. Soc.* **2001,** *123,* 6543–6554.

[16] Amir-Ebrahimi, V.; Corry, D. A.; Hamilton, J. G.; Thompson, J. M.; Rooney, J. J. *Macromolecules* **2000,** *33,* 717–724.

[17] Hamilton, J. G.; Frenzel, U.; Kohl, F. J.; Weskamp, T.; Rooney, J. J.; Herrmann, W. A.; Nuyken, O. *J. Organomet. Chem.* **2000,** *606,* 8–12.

[18] Schellekens, M. A. J.; Klumperman, B. *J. Macromol. Sci., Rev. Macromol. Chem. Phys.* **2000,** *C40,* 167–192.

[19] Schwab, P.; Grubbs, R. H.; Ziller, J. W. *J. Am. Chem. Soc.* **1996,** *118,* 100–110.

[20] Scholl, M.; Ding, S.; Lee, C. W.; Grubbs, R. H. *Org. Lett.* **1999,** *1,* 953–956.

[21] Ivin, K. J.; Mol, J. C. *Olefin Metathesis and Metathesis Polymerization;* Academic Press: London, 1997.

[22] Grubbs, R. H., Ed.; *Handbook of Metathesis;* Wiley-VCH: Weinheim, 2003.
[23] Sanford, M. S.; Ulman, M.; Grubbs, R. H. *J. Am. Chem. Soc.* **2001,** *123,* 749–750.
[24] Lang, H.; Moser, H. E. *Helv. Chim. Acta* **1994,** *77,* 1527–1540.
[25] Miller, S. J.; Kim, S. H.; Chen, Z. R.; Grubbs, R. H. *J. Am. Chem. Soc.* **1995,** *117,* 2108–2109.
[26] Bielawski, C. W.; Scherman, O. A.; Grubbs, R. H. *Polymer* **2001,** *42,* 4939–4945.
[27] Lynn, D. M.; Mohr, B.; Grubbs, R. H. *J. Am. Chem. Soc.* **1998,** *120,* 1627–1628.
[28] Hillmyer, M. A.; Grubbs, R. H. *Macromolecules* **1995,** *28,* 8662–8667.
[29] Hillmyer, M. A.; Grubbs, R. H. *Macromolecules* **1993,** *26,* 872–874.
[30] Wu, Z.; Grubbs, R. H. *Macromolecules* **1994,** *27,* 6700–6703.
[31] Hahn, S. F. *J. Polym. Sci., Part A: Polym. Chem.* **1992,** *30,* 397–408.
[32] Harwood, H. J.; Russell, D. B.; Verthe, J. J. A.; Zymonas, J. *Makromol. Chem.* **1973,** *163,* 1–12.
[33] Mango, L. A.; Lenz, R. W. *Makromol. Chem.* **1973,** *163,* 13–36.
[34] Nakagawa, T.; Okawara, M. *J. Polym. Sci., Part A-1* **1968,** *6,* 1795–1807.
[35] Katsuraya, K.; Hatanaka, K.; Matsuzaki, K.; Amiya, S. *Polymer* **2001,** *42,* 9855–9858.
[36] Pangborn, A. B.; Giardello, M. A.; Grubbs, R. H.; Rosen, R. K.; Timmers, F. J. *Organometallics* **1996,** *15,* 1518–1520.
[37] Carlotti, S. J.; Giani-Beaune, O.; Schue, F. *J. Appl. Polym. Sci.* **2001,** *80,* 142–147.
[38] Jernow, J. L.; Gray, D.; Closson, W. D. *J. Org. Chem.* **1971,** *36,* 3511–3515.
[39] Alvarez, E.; Diaz, M. T.; Perez, R.; Ravelo, J. L.; Regueiro, A.; Vera, J. A.; Zurita, D.; Martin, J. D. *J. Org. Chem.* **1994,** *59,* 2848–2876.
[40] Yates, P.; Lewars, E. G.; McCabe, P. H. *Can. J. Chem.* **1972,** *50,* 1548–1556.
[41] Horikawa, T.; Norimine, Y.; Tanaka, M.; Sakai, K.; Suemune, H. *Chem. Pharm. Bull.* **1998,** *46,* 17–21.
[42] Takahashi, A.; Aso, M.; Tanaka, M.; Suemune, H. *Tetrahedron* **2000,** *56,* 1999–2006.
[43] Kawazoe, K.; Furusho, Y.; Nakanishi, S.; Takata, T. *Synth. Comm.* **2001,** *31,* 2107–2112.

Chapter 9

Computational Study on the Effect of Controlled Stereochemistry on Oxygen Permeability in EVOH Materials

This work was done as a collaborative effort with Dr. Valeria Molinero in the Goddard group at Caltech.

9.1 Abstract

The purpose of this research is to explore the microscopic structure and dynamics of two ethylene vinyl alcohol (EVOH) copolymers differing only in the relative stereochemistry between neighboring 1,2-diols by means of molecular dynamics simulations. The spatial distribution of hydroxyl groups, their hydrogen bonding pattern, and free volume distribution were analyzed in an attempt to explain the different properties experimentally observed for these two materials which were detailed in Chapter 8. As expected, the local topology of the 1,2-diols indeed effects the global three-dimensional polymer structures, as characterized by their hydrogen bond networks.

9.2 Introduction

Ethylene vinyl alcohol (EVOH) copolymers possess excellent barrier properties, especially towards oxygen gas diffusion.[1, 2] They have therefore found many commercial applications in the food packaging as well as in the biomedical industries.[1, 3, 4] Until recently, regioregular and stereoregular EVOH materials could not be synthesized. Rather, these copolymers were made through the free-radical copolymerization of vinyl acetate and ethylene, which resulted in varying amounts of uncontrolled branching. Through the use of ring-opening metathesis polymerization (ROMP) with functional group tolerant late transition metal ruthenium olefin metathesis catalysts, regio- and stereo-regular EVOH materials can now be synthesized as illustrated in Scheme 9.1.[4*]

It was evident from experimental results that a difference in stereochemistry between neighboring alcohol functionalites in EVOH have a dramatic effect on the structure of the copolymer both in solution as well as in the solid state.[5] In order to gain a better insight into the role that stereochemistry plays in the material morphology and performance, a detailed set of molecular dynamic simulations was undertaken.

*See Chapter 8.

Scheme 9.1: General sythetic route to syn-(polymer **5**) and anti-diols (polymer **6**) along EVOH backbone from the *trans*- and *cis*-acetonide monomers **1** and **2**, respectively.

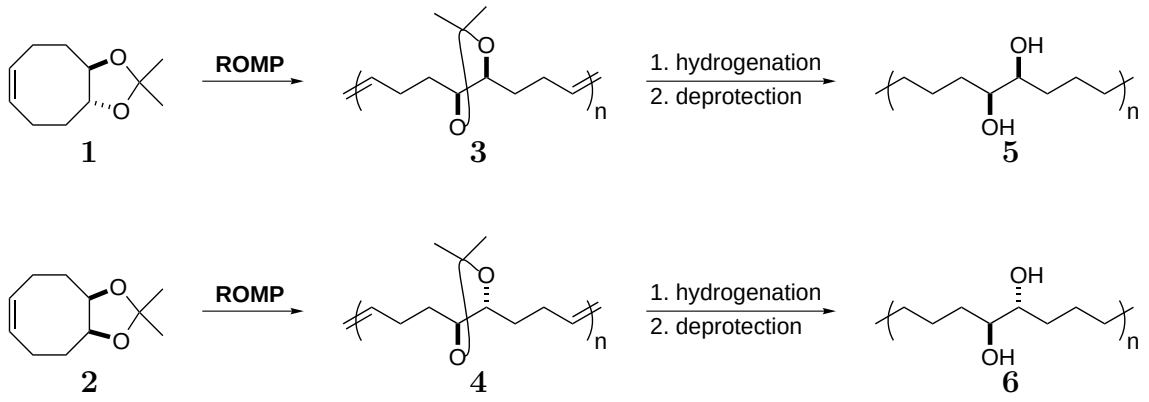

1 **3** **5**

2 **4** **6**

9.3 Simulation Methods

The initial sample EVOH structures of **5** and **6** were made using the Amorphous Builder of Cerius2,[6] which uses Monte Carlo techniques to build an amorphous structure with a three dimensional periodic cell. This Monte Carlo build was followed with an extensive series of annealing simulations in which the volume and temperature were varied systematically to achieve a fully equilibrated system at the target temperature and pressure. Each simulated system consists of four wholly syn or anti EVOH 20-mer chains (total number of atoms in the system is 2088). Three independent samples were constructed for both polymers **5** and **6**.

The annealing procedure for constructing the amorphous structure is as follows. Since the experimental data indicates that the density is 1.09 g/cm^3 at 300 K for EVOH polymer **5**, the initial polymer structure was prepared using a supercell appropriate for a density of 1.1 g/cm^3. Monte Carlo techniques were employed to construct initial configurations at 60% of the target density (1.1 g/cm^3) which were then relaxed by applying the following annealing procedure: First, the structure was gradually expanded by 50% of its initial volume over a period of 50 ps while the temperature was simultaneously increased from 300 K to 700 K. Next, NVT molecular dynamics (MD) simulations were performed at 700 K with the expanded volume

for 50 ps. Next, the structure was compressed back to the initial volume over 50 ps while cooling the temperature to the target temperature of 300 K. This process was repeated five times. Then, at the final target density (1.1 g/cm^3), 100 ps of NVT MD (fixed volume and Nose-Hoover thermostat[7–10] at 300 K) was carried out. This was followed by a step-wise increase of the temperature to 430 K where an NVT simulation for 100 ps followed by an NPT simulation for 400 ps to relax the density of the system were carried out. This was followed by a continuous cooling ramp of temperature from 430 to 300 K over a 520 ps timescale at constant pressure (1 atm). The annealing simulations were performed with LAMMPS (Large-scale Atomic/Molecular Massively Parallel Simulator) code from Plimpton at Sandia (modified to handle our force fields).[11, 12] The equations of motion were integrated using the Verlet algorithm[13] with a time step of 1.0 fs, and the Particle-Particle Particle-Mesh (PPPM) method[14] was used for the electrostatic interactions.

After annealing the structures as described above, NPT MD simulations were performed with the LAMMPS code at 300 K for 1 ns. This led to a final density of 1.03 g/cm^3 $\pm$ 0.02 g/cm^3 for both **5** and **6** polymers at 300 K which compares well with the experimental value of 1.09 g/cm^3 for **5**.

To describe inter- and intra-molecular interactions, the OPLS-AA force field was employed.[15–18] The standard geometric combination rules for the cross van der Waals interactions were used and the total potential energy is given as follows:

$$E_{total} = E_{vdW} + E_{Q} + E_{bond} + E_{angle} + E_{torsion}$$

where E_{total}, E_{vdW}, E_{Q}, E_{bond}, E_{angle}, and $E_{torsion}$ are the total energies and the van der Waals, electrostatic, bond stretching, angle bending, and torsion components, respectively.

9.4 Results and Discussion

9.4.1 Hydrogen Bond Analysis

An attempt was made to identify the glass transition temperature, T_g, for both **5** and **6** by analyzing plots of energy vs temperature and volume vs temperature of the cooling ramps described above. Unfortunately, no significant change in slope was observed in either system. However, a drastic change in atom mobility as a function of temperature was noted. At 430 K, both systems possessed liquid-like mobilities while at 300 K, the atom displacement was < 2 Å for 500 ps as seen in Figure 9.1. This suggests that both polymers are in the glassy state at 300 K in agreement with the experimentally determined T_g of 34.5 and 50 °C for **5** and **6**, respectively. This conclusion is based on the low value of the atom mobilities and the appearance of a plateau evident in Figure 9.1. It is worth noting that the mobility of the hydroxyl group (O) is higher than that of the polymer backbone (C) atoms suggesting that if any hydrogen bonding exists, it does not impose a constraint on the -OH librations.

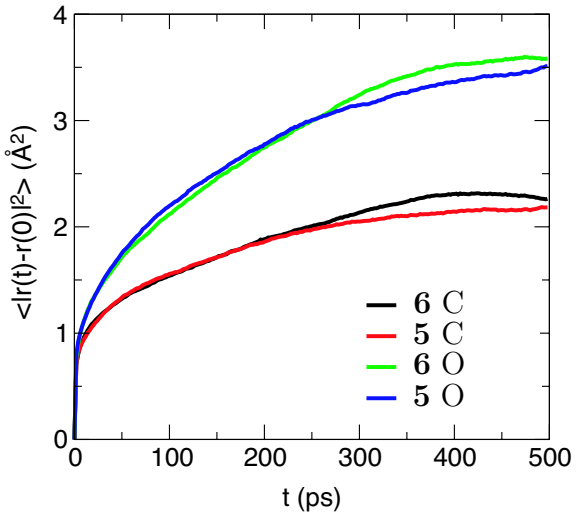

Figure 9.1: Mean square displacement of carbon and oxygen atoms in both syn diol polymer **5** and anti diol polymer **6** at 300 K.

The local topology of the neighboring 1,2-diols is quite different for EVOH polymers **5** and **6**. The formation of 1,2-hydrogen bond interaction between the syn diols

in **5** is prevalent as seen in Figure 9.2. On the other hand, 1,2-hydrogen bonds are not observed for the anti diols in **6** (Figure 9.2). In order to form a neighboring intramolecular hydrogen bond in **6** it is necessary to greatly alter the polymer conformation. The structure resulting from this conformational change is likely to have an unfavorable effect on packing of the polymer chains. Furthermore, in no case are any hydrogen bonding interactions between adjacent neighboring pairs observed. The correlation of intra-chain hydrogen bonds is short ranged and micelle-like structures with segregated hydroxyl domains are not observed.

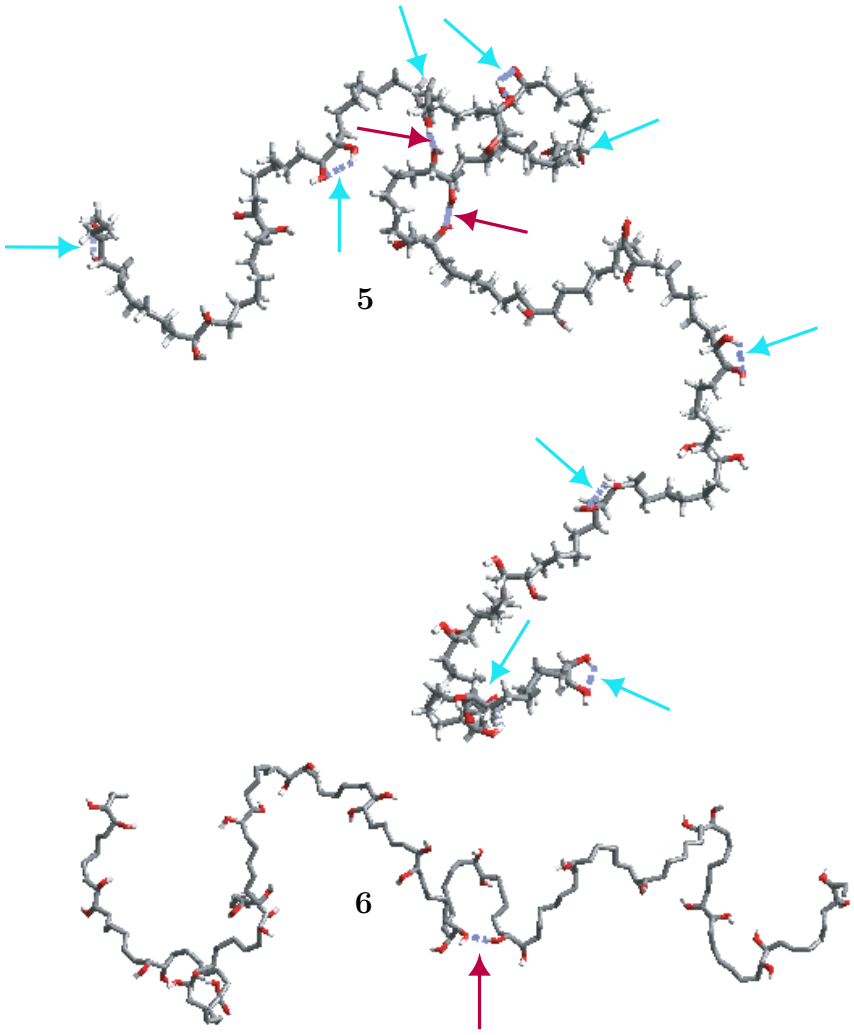

Figure 9.2: Types of intra-chain hydrogen bonding in both **5** and **6**. The blue arrows indicate the presence of neighboring 1,2-diol intramolecular hydrogen bonds and the red arrows point to non-neighboring intramolecular hydrogen bonds.

In an attempt to further characterize the hydrogen bond (H-bond) patterns in the systems, the three-dimensional H-bonding networks in both polymers and computed the distribution of H-bonding clusters were analyzed. The hydrogen bond connectivity was defined using a geometric criterion. A hydrogen bond was considered to be formed if the donor hydrogen and acceptor oxygen were less than 2.5 Å apart. If at least one hydrogen bond exists between two hydroxyl groups, they were assumed to belong to the same cluster. Figure 9.3 shows the hydrogen bond networks for typical configurations of polymers **6** and **5**.

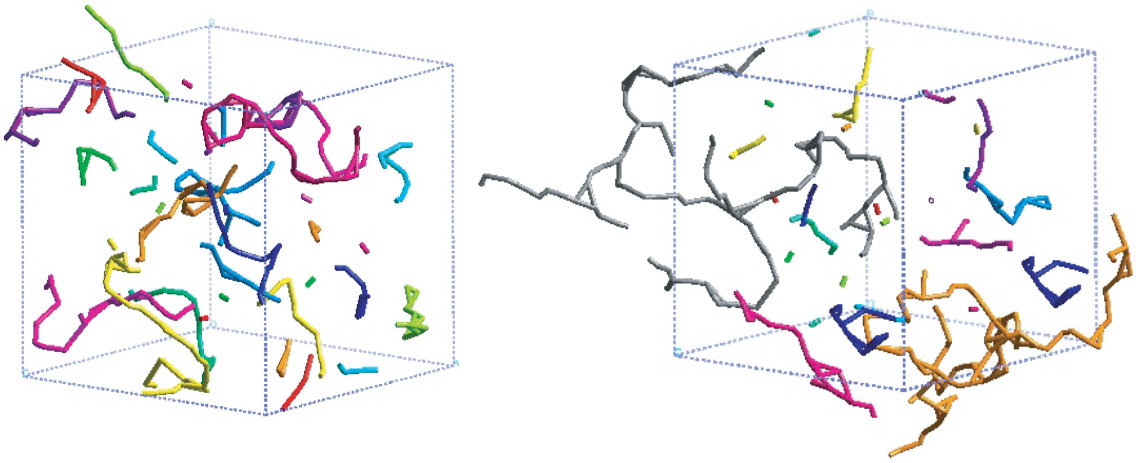

anti diols (**6**) syn diols (**5**)

Figure 9.3: 3-D representation of extended hydrogen bonding in EVOH.

Both polymers form mainly one-dimensional clusters. This is expected as each hydroxyl group has only one hydrogen bond donor and acceptor. However, the syn relationship of the diols in polymer **5** displays a characteristically longer connectivity than is observed in **6**. The average length of the hydrogen bond clusters were quantified and differ by more than 50%: the average number of hydroxyl groups in the cluster is 4.0 and 6.6 for anti and syn polymers, respectively. Moreover, the difference in the distribution of the cluster sizes for the two polymers as shown by the graph in Figure 9.4 is striking. The probability of finding clusters with > 20 hydroxyl groups is zero for the anti polymer **6**. Conversely, syn polymer **5** possesses a broad distribution of cluster sizes. These distribution are in agreement with the qualitative view

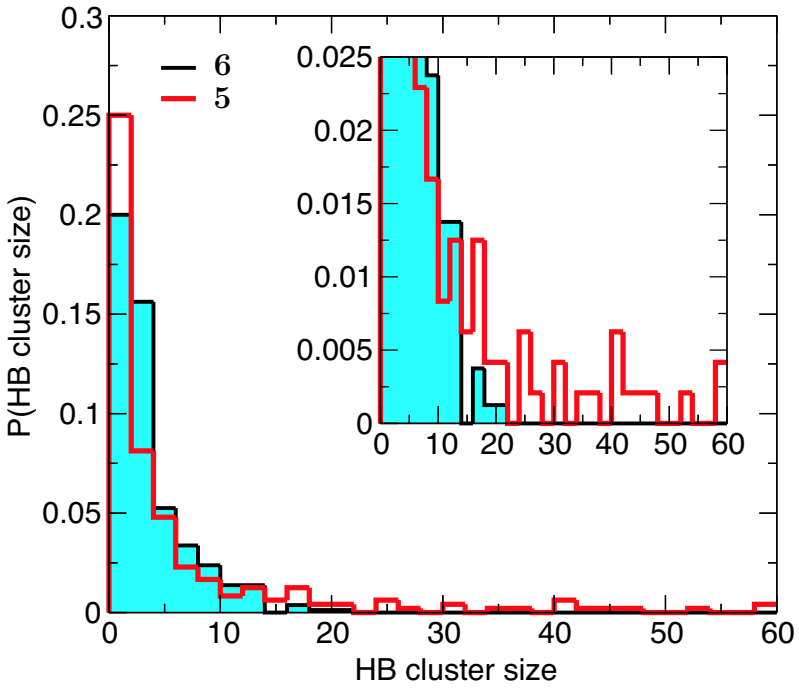

Figure 9.4: Probability of hydrogen bond cluster sizes.

illustrated by the Figure 9.3.

9.4.2 Free Volume Analysis

The free volume (FV) for the two polymers were computed. The FV is defined as the volume fraction of the total volume available for the probe. The FV accessible to a probe of radius R_p was calculated over a three-dimensional grid of size 0.1 Å, and measuring the space occupied by spheres of radius $R_a + R_p$, where R_a is the contact radius (1.2, 1.52, and 1.70 Å for H, O, and C, respectively). The void percolation radius R_{pc} is defined as the largest probe that senses accessible FV channels percolated in all directions. A channel is percolated if it is connected with its periodic images in the three cartesian directions. In a percolated structure, the ratio between the volume of the largest (percolated) void and any other void is very big. This is illustrated in Figure 9.5 which shows the FV fraction largest and second largest voids for both polymers equilibrated at 300 K. The arrow in Figure 9.5 indicates a percolating probe radius, R_{pc}, which is approximately 0.6 Å. The R_{pc} is smaller than any molecular

solute such as oxygen or water; it is close to the 0.55 Å for a glass of random close-packed spheres and well below the 0.9–1.1 Å computed for atactic polypropylene.[19]

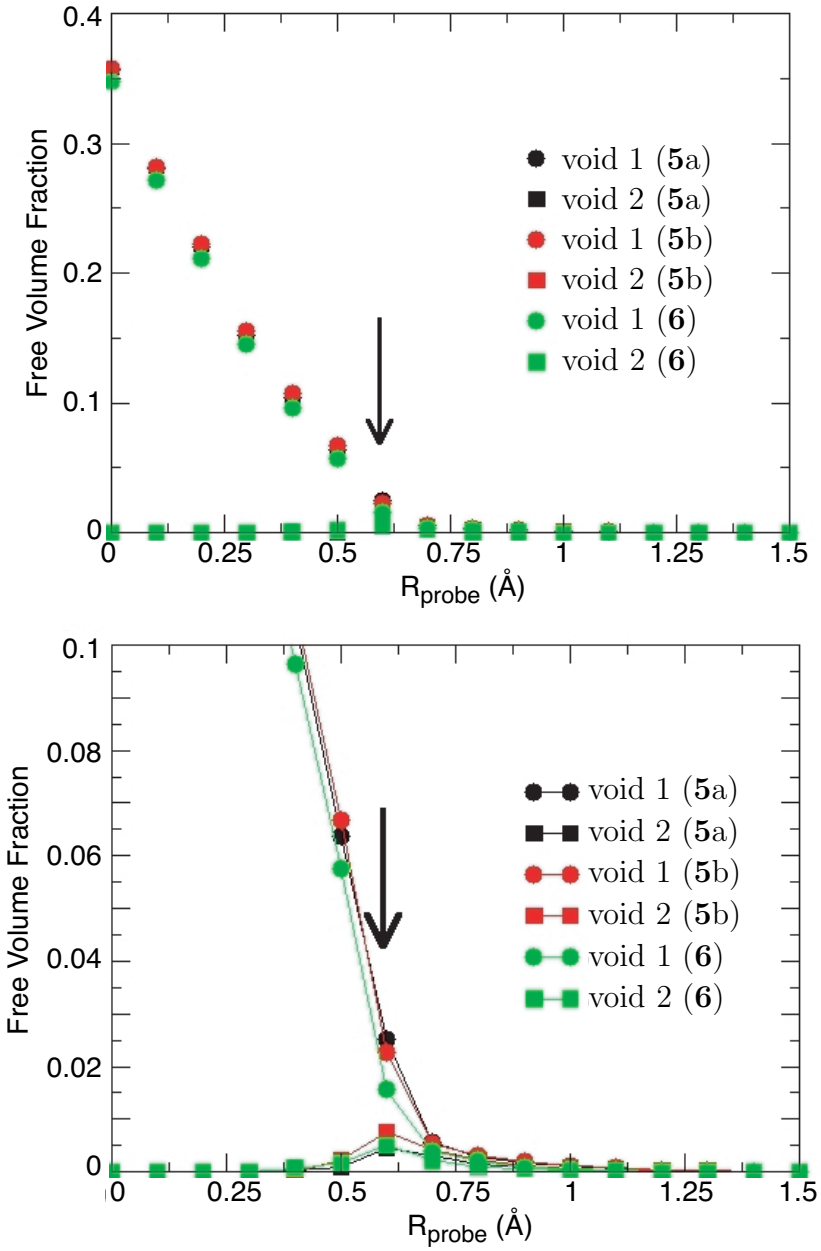

Figure 9.5: Comparison of void spaces in syn and anti EVOH copolymers. **5**a and **5**b are two separate samples of the syn diol polymer.

The low FV fractions for R_p comparable to the size of oxygen (see Figure 9.6)

in these polymers may be related to the exceptional O_2 barrier properties exhibited by **5**.[20–22] As a result of these simulations, comparable or even better barrier properties for **6** based on its lower FV percentage are anticipated (Figure 9.6). Moreover, polymer **6** displays a T_g well above ambient temperatures.

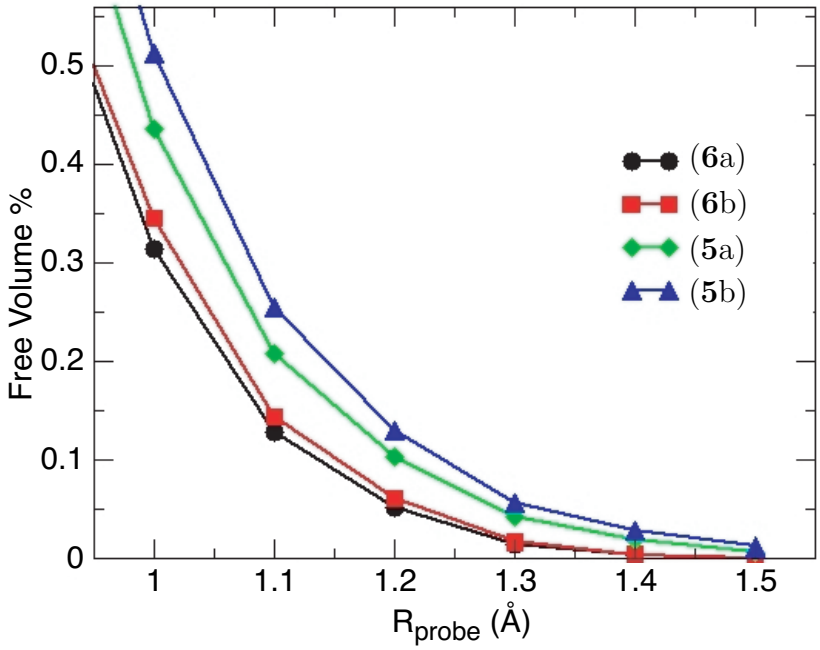

Figure 9.6: Comparison of void spaces in syn and anti EVOH copolymers. **6**a and **6**b and **5**a and **5**b are two separate samples of the anti and syn diol polymers, respectively.

At 300 K the hydroxyl groups are able to fluctuate over distance comparable to the size of O_2 (Figure 9.1). This implied that the voids in the systems evolve and suggested an exploration of the void dynamics. A significant restructuring of the FV voids on the nanosecond scale for both polymers at 300 K is observed. This is shown for polymer **5** in Figure 9.7 and for polymer **6** in Figure 9.8. Furthermore, the voids are small and well-dispersed throughout the cell consistent with the good packing in both systems.

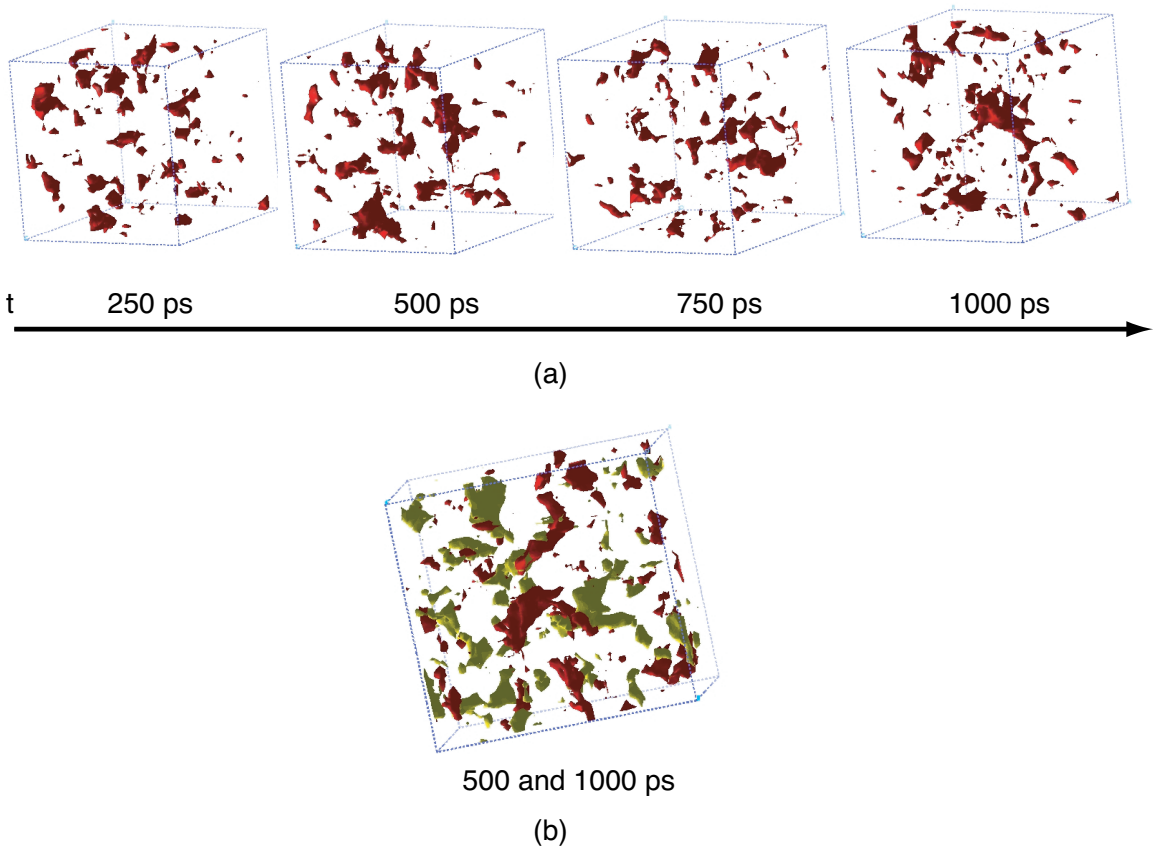

Figure 9.7: (a) Time evolution of the free volume for EVOH copolymer **5** in a 1 ns dynamics simulation at 300 K with a 1 Å probe radius. (b) An overlay of the free volumes at 500 and 1000 ps, indicating that different void spaces are created throughout the dynamics simulation.

9.4.3 Oxygen Diffusivity

In an attempt to determine the mobility of oxygen molecules in the EVOH polymers, molecular oxygen in the equilibrated structure for **5** and **6** was loaded at 300 K. The molecules were inserted at constant pressure using the sorption module of Cerius2 that implements a Grand Canonical Monte Carlo method. Based on standard solubilities of O_2 in organic polymers, *zero* oxygen molecules should be found in the cells (cell dimension is approximately 26 Å). To improve the collection of mobility data, an extremely high concentration of five O_2 molecules in both polymer systems was imposed. The pressures required to impregnate 5 oxygens were significantly higher for **6** than for **5** in agreement with the lower FV of **6**. The resultant mobilities averaged

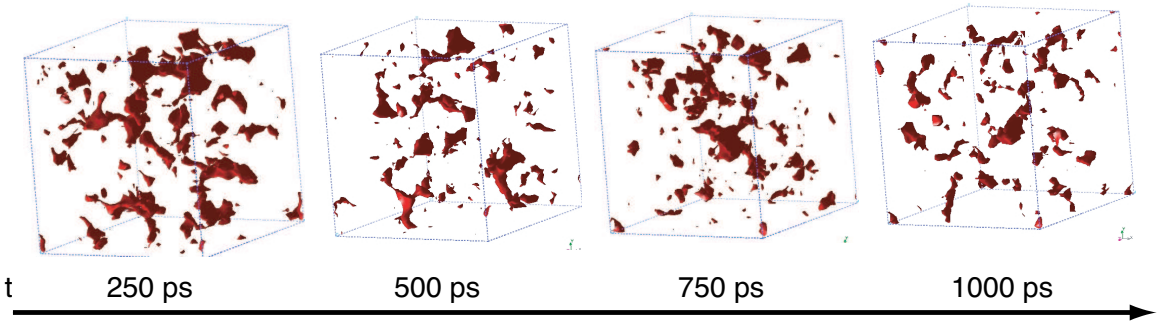

Figure 9.8: Time evolution of the free volume for EVOH copolymer **6** in a 1 ns dynamics simulation at 300 K with a 1 Å probe radius.

over a trajectory of 5 ns are displayed in Figure 9.9 for polymer **5** at 300 K. Note, the increased mobilities of the polymer (C and O) with respect to those observed in Figure 9.1 at the same temperature. The higher polymer mobility in the presence of oxygen indicates a plasticizing effect of this high O_2 concentration. Similar results have been observed previously with experiments of high pressures of Xe in polystyrene blends.[23] This is not surprising with the high loading of O_2 and the proximity to the expected T_g (experimentally determined) for **5**.

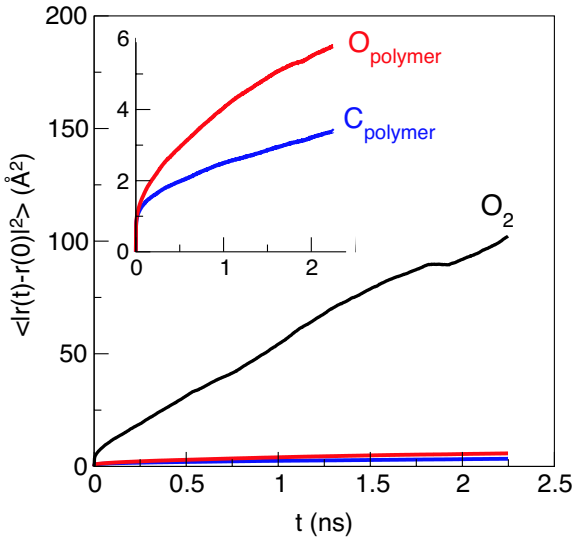

Figure 9.9: Average displacement of atoms in polymer and O_2 in molecular dynamics run.

9.5 Conclusions

The microscopic structure of both EVOH copolymers has been characterized in terms of hydrogen bond and FV networks. The FV is very low compared to other polymers indicating a good packing for both syn and anti diol polymers. The equilibrium densities for both polymers at 300 K were comparable ($1.03\ g/cm^3 \pm 0.02\ g/cm^3$) and in good agreement with an experimental value of $1.09\ g/cm^3$. Though small, the FV voids are still mobile at 300 K in due to the hydroxyl group fluctuations. No significant differences for the mobility between the two EVOH copolymesr at 300 K was found. A striking difference in the hydrogen bond clustering was observed for these polymers. While the anti diol polymer does not form neighboring 1,2-hydrogen bonds, these features are abundant in the syn diol polymer. Perhaps more significant is the difference in extension of the hydrogen bond networks. Polymer **6** displays many short H-bond threads while **5** displays a broader distribution of cluster length with a high proportion of clusters that span over lengths comparable to the simulations cell. The extended H-bond array of polymer **5** does not, however, follow along the periphery of a single polymer chain.

References Cited

[1] Lagaron, J. M.; Powell, A. K.; Bonner, G. *Polym. Testing* **2001,** *20,* 569–577.

[2] Lopez-Rubio, A.; Lagaron, J. M.; Gimenez, E.; Cava, D.; Hernandez-Munoz, P.; Yamamoto, T.; Gavara, R. *Macromolecules* **2003,** *36,* 9467–9476.

[3] Ramakrishnan, S. *Macromolecules* **1991,** *24,* 3753–3759.

[4] Scherman, O. A.; Kim, H. M.; Grubbs, R. H. *Macromolecules* **2002,** *35,* 5366–5371.

[5] Chapter 8 of this thesis.

[6] Accelrys Inc. *Cerius2 Modeling Environment, Release 4.0;* Accelrys Inc.: San Diego, 1999.

[7] Nose, S.; Klein, M. L. J. *Chem. Phys.* **1983,** *78,* 6928–6939.

[8] Nose, S. *J. Chem. Phys.* **1984,** *81,* 511–519.

[9] Nose, S. *Mol. Phys.* **1984,** *52,* 255–268.

[10] Nose, S. *Mol. Phys.* **1986,** *57,* 187–191.

[11] Plimpton, S. J. *J. Comp. Phys.* **1995,** *117,* 1.

[12] Plimpton, S. J.; Pollock, R.; Stevens, M. In the Eighth SIAM Conference on Parallel Processing for Scientific Computing, Minneapolis, 1997.

[13] Verlet, L. *Phys. Rev.* **1967,** *159,* 98.

[14] Hockney, R. W.; Eastwood, J. W. *Computer simulation using particles;* McGraw-Hill International Book Co.: New York, 1981.

[15] Jorgensen, W. L.; Maxwell, D. S.; Tirado-Rives, J. *J. Am. Chem. Soc.* **1996,** *118,* 11225–11236.

[16] Marrink, S. J.; Berendsen, H. J. C. *J. Phys. Chem.* **1996,** *100,* 16729–16738.

[17] Fischer, J.; Lago, S. *J. Chem. Phys.* **1983,** *78,* 5750–5758.

[18] Miyano, Y. *Fluid Phase Equilib.* **1999,** *158–160,* 29–35.

[19] Greenfield, M. L.; Theodorou, D. N. *Macromolecules* **1993,** *26,* 5461–5472.

[20] Banslaben, D. A.; Huynh-Tran, T. C.; Blanski, R. L.; Hughes, P. A.; Roberts, W. P.; Grubbs, R. H.; Hatfield, G. R. Regio-Regular Functionalized Polymeric Packaging Material. US Patent 6,203,923, March 20, 2001.

[21] Banslaben, D. A.; Huynh-Tran, T. C. T.; Blanski, R. L.; Hughes, P. A.; Roberts, W. P.; Grubbs, R. H.; Hatfield, G. R. Regio-Regular Copolymer and Methods of Forming Same. US Patent 6,506,860, January 14, 2003.

[22] Banslaben, D. A.; Huynh-Tran, T. C. T.; Blanski, R. L.; Hughes, P. A.; Roberts, W. P.; Grubbs, R. H.; Hatfield, G. R. Regio-Regular Copolymer and Methods of Forming Same. US Patent 6,153,714, November 28, 2000.

[23] Miyoshi, T.; Takegoshi, K. Terao, T. *Macromolecules* **2002,** *35,* 151–154.